Investigation of In-vivo Total Knee Arthroplasty Biomechanics Using a Dual Fluoroscopic Imaging System

By

Jeremy F. Suggs

B. S. Mechanical Engineering, University of Pittsburgh, 1999

S. M. Mechanical Engineering, Massachusetts Institute of Technology, 2002

SUBMITTED TO THE DEPARTMENT OF MECHANICAL ENGINEERING IN PARTIAL FULFILLMENT OF THE REQUIREMENTS FOR THE DEGREE OF

DOCTOR OF SCIENCE IN MECHANICAL ENGINEERING
AT THE
MASSACHUSETTS INSTITUTE OF TECHNOLOGY

SEPTEMBER 2007

Signature of Author: ______________________________
Department of Mechanical Engineering
July 30, 2007

Certified by: ______________________________
Guoan Li
Associate Professor of Orthopaedic Surgery/Bioengineering
Harvard Medical School
Thesis Supervisor

Certified by: ______________________________
Derek Rowell
Professor of Mechanical Engineering
Thesis Committee Chairman

Accepted by: ______________________________
Lallit Anand
Professor of Mechanical Engineering
Chairman, Department Committee on Graduate Students

Investigation of In-vivo Total Knee Arthroplasty Biomechanics Using a Dual Fluoroscopic Imaging System

by

Jeremy F. Suggs

Submitted to the Department of Mechanical Engineering on July 30, 2007 in Partial Fulfillment of the Requirements for the Degree of Doctor of Science in Mechanical Engineering

ABSTRACT

While contempary total knee arthroplasty has been successful in improving the quality of life for those suffering from severe osteoarthritis, the function of these patients has not reached normal levels for their age group. Thus, there is an increasing need to improve total knee arthroplasty techniques to allow patients to function normally. We currently have limited knowledge about how current knee arthroplasties behave in-vivo, but this information could be pivotal in designing new implants and surgical techniques. Therefore, the objective of this work was to develop the Dual Fluoroscopic Imaging System, a non-invasive imaging system capable of measuring in-vivo knee kinematics in all degrees of freedom. This system was used to investigate factors that may affect patient function after total knee arthroplasty. The feasibility of using kinematic data obtained using this system to analyze wear of the polyethylene insert was also explored

The system was shown to be repeatable and accurate in determining the pose of the TKA components in all degrees of freedom. Six degree-of-freedom kinematics and articular contact motion were measured in-vivo. Data was obtained for patients with two typical classes of TKA, cruciate-retaining and cruciate-substituting, and the function of conventional implants was compared to that of more recent high flexion designs. In general, no differences were detected between these groups. Further, no factors such as age, weight, PCL management, or kinematics, were found to correlate with flexion capability. Future studies should investigate changes in knee structures from the preoperative state to the postoperative state. Preliminary estimates of polyethylene stresses suggested great potential in using the Dual Fluoroscopic Imaging System in developing a model of in-vivo polyethylene wear.

Thesis Committee Chairman: Derek Rowell
Professor of Mechanical Engineering
Massachusetts Institute of Technology

Thesis Supervisor: Guoan Li
Associate Professor of Orthopaedics (Bioengineering)
Harvard Medical School

Committee Member: Alan Grodzinsky
Director, Center for Biomedical Engineering
Professor of Electrical, Mechanical, and Biological Engineering
Massachusetts Institute of Technology

Committee Member: Harry Rubash
Chief of Orthopaedic Surgery
Massachusetts General Hospital
Edith M. Ashley Professor of Orthopaedic Surgery
Harvard Medical School

Acknowledgements

I must first thank my thesis committee for all of their input to this work. I owe a great debt of gratitude to my thesis advisor, Dr. Guoan Li. He has been very enthusiastic, encouraging, and challenging throughout my graduate career. I have especially appreciated his understanding of family pressures. I am also grateful for my invaluable interactions with Dr. Harry Rubash. He has provided deep insight about the study of total knee arthroplasty, and I hope to emulate his humble yet wise style of communication. Professor Derek Rowell has been a great help as my academic advisor and committee chairman, and did a lot to keep me going through this long process. And I appreciate the knowledge I gained from Professor Alan Grodzinsky in the classroom and in committee meetings. I am thankful for all of your support through the years.

I also need to thank all of my colleagues at the Bioengineering Laboratory: George Hanson, Angela Moynihan, Jeffrey Bingham, Sridar Durbhakula, John Velyvis, Young-Min Kwon, Jim Slover, Ephrat Most, Louis DeFrate, Ramprasad Pappanagari, Dr. Park, Dr. Yoo, Dr. Nha, Lu Wan, Sam Van de Velde, Daniel Massimini, Ali Hosseini, Shaobai Wang, Kartik Varadarajan, Conrad Wang, Ervin Wilson, Ara Nazarian, and Vaida Glatt. You all have made the lab a great place to be.

I would like to thank my Mom and Dad and my brother Clayton for their love and support. Without you, I would not have made it hear. I would also like

to thank my in-laws, Claudia, Terry, Meeta, Karl, Bea, Brendon, Ian, and Lydia. You all have been a great help and encouragement throughout our time here in Cambridge.

I must say a special thank you to my wife, Becky, and my children, Jay, Kayla, and Andre. Becky has worked just as hard if not twice as hard as I have, doing most of the raising of our kids while going to school herself. Becky, this would have been impossible without you. "He who finds a wife finds what is good and receives favor from the Lord." *Proverbs 18:22*

And I have to give thanks and honor to God for getting me and my family through this period in our lives. He has blessed us beyond measure.

Table of Contents

List of Figures

List of Tables

Chapter 1. Introduction

1.1 Motivation and Objectives

Millions of Americans suffer from osteoarthritis (OA) of the knee, which is degeneration of the articular cartilage. In cases of severe OA, patients can experience a great amount of pain and lose much of the range of motion (ROM) in the affected knee, which in turn limits their ability to function. Approximately 381,000 primary and 35,000 revision total knee arthroplasties (TKA) were performed in the United States in 2002 to relieve pain and restore knee function in patients suffering from OA (Kurtz, Mowat et al. 2005). Due to the aging and increasing size of the population, the number of primary knee arthroplasties performed annually is expected to increase to at least 474,000 in the year 2030 (Praemer, Furner et al. 1999; Frankowski and Watkins-Castillo 2002; Kurtz, Mowat et al. 2005). In addition, younger patients are having TKA surgeries at an increasing rate (Ranawat, Padgett et al. 1989; Diduch, Insall et al. 1997; Jain, Higgins et al. 2005; Kurtz, Mowat et al. 2005). While contempary TKA has been successful in improving the quality of life for those suffering from OA (March, Cross et al. 1999; Bachmeier, March et al. 2001; Mahomed, Liang et al. 2002), the function of these patients has not reached normal levels for their age group, unlike patients who undergo total hip arthroplasty (Finch, Walsh et al. 1998; March, Cross et al. 1999; Mizner, Petterson et al. 2005; Noble, Gordon et al.

2005). Thus, there is an increasing need to improve TKA techniques to allow patients to function normally.

The healthy human knee can flex up to approximately 150° (Boone and Azen 1979; Dennis, Komistek et al. 1998; Nakagawa, Kadoya et al. 2000; Mulholland and Wyss 2001; Nagura, Dyrby et al. 2002; Steinberg, Hershkovitz et al. 2005), and many activities of daily living require a significant amount of flexion (Laubenthal, Smidt et al. 1972). For example, stair climbing and descent, as well as sitting on chairs, require 90-120° of flexion, and the use of a bathtub requires 135° of flexion (Rowe, Myles et al. 2000). High flexion of the knee is also essential for individuals who are employed in such professions as construction and agriculture, as well as for individuals who participate in recreational activities such as gardening and golfing. In order to kneel, squat, or sit cross-legged for certain religious activities, 165° of flexion is needed (Hefzy, Kelly et al. 1997; Mulholland and Wyss 2001).

Numerous studies have demonstrated that, on average, patients can only flex the knee up to 115°, regardless of the type of TKA design, the patient's age, gender, or pre-operative condition (Insall, Hood et al. 1983; Aglietti, Buzzi et al. 1988; Goldberg, Figgie et al. 1988; Lee, Keating et al. 1990; Rosenberg, Barden et al. 1990; Malkani, Rand et al. 1995; Anouchi, McShane et al. 1996; Emmerson, Moran et al. 1996; Ranawat, Luessenhop et al. 1997; Dennis, Komistek et al. 1998; Kawamura and Bourne 2001; Bellemans, Banks et al. 2002; Banks, Bellemans et al. 2003; Kotani, Yonekura et al. 2005; Matsumoto, Tsumura et al. 2005; Victor, Banks et al. 2005) (Table 1). These data indicate that there may be a common biomechanical mechanism that limits knee flexion after TKA, which has not been clearly described in the orthopaedic literature. The factors that limit higher knee flexion remain unclear (Li, Most et al. 2004). The reduced range of flexion after TKA limits the patients' knee joint function. As a result, enhancing knee flexion has been a goal of TKA surgery (Anouchi, McShane et al. 1996; Pope, Corcoran et al. 1997; Kawamura and Bourne 2001; Argenson, Komistek et al. 2004; Argenson, Scuderi et al. 2005).

Implant failure is another major focus in TKA research, and polyethylene wear is a leading cause for revision (Hood, Wright et al. 1983; Bohl, Bohl et al. 1999; NIH 2000; Harman, Banks et al. 2001; Banks, Harman et al. 2002; Berzins, Jacobs et al. 2002; Sharkey, Hozack et al. 2002; NIH 2003; Vince 2003; Berend, Ritter et al. 2004; Clarke, Math et al. 2004; Huddleston, Wiley et al. 2005; Morgan, Battista et al. 2005; Wright 2005). Studies of wear in TKA have focused on the tibial plateau, the primary articulation in the joint. However, wear of the polyethylene contacting the metal tibial plate, or "backside wear", and wear on the anterior face of the tibial post have also received attention (Banks, Harman et al. 2002; Callaghan, O'Rourke et al. 2002; Harman, Banks et al. 2007).

Many have felt that patient function after TKA, including ROM and polyethylene wear, is related to the kinematics of the knee, but acquiring full and accurate kinematics has been a challenge. This work discusses past study of TKA and presents the development, validation, and implementation of the Dual Fluoroscopic Imaging System, a markerless and non-invasive technique capable of measuring joint kinematics in all 6 degrees of freedom. The technique is used to explore possible differences in kinematics between patients with excellent function and patients with limited ROM. The feasibility of using the 6 DOF kinematics to estimate the in-vivo polyethylene stresses through finite element analysis is also investigated.

1.2 Organization

This thesis has four main sections. The first is chapter 3, which presents the development and validation of the imaging system. Chapters 4 and 5 discuss results from patients with cruciate-retaining implants, while chapter 6 discusses posterior-stabilized implants. Chapter 7 investigates the distribution of maximum flexion across both types of implants. Chapter 8 begins to look at the stresses experienced by the articular polyethylene insert by combining data obtained through dual fluoroscopic imaging with finite element analysis. The work is based on the following papers:

Li G, Suggs J, Hanson G, Durbhakula S, Johnson T, Freiberg A. Three-dimensional tibiofemoral articular contact kinematics of a cruciate-retaining total knee arthroplasty. J Bone Joint Surg Am. 2006 Feb;88(2):395-402.

Hanson GR, Suggs JF, Freiberg AA, Durbhakula S, Li G. Investigation of in vivo 6DOF total knee arthoplasty kinematics using a dual orthogonal fluoroscopic system. J Orthop Res. 2006 May;24(5):974-81.

Hanson GR, Suggs JF, Kwon YM, Freiberg AA, Li G. In vivo anterior tibial post contact after posterior stabilizing total knee arthroplasty. J Orthop Res. 2007 Jun 7; [Epub ahead of print]

Suggs JF, Kwon YM, Durbhakula SM, Hanson GR, Li G, Freiberg AA. In-vivo Flexion and Kinematics of the Knee after TKA – Comparison of a Conventional and a High Flexion Cruciate-Retaining Total Knee Arthroplasty Design. Submitted to Journal of Bone and Joint Surgery – Br

Suggs JF, Hanson GR, Park SE, Moynihan AL, Freiberg AA, Li G. Patient Function after a Posterior Stabilizing Total Knee Arthroplasty – Cam-post Engagement and Knee Kinematics. Submitted to Knee Surgery, Sports Traumatology, Arthroscopy.

Suggs JF, Hanson GR, Freiberg AA, Rubash HE, Li G. Determination of In-vivo TKA Contact Area Using Dual Fluoroscopic Imaging. Proceedings of Summer Bioengineering Conference, Amelia Island, Florida, 2006

Suggs JF, Hanson GR, Li G. In-vivo Tibiofemoral Contact Stress in the Knee after TKA. Proceedings of Summer Bioengineering Conference, Keystone Colorado, 2007

Chapter 2. Review of the Study of Flexion after TKA

2.1 Factors Affecting Flexion

The main goal of total knee arthroplasty is to restore the function of the knee in patients suffering from severe cartilage degeneration, and the amount of the flexion the patient achieves postoperatively has been a primary measure of the level of restoration. Investigators have reported various factors that may affect knee flexion after TKA. These factors can be broken into 3 categories: Preoperative, Intraoperative, and Postoperative.

2.1.1 Preoperative Factors

Previous investigators have studied the effects of preoperative factors that might limit flexion after total knee arthroplasty (Ritter and Stringer 1979; Schurman, Parker et al. 1985; Tew, Forster et al. 1989; Maloney and Schurman 1992; Parsley, Engh et al. 1992; Harvey, Barry et al. 1993; Anouchi, McShane et al. 1996; Lizaur, Marco et al. 1997; Schurman, Matityahu et al. 1998; Kawamura and Bourne 2001; Ritter, Harty et al. 2003; Kotani, Yonekura et al. 2005; Rowe, Myles et al. 2005; Evans, Parsons et al. 2006). One of the first proposed correlates to range of motion after TKA was preoperative flexion (Ritter and

Stringer 1979). In a study of 145 total knee arthroplasties, Ritter and Stringer found that postoperative flexion may be determined by preoperative flexion, particularly in cases where the preoperative flexion was less than 75°. They did not see any correlation between postoperative flexion and prosthesis design, gender, age, or diagnosis of rheumatoid or osteoarthritis. In a later study of 4727 knees, Ritter et al. again found preoperative flexion to be the strongest predictor of postoperative flexion (Ritter, Harty et al. 2003). They also found weaker correlations between postoperative flexion and gender, age, and preoperative tibiofemoral alignment.

In a multi-center, prospective study of 282 knees, Anouchi et al. reported that patients with pre-operative flexion of less than 90° gained the most flexion, while patients with flexion greater than 105° prior to surgery tended to retain or lose some motion after surgery (Anouchi, McShane et al. 1996). Age, gender, weight, and previous surgery were not significantly correlated with the post-operative range of motion. Kotani et al. did not find any correlation between postoperative ROM and age or body mass index (Kotani, Yonekura et al. 2005). Similarly, other studies have noted that patients with the least pre-operative motion increased their flexion range the most, whereas those with the most pre-operative motion tended to lose motion after surgery (Schurman, Parker et al. 1985; Parsley, Engh et al. 1992; Harvey, Barry et al. 1993; Lizaur, Marco et al. 1997; Kawamura and Bourne 2001; Rowe, Myles et al. 2005). Despite the relationship between preoperative and postoperative knee flexion, postoperative knee flexion has been limited to approximately 115° (Insall, Hood et al. 1983;

Insall, Binazzi et al. 1985; Aglietti, Buzzi et al. 1988; Goldberg, Figgie et al. 1988; Lee, Keating et al. 1990; Rosenberg, Barden et al. 1990; Dennis, Clayton et al. 1992; Ranawat, Flynn et al. 1993; Rand 1993; Malkani, Rand et al. 1995; Emmerson, Moran et al. 1996; Ranawat, Luessenhop et al. 1997; Kotani, Yonekura et al. 2005).

2.1.2 Intraoperative Factors

Several studies have looked at the effect of the surgical approach on the outcome of TKA (Parsley, Engh et al. 1992; Keating, Faris et al. 1999; Parentis, Rumi et al. 1999; Matsueda and Gustilo 2000; Tanavalee, Thiengwittayaporn et al. 2004; Berger, Sanders et al. 2005; Laskin 2005). The concept behind these studies is that minimized disruption to certain soft tissues in the knee will result in improved function after surgery. In prospective, randomized studies comparing the midvastus and median parapatellar approaches, no significant differences were shown in range of motion, strength, knee scores, tourniquet time, or proprioception (Keating, Faris et al. 1999; Parentis, Rumi et al. 1999). In a retrospective study of the subvastus and median parapatellar techniques (Parsley, Engh et al. 1992; Matsueda and Gustilo 2000), the type of approach once again was not found to improve range of motion. The choice of surgical approach, including minimally invasive surgeries (MIS) (Tanavalee, Thiengwittayaporn et al. 2004; Berger, Sanders et al. 2005; Laskin 2005), does not seem to increase the ultimate flexion of the knee but, theoretically, may allow for faster rehabilitation.

Another surgical consideration is the release of various soft tissues around the knee (Harvey, Barry et al. 1993; Arima, Whiteside et al. 1998; Mihalko, Whiteside et al. 2003; Ritter, Harty et al. 2003; Laskin and Beksac 2004; Argenson, Scuderi et al. 2005; Victor, Banks et al. 2005; Mizu-Uchi, Matsuda et al. 2006). It has been suggested that release of the posterior capsule (Argenson, Scuderi et al. 2005), partial release of the PCL (Arima, Whiteside et al. 1998; Laskin and Beksac 2004), or release of the medial or lateral tissues (Victor, Banks et al. 2005; Mizu-Uchi, Matsuda et al. 2006) may be necessary to afford the patient normal function. Ritter et al. found that patients with a medial release had 3° less ROM, but they attribute this difference to the preoperative varus deformity that necessitated the medial release as opposed to the release itself (Ritter, Harty et al. 2003). Harvery et al. reported that soft tissue release did not affect ROM (Harvey, Barry et al. 1993). While there has been substantial discussion concerning soft-tissue release, there has been relatively little objective investigation into the mechanical effect releasing various tissues in the context of total knee arthroplasty. Mihalko et al measured the effect releasing medial structures and lateral structures on the joint gap in an in-vitro study (Mihalko, Whiteside et al. 2003). They found that the superficial MCL and LCL had a significant restraining effect throughout flexion but mostly at flexion greater than 90°.

Removal of posterior femoral and tibial osteophytes has also been recognized as a factor that affects knee flexion and is sometimes part of releasing the posterior capsule (Li, Schule et al. 2003; Ritter, Harty et al. 2003;

Laskin and Beksac 2004; Argenson, Scuderi et al. 2005; Sugama, Kadoya et al. 2005; Yau, Chiu et al. 2005). Failure to remove the posterior osteophytes may result in early tibial impingement and, thus, reduce flexion. Removal of all the posterior osteophytes may also help in achieving full extension of the knee as they cause tenting of the posterior capsule.

Whether or not to retain the PCL has been a controversial topic in the research on TKA techniques (Andriacchi and Galante 1988; Becker, Insall et al. 1991; Walker and Garg 1991; Banks, Markovich et al. 1997; Bolanos, Colizza et al. 1998; Dennis, Komistek et al. 1998; Stiehl, Dennis et al. 2000; Li, Zayontz et al. 2001; Li, Gill et al. 2002; Most, Zayontz et al. 2003; Jacobs, Clement et al. 2005; Kotani, Yonekura et al. 2005; Victor, Banks et al. 2005; Fantozzi, Catani et al. 2006). PCL retention has been thought to have the potential advantage of a better passive range of knee flexion, improved rollback of the femur, and enhanced joint stability (Andriacchi and Galante 1988; Walker and Garg 1991; Li, Gill et al. 2002). An alternative to PCL retention is the PCL-substituting TKA, which replaces the PCL with a spine on the tibial polyethylene insert that engages with a cam built into the femoral component. The advantages of PCL-substituting is more consistent results compared to PCL-retention (Argenson, Scuderi et al. 2005; Fantozzi, Catani et al. 2006). In general, PCL-retaining and PCL-substituting designs have had similar kinematics (Stiehl, Dennis et al. 2000; Li, Zayontz et al. 2001; Victor, Banks et al. 2005). Given these kinematic similarities, it is not surprising that no definite clinical differences have been reported (Becker, Insall et al. 1991; Bolanos, Colizza et al. 1998). (Check for a paper by Tanzer on this subject)

Component geometry has also been suggested as a factor in patient function after TKA (Maloney and Schurman 1992; Akagi, Nakamura et al. 2000; D'Lima, Poole et al. 2001; Argenson, Komistek et al. 2004; Argenson, Scuderi et al. 2005). Contemporary femoral components have a smaller radius of curvature in the posterior portion of the condyles compared to the distal portion, similar to the native knee (Walker 2000). This difference is intended to allow femoral rollback and flexion. Some have warned that the reduced radius of curvature in the posterior condyles decreases the flexion moment generated by the quadriceps and, thus, may limit the functional flexion range utilized by the patient (D'Lima, Poole et al. 2001; Kurosaka, Yoshiya et al. 2002; Laskin and Beksac 2004). In addition, the increased quadriceps force needed to maintain the desired flexion moment may lead to an increased rate of patellofemoral complications. Wilson et al reported that TKA patients used significantly less ROM during level walking and stair descent compared to an age-matched control group, but found no difference in quadriceps strength (Wilson, McCann et al. 1996). Despite various modifications to component geometries (Maloney and Schurman 1992; Akagi, Nakamura et al. 2000; Argenson, Komistek et al. 2004; Argenson, Scuderi et al. 2005), the ultimate range of flexion still remains limited.

Closely related to soft-tissue release is the size of the components, since it affects the tension in the tissues around the knee (Laskin and Beksac 2004). A component that is too small may result in a reduced posterior condyle offset and cause impingement in flexion (Bellemans, Banks et al. 2002), although this may be more of a concern for PCL-retaining designs than for PCL-substituting (Kim, Sohn et al. 2005). On the other hand, a femoral component that is too large may result in a tight flexion gap. It may also cause "overstuffing" of the knee joint (Li, Papannagari et al. 2005). This, too, may result in unsatisfactory clinical outcome due to reduced flexion. Thus, accurate sizing of the components is important in obtaining satisfactory range of motion after TKA.

The positioning of the components relative to the bones is another part of the surgical technique that can affect the function of the implant (Piazza, Delp et al. 1998; Callaghan, O'Rourke et al. 2002; Laskin and Beksac 2004; Argenson, Scuderi et al. 2005; Catani, Fantozzi et al. 2006). The relative anterior-posterior position of the tibial component on the cut tibial surface may affect rollback. The more posterior the tibial component is placed, the greater the capacity for posterior femoral translation, which would have a beneficial effect on flexion (Li, Most et al. 2004). Position (Walker and Garg 1991) and rotation (Berger, Crossett et al. 1998) of the femoral component have also been shown to influence flexion. Callaghan et al. warned against placing the femoral component in flexion or the tibia in excessive posterior slope as this may cause anterior impingement in PCL-substituting designs (Callaghan, O'Rourke et al. 2002).

The normal tibia has a natural posterior slope of approximately 10° (Kuwano, Urabe et al. 2005). Many TKAs are designed so that the tibia is cut with a posterior slope (usually between 3° and 10°). Failure to appreciate the posterior tibial slope may result in a tight flexion gap, which will limit flexion.

Conversely, an excessive posterior slope may also result in flexion gap laxity, which may lead to flexion instability and failure of the TKA (Walker and Garg 1991; Singerman, Dean et al. 1996). Catani et al. reported a mild to moderate correlation between maximum knee flexion and tibial slope during chair rising/sitting and step up/down activities (Catani, Fantozzi et al. 2006). However, many studies have failed to find a correlation between tibial slope and ROM (Kotani, Yonekura et al. 2005)

The flexion angle of the knee during closure has been considered to be another factor that can affect the ultimate range of motion of a knee. Emerson et al. (Emerson, Ayers et al. 1996; Emerson, Ayers et al. 1999) have reported that knees closed in 90-110° degrees of flexion have significantly more flexion (118°) compared to knees closed in extension (113°) at one-year follow-up. However, another study (Masri, Laskin et al. 1996) failed to show any benefit of capsular closure in flexion in relation to early post-operative rehabilitation at three months.

2.1.3 Postoperative Factors

Post-operative factors have been examined closely to determine the effect on the ultimate range of motion after TKA. Numerous articles have looked at post-operative rehabilitation as a means of optimizing flexion. Two factors that have been investigated are the use of a continuous passive motion device (Leach, Reid et al. 2006) and quadriceps strengthening regimes (Silva, Shepherd et al. 2003; Moffet, Collet et al. 2004; Mizner, Petterson et al. 2005). Several prospective, clinical trials have failed to show the effect of rehabilitation in optimizing the ultimate range of motion (Fox and Poss 1981; Romness and Rand 1988; Kumar, McPherson et al. 1996; Pope, Corcoran et al. 1997; Chen, Zimmerman et al. 2000; MacDonald, Bourne et al. 2000; Teeny, York et al. 2005; Leach, Reid et al. 2006).

2.2 Methods of Investigation

Numerous researchers have investigated the function of the knee after total knee arthroplasty, and they have done so using several different techniques. These techniques are reviewed here in four categories: Clinical, In-vitro, Computational, and In-vivo.

2.2.1 Clinical Methods

Several methods have been used to explore knee function following total knee arthroplasty. These methods can be broken down into four categories. The first is Clinical, referring to methods based on tools commonly available in a clinical setting, such as goniometers or surveys. Most studies of TKA function fall into this category because the methodology is typically easy to implement and can be performed on large numbers of subjects relatively quickly. Clinical studies often record outcomes, such as range of motion, knee scores, or survivorship (Anouchi, McShane et al. 1996; Lizaur, Marco et al. 1997; Finch, Walsh et al. 1998; March, Cross et al. 1999; Robertsson, Dunbar et al. 2000; Bachmeier, March et al. 2001; Kawamura and Bourne 2001; Weale, Halabi et al. 2001; Mahomed, Liang et al. 2002; Yamazaki, Ishigami et al. 2002; Ritter, Harty et al. 2003; Aglietti, Baldini et al. 2005; Bertin 2005; Huang, Su et al. 2005; Kim, Sohn et al. 2005; Kotani, Yonekura et al. 2005; Seon, Song et al. 2005; Evans, Parsons et al. 2006; Gupta, Ranawat et al. 2006; Jones 2006; Sathappan, Wasserman et al. 2006; Bin and Nam 2007). Examples of the power of clinical studies are papers by Miner et al. and Ritter et al., which include data from almost 700 knees and over 4700 knees, respectively (Miner, Lingard et al. 2003; Ritter, Harty et al. 2003). While these methods can be used to collect a vast amount of data, they often lack valuable information about the mechanics of the knee joint, making it difficult to draw ways of improving patient function from the results.

2.2.2 In-vitro Methods

The second category of methods is In-vitro. Cadaveric studies of total knee arthroplasty have been performed with various mechanical systems (Whiteside, Kasselt et al. 1987; Anouchi, Whiteside et al. 1993; Luger, Sathasivam et al. 1997; Singerman, Pagan et al. 1997; Zavatsky 1997; Miller, Goodfellow et al. 1998; Weale, Feikes et al. 2002; Browne, Hermida et al. 2005; Patil, Colwell et al. 2005; Werner, Ayers et al. 2005). Add Greenwald to list One system that has been used extensively is the Oxford Rig (Zavatsky 1997; Miller, Goodfellow et al. 1998; Weale, Feikes et al. 2002; Walker and Haider 2003; Browne, Hermida et al. 2005; Patil, Colwell et al. 2005). The rig was designed to simulate a chair rise or step up activity. A vertical load is applied at the simulated hip joint, which is free to rotate as well as translate vertically. The quadriceps tendon is attached to a force transducer, and the force applied to the tendon can be manipulated to flex, extend, or stabilize the knee. The simulated ankle joint is free to rotate but is fixed in translation. An optical tracking system is sometimes used in conjunction with the rig to obtain knee kinematics with flexion. This system is particularly useful for investigating patellofemoral kinematics (Miller, Murray et al. 1997; Browne, Hermida et al. 2005).

The Bioengineering Laboratory has been conducting in-vitro studies for quite some time using a robotic testing system (Most 2000; Li, Zayontz et al. 2001; Li, Most et al. 2002; Li, Schule et al. 2003; Most, Li et al. 2003; Most, Zayontz et al. 2003; Li, Most et al. 2004; Li, Zayontz et al. 2004; Suggs, Li et al. 2004; Suggs, Li et al. 2006). This system can be operated in force control or displacement control mode, and various loading conditions can be applied to the knee, including quadriceps and hamstrings loads. A testing protocol can be applied repeatedly to the same knee specimen in multiple states (e.g. intact, injured, reconstructed). This system has been used to explore the affect of various factors, such as retaining or substituting the posterior cruciate ligament and or using a mobile bearing instead of a fixed bearing implant, on TKA kinematics.

The advantages in-vitro investigations include the potential for tight control of the experimental environment and an increased range of protocols that can be performed on cadaveric specimens compared to what can be done to living subjects. While these techniques allow researchers to observe the mechanics of

TKA implants, the major disadvantage is the difficulty in relating the experimental conditions to physiological conditions.

2.2.3 Computational Methods

Computational models can be a relatively quick and inexpensive way to explore the effects of design and loading modifications on TKA function. Delp et al. used a two-dimensional model to analyze design parameters that affect the possibility of dislocation in PCL-substituting TKA (Delp, Kocmond et al. 1995; Kocmond, Delp et al. 1995; Piazza, Delp et al. 1998). Two-dimensional models have also been used to investigate wear of the polyethylene in TKA (Wimmer and Andriacchi 1997; Godest, de Cloke et al. 2000). Several groups have developed more sophisticated three-dimensional models (Bartel, Bicknell et al. 1986; Sathasivam and Walker 1997; D'Lima, Chen et al. 2001; Piazza and Delp 2001; D'Lima, Chen et al. 2003; Fregly, Bei et al. 2003; Fregly, Sawyer et al. 2005; Guess and Maletsky 2005; Guess and Maletsky 2005; Halloran, Petrella et al. 2005; Laz, Pal et al. 2006; Laz, Pal et al. 2006; Rawlinson, Furman et al. 2006; Huang, Liau et al. 2007; Knight, Pal et al. 2007). Most of these studies are also focused on polyethylene wear. The weakness of the computational approach has been the appropriateness of the boundary conditions applied to the model. Either the model inputs have been based on data from knee simulators or inputs for some degrees of freedom have been derived from in-vivo data while the other degrees of freedom were left unconstrained. Thus, there is a question as to how well the modeled environment represents truly in-vivo conditions, which in turn creates some uncertainty in the conclusions drawn from these studies.

2.2.4 In-vivo Methods

The final category, acquiring in-vivo data on the mechanics of the knee after TKA, is the ideal mode of investigating TKA function. However, acquiring in-vivo data in an ethical manner can be a challenge. A few research groups have developed instrumented, telemetric TKA components that measure in-vivo forces once implanted in a patient (Foster, Werner et al. 1980; Kaufman, Kovacevic et al. 1996; Taylor, Walker et al. 1998; Morris, D'Lima et al. 2001; Taylor and Walker 2001; D'Lima, Patil et al. 2005; Kirking, Krevolin et al. 2006). The use of telemetry to measure forces across the knee joint was first introduced by Foster et al. (Foster, Werner et al. 1980), but two other groups have been more prolific in their used of the method. Taylor and Walker have used an instrumented femoral component to measure axial forces, torque, and bending moments in the distal femur (Taylor, Walker et al. 1998; Taylor and Walker 2001). The group led by Colwell has used an instrumented tibia instead of a femur (Kaufman, Kovacevic et al. 1996; Morris, D'Lima et al. 2001; D'Lima, Patil et al. 2005; D'Lima, Townsend et al. 2005; D'Lima, Patil et al. 2006; Kirking, Krevolin et al. 2006). Both groups report forces during activities, such as walking and stair ascent, with peak forces reaching over 3 times body-weight. While this information is invaluable in efforts to improve TKA designs, this method has been used on very few patients (published data has come from only 3 patients), limiting its application to the general patient population.

Knowing the in-vivo kinematics of the knee after TKA is also very important in assessing TKA function, and gait analysis was one of the first techniques used to measure TKA kinematics (Rittman, Kettelkamp et al. 1981; Andriacchi, Galante et al. 1982; Jevsevar, Riley et al. 1993; Wilson, McCann et al. 1996; Kramers-de Quervain, Stussi et al. 1997; Andriacchi, Dyrby et al. 2003Bolanos, 1998 #271; Nagura, Otani et al. 2005). Gait analysis uses skin markers to estimate the motion of the underlying bones. While this method can be used to measure kinematics for a wide variety of activities over a large spatial region, there is intrinsic error in the results due to relative motion between the skin and bones of interest. Another method of obtaining in-vivo kinematics is Roentgen Stereophotogrammetric Analysis (RSA) (Nilsson, Karrholm et al. 1990; Nilsson, Karrholm et al. 1991; Karrholm, Jonsson et al. 1994; Uvehammer, Karrholm et al. 2000). RSA alleviates the problem of relative motion between the markers and the bones by placing the markers inside the bones and tracking them radiographically. Despite its increased accuracy, this method is quite invasive, especially for control subjects, due to the need to implant markers.

Single-plane fluoroscopy has been used for over a decade to investigate in-vivo TKA kinematics (Yamazaki, Watanabe et al. 2005; Catani, Fantozzi et al. 2006; Fantozzi, Catani et al. 2006). Banks has been one of the pioneers in matching three-dimensional CAD models of implants to two-dimensional fluoroscopic images to calculate in-vivo kinematics (Banks and Hodge 1996;

Banks, Markovich et al. 1997; Harman, Markovich et al. 1998; Bellemans, Banks et al. 2002; Banks, Bellemans et al. 2003; Banks, Harman et al. 2003; Incavo, Mullins et al. 2004; Banks, Fregly et al. 2005; Fregly, Sawyer et al. 2005; Victor, Banks et al. 2005; Moro-Oka, Muenchinger et al. 2006; Coughlin, Incavo et al. 2007; Zhao, Banks et al. 2007). He developed an algorithm that used a library of pre-calculated implant profiles to increase the efficiency of the matching process. Initial tests reported in-plane accuracies of 0.5 mm and 0.3° for translation and rotation, respectively. However out-of-plane accuracies were up to 8.3 mm and 1.9°, respectively.

Dennis and Komistek have also based much of their research on the use of single-plane fluoroscopy (Stiehl, Komistek et al. 1995; Dennis, Komistek et al. 1996; Dennis, Komistek et al. 1998; Dennis, Komistek et al. 1998; Hoff, Komistek et al. 1998; Stiehl, Komistek et al. 2000; Dennis, Komistek et al. 2001; Argenson, Komistek et al. 2002; Bertin, Komistek et al. 2002; Komistek, Allain et al. 2002; Dennis, Komistek et al. 2003; Mahfouz, Hoff et al. 2003; Argenson, Komistek et al. 2004; Dennis, Komistek et al. 2004; Komistek, Dennis et al. 2004; Argenson, Scuderi et al. 2005; Komistek, Kane et al. 2005; Lee, Matsui et al. 2005; Mahfouz, Hoff et al. 2005; Sugita, Sato et al. 2005; Yoshiya, Matsui et al. 2005). Initially, their groups methodology also used a library of pre-calculated implant silhouettes to match to the fluoroscopic images, but they later began generating simulated images of the implant models to compare to the actual fluoroscopic images (Mahfouz, Hoff et al. 2003). The technique eliminated the need for image segmentation, which they believed introduced error into the analysis. However, they reported in-plane translation accuracy of 0.65 mm, out-of-plane translation accuracy of 3.2 mm, and rotational accuracy of 1.5°, which are very similar to the accuracy values reported by Banks.

These single-plane fluoroscopic techniques have been used extensively to evaluate differences in TKA designs, such as PCL-retaining versus PCL-substituting or fixed-bearing versus mobile bearing. They are relatively accurate compared to gait analysis and less invasive than RSA. However, useful data from these studies is limited to in-plane kinematics. Certainly, sagittal plane kinematics are very important, but in order to investigate topics such as the relationship between contact patterns and wear or the ability of total knee arthroplasty to truly restore healthy knee function all six degrees of freedom need to be assessed.

A wealth of information concerning the function of the knee after total knee arthroplasty has been accrued using all of these Clinical, In-vitro, Computational, and In-vivo methods. This information has resulted in some improvement in TKA function, including ROM and survorship, over the earliest knee arthroplasty implants. However, knee function after TKA is still limited compared to otherwise healthy knees, and there has been no improvement in TKA function over the past couple of decades, suggesting that there are still some underlying biomechanical factors that are limiting patients after total knee arthroplasty. We believe that in order to decipher these factors, we need a robust, relatively non-invasive tool that is accurate in all degrees of freedom.

Chapter 3. Investigation of Six Degree of Freedom Kinematics Using Dual Fluoroscopic Imaging System

3.1 Introduction

Recent studies have used fluoroscopy to investigate *in vivo* total knee arthroplasty (TKA) kinematics due to its accessibility and low radiation dosage (Banks and Hodge 1996; Zuffi, Leardini et al. 1999; Dennis, Komistek et al. 2003; Mahfouz, Hoff et al. 2003; Watanabe, Yamazaki et al. 2004). In these studies, a single sagittal image of the knee was taken with a fluoroscope. Kinematics were then derived by matching a 3D model of the TKA to the 2D fluoroscopic image. While 3D model matching can theoretically be achieved using a single image, studies have found that the use of just a single image may not result in the same accuracy in the out-of-plane degrees-of-freedom (DOF) compared to the in-plane motion (Li, Wuerz et al. 2004; Fregly, Rahman et al. 2005). These studies usually reported anteroposterior motion of the tibiofemoral contact in the medial and lateral compartments. Currently, determination of TKA kinematics in 6DOF still presents a challenge in the field of biomechanics.

Recently, Li et al. acquired orthogonal fluoroscopic images using a single 3D fluoroscope to quantify *in vivo* kinematics of a normal knee during a quasi-static single leg lunge (Li, Wuerz et al. 2004). Using sphere and cylinder models, the study showed that translation and rotation errors were within 0.1 mm and 0.1°, respectively, for all DOF. The study of Li et al. suggests that a biplane fluoroscopic technique has an advantage over a single plane technique due to the ability to detect out-of-plane translation and rotation. Thus far, no study has reported the application of fluoroscopic biplanar matching to the kinematic analysis of TKA.

In this chapter, the repeatability and accuracy of measuring TKA position and orientation using the fluoroscopic system were evaluated. A parametric study was also performed to quantify the differences between using the dual fluoroscopic system and a single image fluoroscopic technique to image complex geometry such as TKA components.

3.2 Methodology

3.2.1 Dual orthogonal fluoroscopic system setup

Two fluoroscopes were positioned in such a way that the two image intensifiers were perpendicular to each other (Fig. 3.1). The knee joint was positioned in front of the two image intensifiers and imaged simultaneously by the fluoroscopes in order to acquire orthogonal images of the knee from the posteromedial and posterolateral directions.

A 3D modeling program (Rhinoceros®, Robert McNeel & Associates, Seattle, WA) was used in order to replicate the dual orthogonal fluoroscopic system in a computer (Fig. 3.2A). The source of each fluoroscope was represented in the modeling program by a perspective projection camera, and each intensifier was represented by a drawing plane. The virtual fluoroscopes were placed in the same relative position as the actual fluoroscopes during image acquisition. The image from each fluoroscope was then placed at the calculated intensifier location. Three dimensional computer aided design (CAD) models of the TKA components (supplied by the manufacturer) were then imported into the modeling program and matched to the fluoroscopic images.

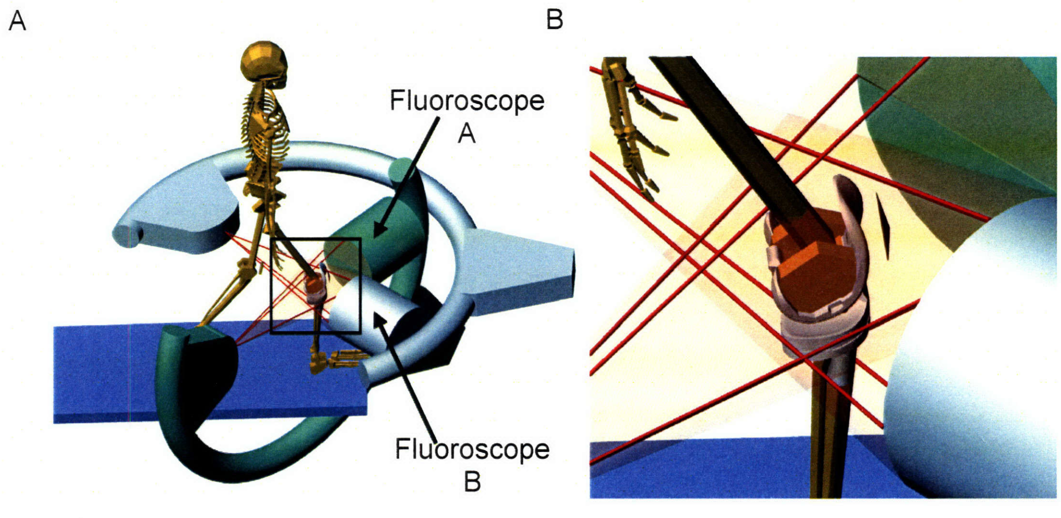

Fig. 3.1 A) The knee joint in view of the dual orthogonal fluoroscopic system **B)** a close-up of the TKA.

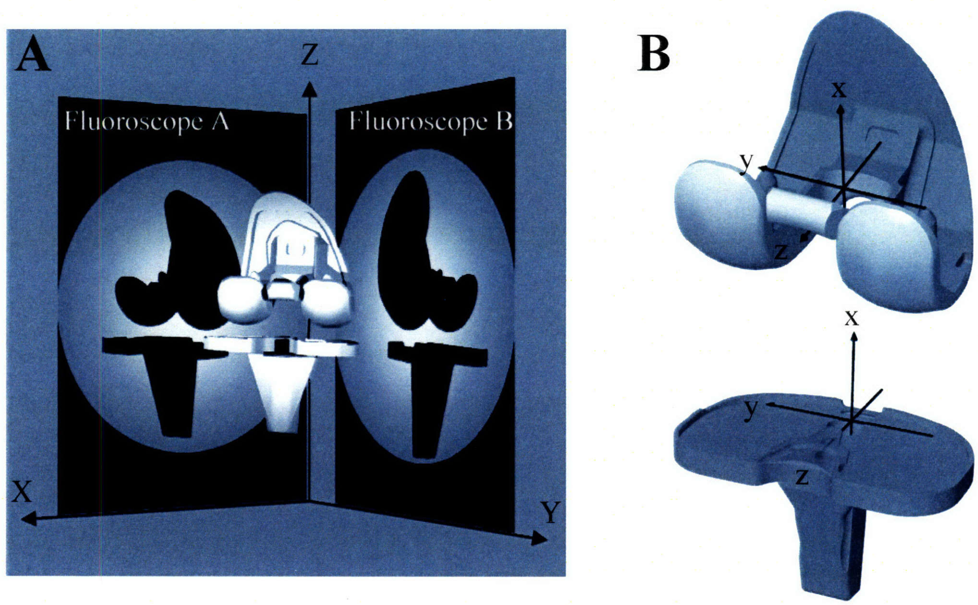

Fig. 3.2 A) Virtual setup of the dual orthogonal imaging system in which the TKA components are in view of both Fluoroscopes A and B and **B)** Femoral and tibial coordinate systems.

During the matching process, the component models of the TKA were translated and rotated independently in the software. The 3D modeling software allowed the observer to view all translational and rotational manipulations of the model components instantaneously and simultaneously from both perspectives (from the two fluoroscope sources). The software also allowed the model to be translated and rotated in increments of less than 0.01 mm and 0.01°, respectively. The tibial and polyethylene components were treated as one assembled piece, but the polyethylene could be hidden for an unobstructed view of the tibial silhouette during the matching process. The geometry of the polyethylene insert was not used in the matching process, since it was not discernibly visible under fluoroscopy. The 3D models were considered "matched" when the model, as viewed from both respective virtual sources, overlapped its silhouette on the fluoroscopic images.

3.2.2 Repeatability of 3D matching using the dual orthogonal fluoroscopic system

The dual orthogonal fluoroscopic system was tested in order to assess the ability of the observer to repeatedly reproduce the same position and orientation of the *in vivo* TKA components over the course of multiple trials. Two patients (under IRB approval), one with cruciate retaining and the other with posterior substituting TKA (NexGen® CR and NexGen® LPS, Zimmer, Warsaw IN), were asked to flex their knee to a random position within view of both fluoroscopes during image acquisition (Fig. 3.1). Three-dimensional CAD models of the components were then matched 15 times to the corresponding orthogonal images using the 3D modeling program. For each trial, the components were introduced in a random manner that in no way resembled the correct position and orientation. Each component was manually manipulated in 6DOF and matched to the silhouettes on both intensifiers simultaneously.

The position and orientation of the components were determined by the position and orientation of their local coordinate systems (defined by geometric landmarks on the 3D component models) in a global coordinate system (X, Y, Z in Fig 3.2A). The y-axis (flexion/extension axis) of the femoral component was defined as a line connecting the tips of the pegs (Fig. 3.2B). The x-axis (internal/external axis) was defined as a line parallel to the pegs and perpendicular to the y-axis placed at the midpoint of the y-axis. The z-axis (varus/valgus axis) was defined as the cross product of the x- and y-axes. The z-axis of the tibial component was defined as the line of symmetry on the base of the polyethylene. The y-axis of the tibial component was defined as a line connecting two landmarks on the polyethylene base and was perpendicular to the z-axis (Fig. 3.2B). The x-axis was defined as the cross product of the y- and z-axes. The positions of the femoral and tibial components were reported as the location of the component origins in a global coordinate system. Component rotations were reported as the rotation of the local coordinate system referenced to the global coordinate system using Eulerian angles assuming a y-z-x rotation sequence. The repeatability of the matching procedure was determined by the variation (measured using standard deviation) of the component positions determined from the 15 independent trials.

3.2.3 Accuracy of 3D matching using the dual orthogonal fluoroscopic system

To assess the accuracy of the matching process of the TKA components using the orthogonal images, the true position of the TKA components had to be known. Since the true position of in-vivo TKA is unknown, an idealized testing condition was used. To do this, the component models were placed in known positions within the virtual imaging system (Fig. 3.2A). These known positions were defined as the Gold Standard. The Gold Standard was synthetically imaged at full extension using the two virtual fluoroscopes, and the components were then matched to the synthetic images 15 times in the same fashion as in the repeatability test. The accuracy of the matching method was determined by comparing the position and orientation of the matched TKA to the Gold Standard.

3.2.4 Out-of-plane parametric study of the single plane imaging technique

The sensitivity to out-of-plane motion when using a single plane image to determine joint position was evaluated with the dual orthogonal fluoroscopic system, since single image techniques have been widely used for joint kinematics measurement (Banks and Hodge 1996; Zuffi, Leardini et al. 1999; Dennis, Komistek et al. 2003; Mahfouz, Hoff et al. 2003; Watanabe, Yamazaki et al. 2004; Fregly, Rahman et al. 2005). A parametric test was performed to determine the effect of out-of-plane translation on in-plane projection using the 3D model of the femoral TKA component. Four points on the component surface (top, bottom, left and right) were chosen in order to quantitatively track the changes in the component projection on the intensifier (Fig. 3.3A). The bottom and left points were close to the image center, while the top and right points were close to the edge of the image. The femoral component was translated 10 mm in the normal direction away from the intensifier plate in 1 mm increments. After each incremental out-of-plane translation, the points were projected onto the in-plane intensifier, and the projected positions were measured as the sensitivity of component projection to out-of-plane motion.

A

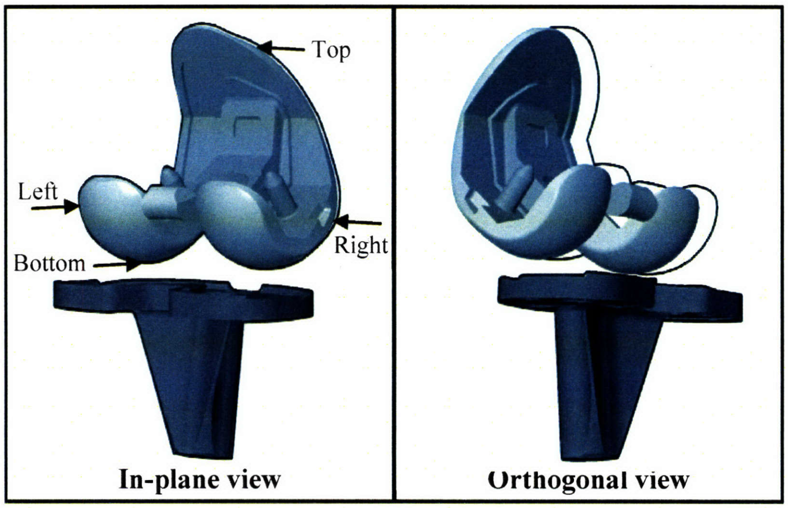

B

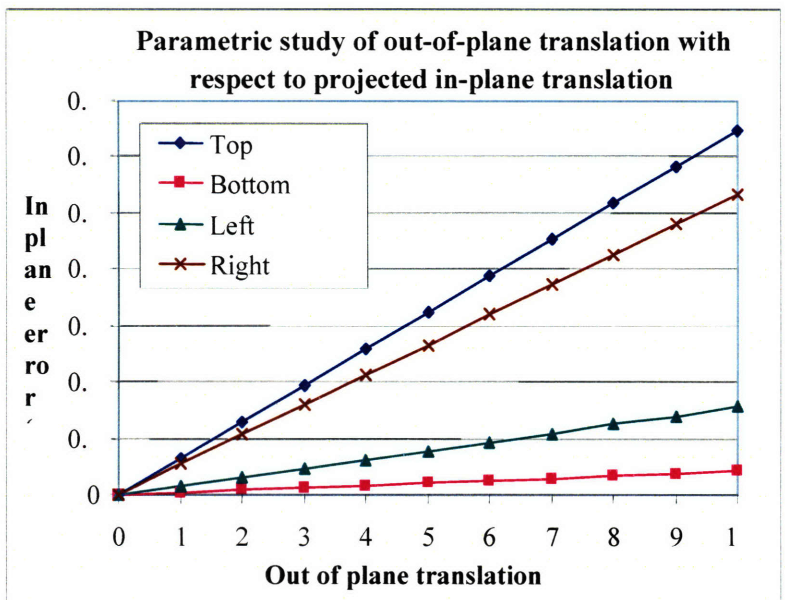

Fig. 3.3 A) A schematic diagram showing the sensitivity of out-of-plane error to in-plane accuracy. **B)** Effects of projected distance on out-of-plane translation in which four points (top, bottom, left and right) as seen in Fig. 1.3A were tracked throughout a 10 mm range of out-of-plane translation.

3.3 Results

3.3.1 Repeatability Test

The matching process of the dual orthogonal fluoroscopic system was highly repeatable in determining the 6DOF positions and orientations for both the CR and PS TKA components (Table 3.1). All positions and orientations for the repeatability test are reported with respect to the X-, Y- and Z-axes of the global coordinate system. For the CR TKA, the mean femoral position was 111.18 ± 0.09 mm, 182.67 ± 0.07 mm and 137.34 ± 0.07 mm along the X-, Y- and Z-axes, respectively. The mean tibial position was 102.62 ± 0.05 mm, 186.27 ± 0.16 mm and 102.21 ± 0.10 mm, respectively. The mean femoral orientation (assuming a y-z-x rotation sequence) was -51.082° ± 0.45°, 2.05° ± 0.35° and 179.84° ± 0.15°, respectively. The mean tibial orientation was -94.74° ± 0.13°, -8.04° ± 0.50°, -177.87° ± 0.12°, respectively.

For the PS TKA, the mean femoral position was 147.52 ± 0.12 mm, 209.00 ± 0.13 mm and 215.95 ± 0.07 mm along the X-, Y- and Z-axes, respectively. The mean tibial position was 140.14 ± 0.11 mm, 191.04 ± 0.12 mm and 185.55 ± 0.14 mm, respectively. The mean femoral orientation was -95.42° ± 0.50°, -61.68° ± 0.56° and -166.12° ± 0.33°, respectively. The mean tibial orientation was -97.03° ± 0.26°, -56.97° ± 0.44° and -167.73° ± 0.21°, respectively.

Repeatability and Accuracy of Femoral and Tibial Component Placement

	Trial	X	Y	Z	Rot X	Rot Y	Rot Z
Femur	SD, CR	111.178 ± 0.094	182.673 ± 0.067	137.340 ± 0.070	179.844° ± 0.146°	-51.082° ± 0.446°	2.048° ± 0.354°
	RMS, CR	0.091	0.065	0.068	0.141°	0.431°	0.342°
	SD, PS	147.521 ± 0.117	208.999 ± 0.126	215.948 ± 0.074	-166.121° ± 0.325°	-95.417° ± 0.504°	-61.681° ± 0.561°
	RMS, PS	0.113	0.122	0.071	0.314°	0.487°	0.542°
	Error ± SD	0.044 ± 0.094	0.041 ± 0.068	0.015 ± 0.109	0.230° ± 0.146°	0.146° ± 0.135°	0.076° ± 0.339°
	RMS Error	0.101	0.078	0.107	0.270°	0.196°	0.336°
Tibia	SD, CR	102.616 ± 0.050	186.273 ± 0.164	102.212 ± 0.100	-177.870° ± 0.120°	-94.744° ± 0.133°	-8.038° ± 0.501°
	RMS, CR	0.048	0.159	0.096	0.116°	0.129°	0.484°
	SD, PS	140.135 ± 0.111	191.041 ± 0.124	185.548 ± 0.141	-167.732° ± 0.214°	-97.034° ± 0.259°	-56.971° ± 0.443°
	RMS, PS	0.108	0.120	0.136	0.206°	0.250°	0.428°
	Error ± SD	-0.014 ± 0.050	-0.113 ± 0.103	0.006 ± 0.065	0.086° ± 0.081°	0.108° ± 0.077°	0.184° ± 0.475°
	RMS Error	0.050	0.150	0.064	0.116°	0.131°	0.494°

Table 3.1: Position and orientation results from the repeatability study are reported as the mean ± SD and Root Mean Square (RMS) for each of the imaged positions. Two TKA components were used (indicated as "CR" and "PS" in the table). Error mean ± SD and RMS of the error are reported for the accuracy study.

3.3.2 Accuracy Test

The matching process showed a high accuracy in the determination of the femoral and tibial component position and orientation in 3D space over 15 trials (Table 3.1). For the accuracy test, all positions are reported with respect to the global coordinate system and orientations are reported with respect to the Gold Standard coordinate system. The mean errors in femoral position when compared to the Gold Standard were 0.04 ± 0.09 mm (mean error ± SD), 0.04 ± 0.07 mm, and 0.02 ± 0.11 mm along the global X-, Y- and Z-axes, respectively. The mean errors of the tibial position were -0.01 ± 0.05 mm, -0.11 ± 0.10 mm and 0.01 ± 0.07 mm, respectively. The mean errors in femoral orientation were 0.15 ± 0.14°, 0.08 ± 0.34° and 0.23 ± 0.15°, assuming a y-z-x rotation sequence. The tibial orientation error was 0.11 ± 0.08°, 0.18 ± 0.48° and 0.09 ± 0.08°, respectively.

3.3.3 Parametric Test

When a single image was used to determine the TKA position, component projection was not sensitive to the component position in the out-of-plane direction of the intensifier (Fig. 3.3A & B). For out-of-plane motion of 1 mm, the top and bottom points translated only 0.066 mm and 0.004 mm, respectively in the plane. For out-of-plane motion of 5 mm, the in-plane motion was only 0.324 mm and 0.021 mm for the top and bottom points, respectively. When the femoral component was translated 10 mm in the out-of-plane direction, the top point moved 0.649 mm, while the bottom point moved only 0.042 mm.

3.4 Discussion

This study investigated the ability to repeatably and accurately match a TKA component model to biplanar fluoroscopic images in 6DOF using the dual orthogonal fluoroscopic system and then used this system to investigate 6DOF kinematics of TKA patients during a weight-bearing single leg lunge. In this methodology, 3D models of the TKA components were matched to two orthogonal images simultaneously to determine the positions and orientations of the TKA components. In the repeatability test, femoral and tibial translations had a standard deviation (SD) less than 0.17 mm in all directions for both the CR and PS components. Femoral and tibial rotations had SD less than 0.57° about all three axes. The low SD indicates that the observer can reliably reproduce the same position with orthogonal fluoroscopic images using a manual matching process.

The accuracy test reported the error of the matching process with respect to the known position of a synthetically imaged TKA component set (Gold Standard). With the exception of the tibial y-axis, all mean position errors and SD for both components were less than 0.05 mm and 0.11 mm, respectively. The positional error of the tibial component in the y-direction was -0.11 ± 0.10 mm. Mean rotation errors and SD were all less than 0.24° and 0.48°, respectively. In general, the accuracy and repeatability studies showed similar variations in the data with SD variation within the repeatability study being slightly higher than that found in the accuracy study. This may be due, in part, to the fact that the repeatability test used actual fluoroscopic images of TKA components and included system noise, while the accuracy test used synthetic images of 3D models created in an ideal environment. Another source of error in the repeatability test may be geometric differences between the 3D models and the actual machined TKA components (Kaptein, Valstar et al. 2003).

Previous studies have employed a single plane system in order to determine *in vivo* TKA kinematics. These methodologies have reported acceptable accuracy in the anteroposterior (in-plane) direction. Investigators have performed computer simulations similar to the accuracy test presented in this study and have reported in-plane errors ranging from -0.073 ± 0.136 mm to -0.37 ± 0.22 mm (Banks and Hodge 1996; Zuffi, Leardini et al. 1999; Mahfouz, Hoff et al. 2003). However, due to the limitations of the single plane system, mediolateral (out-of-plane) accuracy was compromised. The aforementioned studies reported mean out-of-plane errors of 0.021 ± 1.395, 1.054 ± 3.031 mm and 1.91 ± 0.27 mm. In a more recent study, computed tomography (CT) 3D knee models were matched to synthetic fluoroscopic images (Fregly, Rahman et al. 2005). That study reported femoral root-mean-square errors of 0.35 mm and 0.25 mm for in-plane position and 8.4 mm for out-of-plane position.

The parametric test of this study indicates that an out-of-plane translation error of 5 mm can occur with in-plane accuracy ranging between 0.021 mm to 0.324 mm depending on the location of the object on the fluoroscopic images (Fig. 1.3B). Using the four tracking points, the in-plane projection of the femoral component showed a linear relation with respect to the out-of-plane motion of the femoral component. The closer the edge of the matched component is to the image center, the less sensitive the matching will be at that edge with respect to out-of-plane motion. Since fluoroscopic resolution is typically between 0.3 and 0.5 mm, it would be difficult to detect out-of-plane translations on the order of 5 mm using only a single image (Li, Wuerz et al. 2004). However, motion of the projected points that would not be discernable in the in-plane projection would be easily detected using an orthogonal image as demonstrated by the dual orthogonal imaging system (Fig. 3.3B).

Previous investigators have utilized biplanar radiographic matching techniques (Lavallee and Szeliski 1995; Penney, Weese et al. 1998; Asano, Akagi et al. 2001; You, Siy et al. 2001; Kaptein, Valstar et al. 2003). Kaptein et al. implemented the use of 3D models of TKA implants with roentgen stereophotogrammetric analysis (RSA) in order to measure three-dimensional motion. However, this technique involves the application of high dose x-rays.

Both Asano et al. and You et al. developed methods of matching models of healthy knees constructed from CT data to biplanar x-ray images, and also require a high dosage x-ray scanner. Compared with previous techniques, the dual orthogonal fluoroscopic technique presents a non-invasive, low dose radiation methodology that eliminates the increased out-of-plane error encountered in single plane imaging and has the potential for investigating dynamic joint motion.

As previously noted, a possible limitation observed with the image matching method was that there might be geometrical differences between the 3D model provided by the component manufacturer and the imaged component due to the machining tolerances. It is suspected that some of the error in matching may be a result of these differences (Zuffi, Leardini et al. 1999; Kaptein, Valstar et al. 2003). The manual matching of each component is rather labor-intensive (approximately 10 to 15 minutes per component), and, as a result, efforts are underway to create an automated matching procedure. Another limitation common to all in vivo kinematic studies is the difficulty in evaluating the system accuracy, since accurate in-vivo TKA position is not known *a priori*. Therefore, an idealized testing was used in this study to determine the accuracy of the matching process in measuring the 6DOF TKA position in 3D space. This accuracy evaluation did not include the effect of all the sources of error in the entire system. However, the fact that the repeatability of the matching using in-vivo fluoroscopic images is similar to the repeatability of the matching process in the idealized environment suggests that the accuracy is also similar.

In summary, the dual orthogonal fluoroscopic system provides an easy and powerful tool for accurately determining 6DOF positions of TKA components in 3D space. This method has been shown to be highly repeatable and able to determine 6DOF kinematics of TKA patients. The advantages of the dual orthogonal fluoroscopic system are that it is sensitive to position and orientation in all DOF, has low radiation dosage, and can be constructed using any pair of readily available fluoroscopes.

Chapter 4. Kinematics of a Cruciate-Retaining Total Knee Arthroplasty

4.1 Introduction

Many studies have reported in-vivo knee kinematics after total knee arthroplasty and have reported inconsistent data on in-vivo motion (Stiehl, Komistek et al. 1995; Dennis, Komistek et al. 1996; Banks, Markovich et al. 1997; Kim, Pelker et al. 1997; Dennis, Komistek et al. 1998; Matsuda, Miura et al. 1999; Stiehl, Komistek et al. 2000; Bertin, Komistek et al. 2002). Matsuda et al. (Matsuda, Miura et al. 1999) measured the anteroposterior laxity of a posterior cruciate ligament-retaining total knee arthroplasty (Miller-Galante 1, Zimmer) in 19 knees using a KT-2000 arthrometer and found inconsistent anteroposterior stability in flexion. Stiehl et al. (Stiehl, Komistek et al. 1995; Stiehl, Komistek et al. 2000) studied a variety of posterior cruciate ligament-retaining knee designs (Porous Coated Anatomic, Howmedica; Ortholoc, Wright Medical Technology; Genesis, Richards; Anatomic Modular Knee, DePuy; Miller-Galante II, Zimmer) using a single plane fluoroscopic technique and found that physiological rollback of the femur was not demonstrated in patients after posterior cruciate ligament-retaining arthroplasty. Similar results were also observed by Kim et al. (Kim, Pelker et al. 1997) with posterior cruciate ligament-retaining designs (Genesis, Richards). One study by Dennis et al. (Dennis, Komistek et al. 1996) found abnormal femoral translation during deep knee-bends in patients after posterior cruciate ligament-retaining arthroplasty (Press-Fit Condylar Designs, Johnson & Johnson) while patients exhibited more normal femoral translation after posterior stabilized arthroplasty. Furthermore, Dennis et al. (Dennis, Komistek et al. 1998) demonstrated that posterior cruciate ligament-retaining design has a range of motion similar to posterior cruciate ligament-substituting design during passive flexion but a decreased range of motion during squatting. Using a similar fluoroscopic technique, however, Banks et al. (Banks, Markovich et al. 1997) found that the range of axial tibial rotation and condylar translation for posterior cruciate ligament-retaining total knee arthroplasty (AMK, DePuy) was similar to the range reported for normal and anterior cruciate ligament deficient knees during a step-up maneuver. Bertin et al. (Bertin, Komistek et al. 2002) found that posterior femoral rollback was reproduced in the posterior cruciate ligament-retaining design (NexGen, Zimmer) and that, on average, patients exhibited internal tibial rotation but with lower magnitude compared to that of the normal knee (Li, Wuerz et al. 2004).

The capability of a posterior cruciate ligament-retaining arthroplasty to restore normal knee kinematics and function remains controversial. All previous investigations have reported tibiofemoral contact kinematics along the anteroposterior direction. No data has been reported on the actual articular contact locations on the three-dimensional tibial plateau surfaces. This information is critical for understanding the biomechanical function of the implant in-vivo and for an explanation of wear pattern and failure mechanisms of the polyethylene insert. Recently, a dual-orthogonal fluoroscopic imaging technique has been introduced as a research tool for the study of in-vivo musculoskeletal joint biomechanics (Li, Wuerz et al. 2004). This technique can accurately determine the 6 degrees-of-freedom kinematics of in-vivo knee joint motion (DeFrate, Sun et al. 2004; Li, DeFrate et al. 2005; Hanson, Suggs et al. 2006). Given the 6 degrees-of-freedom position of the femoral and tibial implant components, the articular contact on the polyethylene insert can be examined.

In this study, we applied this imaging technique to determine the in-vivo 6DOF kinematics and contact locations on the tibial articulating surface of a posterior cruciate ligament-retaining total knee arthroplasty design during weight-bearing flexion activity of the knee. The objective of this study was to determine the contact points on the three-dimensional tibial component articulating surface in both the anteroposterior and mediolateral directions and to compare the contact data of the component design to that of normal knees under the same weight-bearing motion (Li, DeFrate et al. 2005).

4.2 Materials and Methods

4.2.1 Experimental Setup

Twelve patients (1 female, 11 male, at least 6 months post surgery) were randomly recruited among patients after cruciate-retaining total knee arthroplasty using a single design (NexGen CR, Zimmer, Table 4.1). All patients were operated on by the same surgeon and evaluated as clinically successful after surgery with no pain during normal function. A consent form approved by the authors' Institution Review Board was signed by each subject before testing. The subject performed a single leg lunge from 0° to maximal flexion while two orthogonally positioned 12 inch fluoroscopes (GE Medical, Milwaukee, WI) were used to simultaneously image the knee under weight-bearing conditions in 15° intervals from the posteromedial and posterolateral directions (Fig. 4.1).

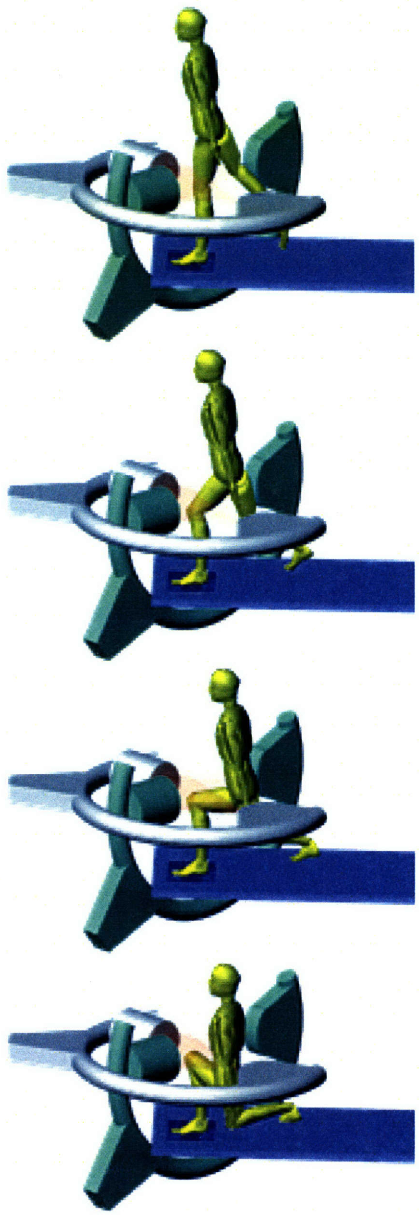

Fig. 4.1 Representation of single leg weight-bearing flexion of the knee while the dual-orthogonal fluoroscopic system captures the knee images.

Table 4.1: Data on the Patients

Average Patient Characteristics

	Age (years)	Weight (lbs)	Height (inches)	Passive Preop ROM (degrees)	Passive Postop ROM (degrees)	Postop Time (months)
Average	68.9	203	71	109	125	32.6
Min Range	46	159	67	90	110	18.9
Max Range	80	247	73	125	138	60.8

A virtual dual orthogonal fluoroscopic system was constructed within a solid modeling software (Rhinoceros®, Robert McNeel & Associates, Seattle, WA) to reproduce the patient's kinematics by manually matching three-dimensional computer models of the components (obtained from the manufacturer) to the acquired fluoroscopic images (Li, Wuerz et al. 2004; Hanson, Suggs et al. 2006). Two cameras were placed within the virtual system to provide the correct orthogonal perspectives with respect to the images (Fig. 4.2). When positioning the component models in three-dimensional space, they were viewed from both camera perspectives simultaneously and were adjusted in 6 degrees-of-freedom until the model overlapped the fluoroscopic profiles on the acquired images. The overlapped, or matched, three-dimensional models replicated the in-vivo position of the femoral and tibial component within the patient's knee joint at the moment of image acquisition (Fig. 4.2).

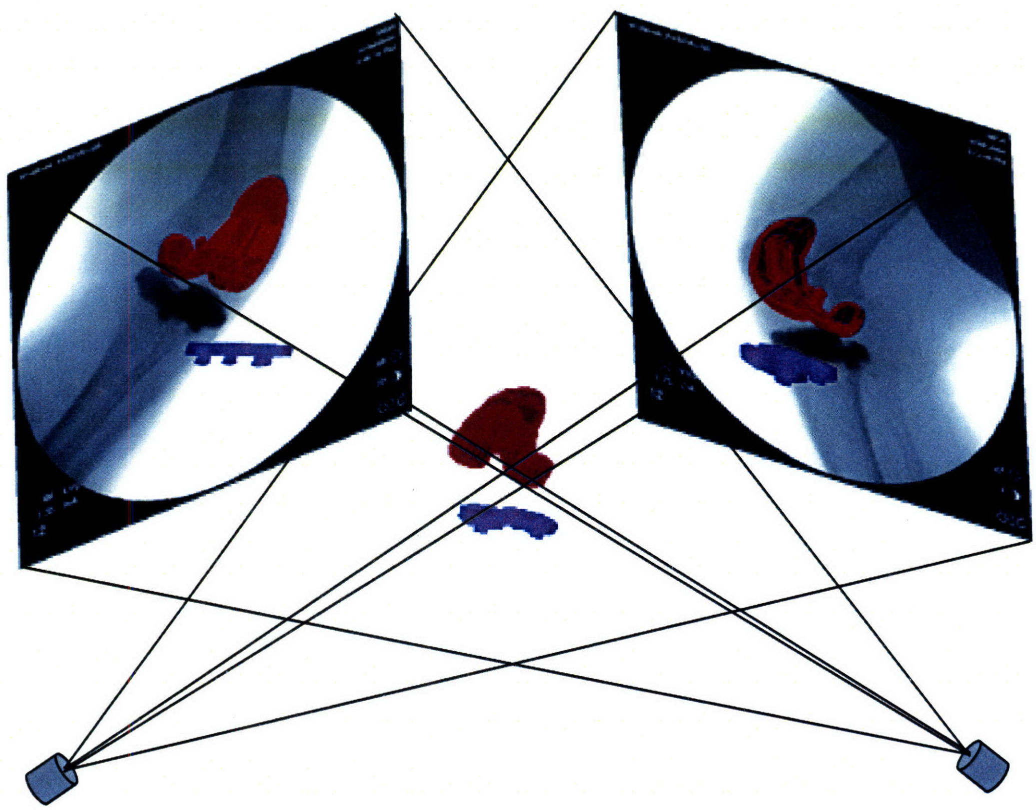

Fig. 4.2 Representation of virtual dual-orthogonal fluoroscopic system used to reproduce in-vivo total knee arthroplasty positions using fluoroscopic images and three-dimensional CAD models of the prosthetic components.

After matching the component model (both the metal femoral component and metal tibial tray) to the orthogonal images, the in-vivo knee position was reproduced by the three-dimensional model. The ultra-high molecular weight polyethylene tibial insert was not visible under fluoroscopy, but its position can be determined based on the tibial component. In 9 subjects (one female, eight males), contact was determined by locating the intersection of the articulating surfaces of the femoral component and polyethylene tibial insert. The centroid of the surface intersection was used to report the point of contact location. In the case that surface overlap was not encountered, contact was determined based on the closest points between the femoral component and polyethylene tibial insert articulating surfaces. Previous validations have tested the average system resolution to be within 0.16 mm for the femoral component and 0.13 mm for the tibial tray component (Li, Wuerz et al. 2004; Hanson, Suggs et al. 2006). Therefore, a closest distance between the two articulating surfaces measuring greater than 0.29 mm was defined as condylar lift-off.

4.2.2 Component geometry and surgical technique

The posterior cruciate ligament-retaining arthroplasty design investigated in this study has an asymmetric femoral component (Zimmer, 2004). The radii of the lateral condyle are larger than those of the medial condyle in the sagittal plane to facilitate axial rotation of the knee during flexion. The radii of the tibiofemoral articulating surfaces are matched in the coronal plane to provide conforming surfaces and thus increase the contact area. The tibial articular surface is also curved in the sagittal plane.

The surgical implantation was conducted using a medial arthrotomy, and intramedullary alignment was used on the femoral side. The femur was cut in 5° of valgus and 3° of external rotation. The epicondylar axis was used to assess the rotational alignment, with the posterior femoral condyles and Whiteside's line as additional references. Tibial alignment was performed using an extramedullary guide. The reference points used were the center of the tibial plateau, the junction of the medial and middle thirds of the tibial tuberosity and the visible part of the tibial crest. The tibial cut was performed with a 7° posterior slope. Prior to placement of the definitive components, a trial reduction was performed with careful attention to the assessment of the flexion and extension gaps, stability, range of motion and patellar tracking. Posterior cruciate ligament tension was assessed by flexing the knee and examining for tibial tray anterior lift-off. The posterior cruciate ligament was also manually palpated to assess for tension, and the flexion gap was examined. The femoral, tibial and patellar prostheses were cemented. The patella was resurfaced in all patients. The extensor mechanism and skin were closed with sutures in a standard fashion.

4.2.3 Data analysis

The anteroposterior and mediolateral contact locations of the medial and lateral compartments were determined for quasi-static single leg lunge motion. The findings were then averaged at each flexion angle. To quantify the location of the contact point on the tibial surfaces, coordinate systems were created on the surfaces of the medial and lateral tibial compartments. The geometric centers of the medial and lateral compartments of the tibial component surface were used as the origins of the coordinate systems for the two compartments (Fig. 4.3A). Anterior and medial coordinates were denoted as positive; posterior and lateral coordinates were denoted as negative. Within each tibial compartment, the half closer to the tibial spine was denoted as the inner portion, and the half farther from the tibial spine was denoted as the outer portion.

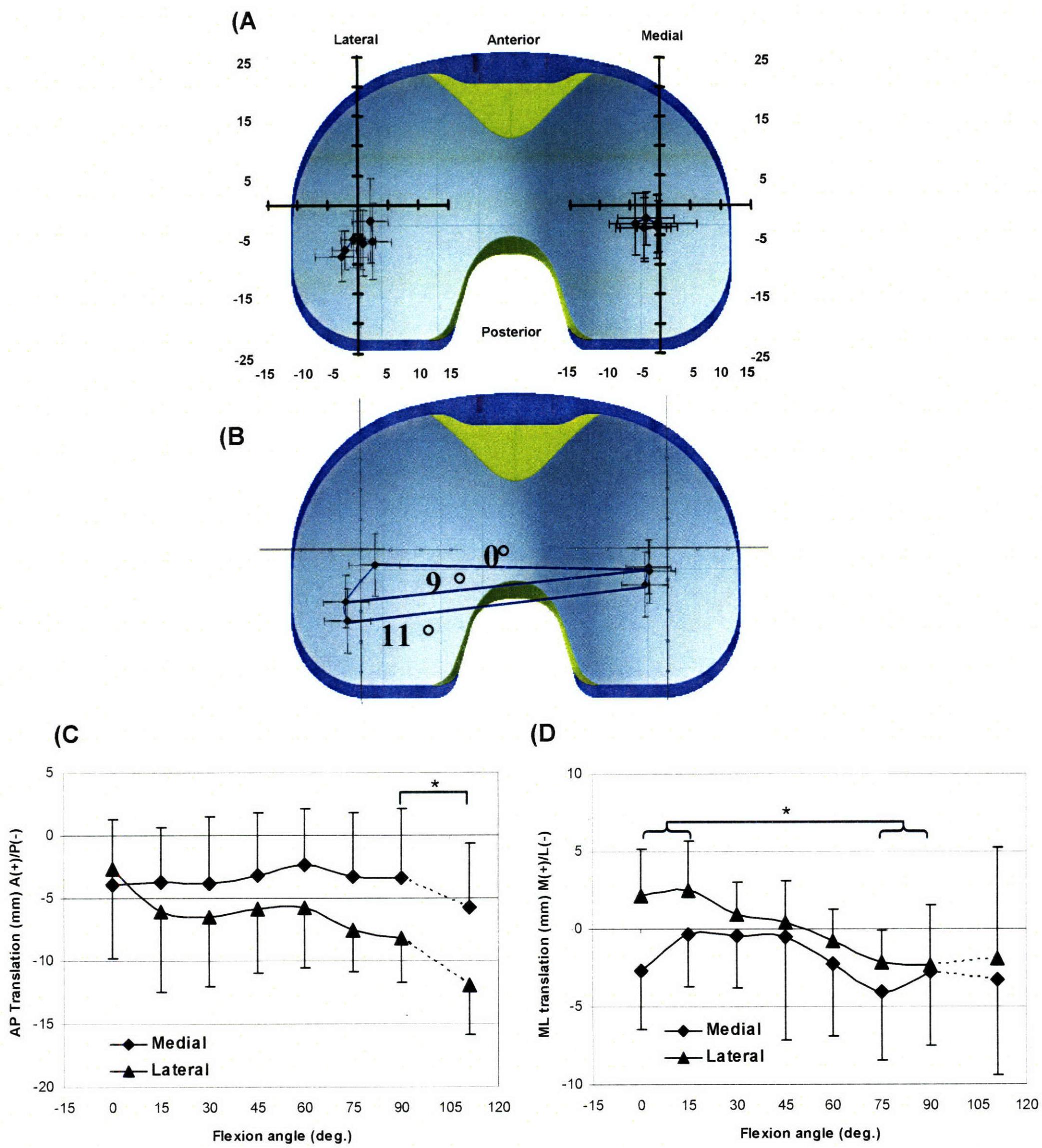

Fig. 4.3 A) Illustration showing the mean in vivo tibiofemoral contact point locations (and standard deviations) during weight-bearing knee flexion from 0-90° at 15° intervals. **B)** Illustration showing the mean contact locations (and standard deviations) at 0°, 90° and 113° (the average maximum flexion); **C)** Graph showing the mean anteroposterior translation (and standard deviation) of the medial and lateral contact points. **D)** Graph showing the mean mediolateral translation (and standard deviation) of the medial and lateral contact points. * $p<0.05$.

All patients achieved more than 90° of flexion after the cruciate retaining total knee arthroplasty, but maximum flexion varied for each patient. The average maximal weight-bearing flexion angle was 113.3 ± 13.1°. To analyze the component contact behavior at maximal flexion, the contact data for all patients at their maximal flexion angles were averaged, analyzed and reported at the mean maximal flexion angle of 113.3°. Therefore, we presented the data in two flexion ranges: from full extension to 90° and from 90° to maximal flexion (Fig. 4.3).

A repeated-measures analysis of variance followed by the Student-Newman-Kuels test was used to study the effect of flexion angle on contact point location in the medial and lateral compartments. Statistical significance was defined as $p < 0.05$.

4.3 Results

4.3.1 6DOF Kinematics

The 6DOF in vivo TKA kinematics of CR TKA patients under weight bearing flexion is shown in Figs. 4.4A and 4.4B. The femur translated anteriorly by 5.29 mm through 45° of flexion and then consistently translated in the posterior direction through maximum flexion by 11.58 mm (Fig. 4.4A). The femur translated proximally by 6.17 mm through 90° of flexion and moved slightly in the distal direction between 90° and maximum flexion. Through 45° of flexion, the femur moved laterally by 1.31 mm, remained relatively constant through 75° and then moved medially by 1.39 mm at maximum flexion (Fig. 4.4A).

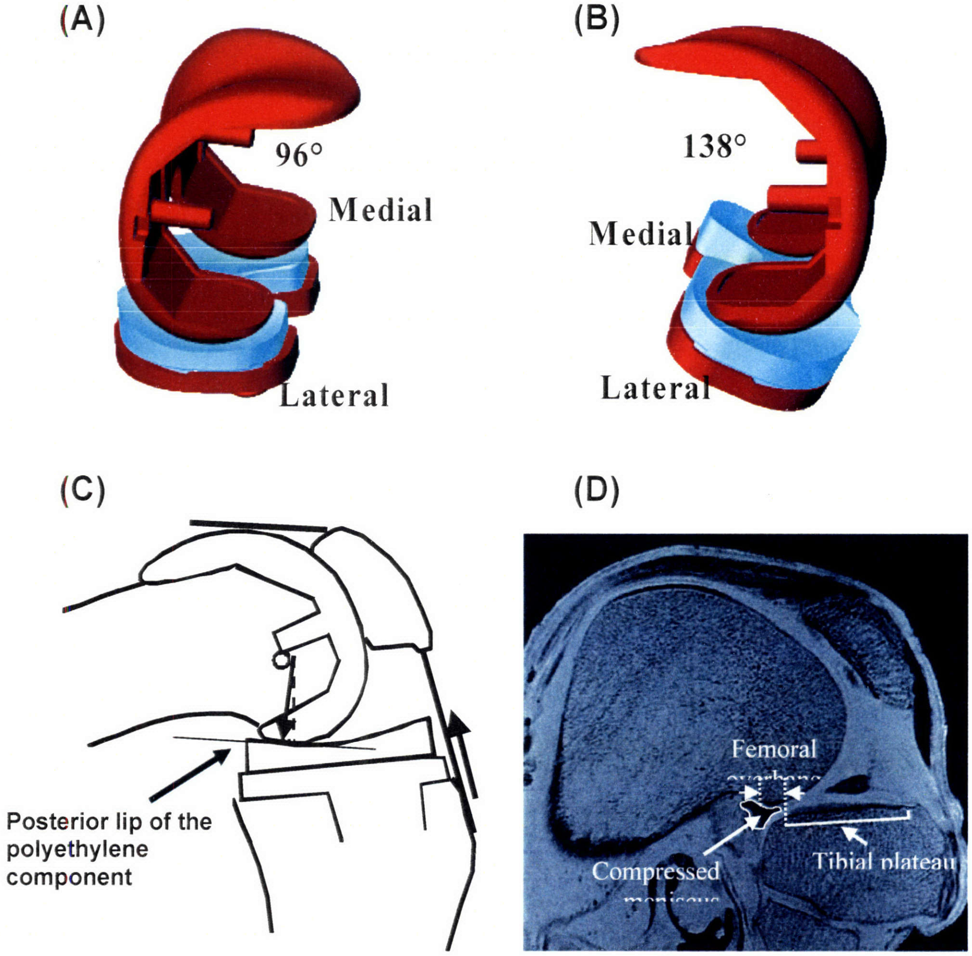

Fig. 4.4 A, B) Virtual representation of two patients after total knee arthroplasty at their maximal flexion angles; **C)** Schematic of tibiofemoral contact at high flexion of the cruciate-retaining total knee arthroplasty being constrained by the increasing height of the posterior lip of the polyethylene and the stretching extensor mechanism; and **D)** Sagittal view of the lateral femoral condyle of a normal knee rolling off the tibial plateau at high flexion.

The tibia rotated internally by 4.79° through 60° of flexion and remained relatively constant through 90° (Fig. 4.4B). An increase in mean internal rotation of only 0.66° occurred between 90° and maximum flexion. Varus rotation increased by 0.86° through 30° of flexion. A valgus rotation of 1.52° was observed between 30° and 90°, and a varus rotation of 0.34° occurred between 90° and maximum flexion.

4.3.2 Tibiofemoral contact location change from full extension to 90°

Medial compartment There was no statistically significant motion of the average medial tibiofemoral contact point from full extension to 90° of flexion in the anteroposterior direction (Figs. 4.3A and C). At full extension, the contact point was -3.9 ± 5.2 mm (mean ± SD) posterior to the midline of the tibial plateau. At 60° of flexion, the contact point was at -2.4 ± 4.6 mm, and at 90°, the contact point was at -3.4 ± 5.6 mm. The total range of the average contact in the anteroposterior direction was 1.5 mm from full extension to 90° of flexion.

In the mediolateral direction, the average tibiofemoral contact points were positioned in the inner half of the medial compartment (Figs. 4.3A and D). At full extension, the contact point was at -2.7 ± 3.8 mm on the inner half of the tibial plateau. The outermost position was -0.3 ± 3.3 mm, which was measured at 15° of flexion. The innermost position was -4.0 ± 4.4 mm, which was measured at 75°

of flexion. The range of the average contact in the mediolateral direction was about 3.7 mm from full extension to 90° of flexion, but this motion was not statistically significant.

Lateral compartment There was no statistically significant motion in the anteroposterior direction from full extension through 45° of flexion (Figs. 4.3A and C). The contact location from 60° through 90° of flexion was significantly posterior to the location at full extension ($p<0.048$). At full extension, the tibiofemoral contact point was positioned at -2.6 ± 7.1 mm. At 60° of flexion, the contact location was at –5.7 ± 4.8 mm ($p=0.048$). At 90°, the contact point was located at -8.2 ± 3.6 mm ($p=0.013$). The total range of the average contact in the anteroposterior direction was 5.6 mm from full extension to 90° of flexion.

In the mediolateral direction, the tibiofemoral contact points were positioned on the inner portion near full extension and shifted to the outer portion 75° and 90° of flexion ($p<0.024$, Figs. 4.3A and D). At full extension, the contact point was at 2.1 ± 3.1 mm. At 75° of flexion, the contact was at -2.2 ± 2.1 mm, and at 90° of flexion the contact was at -2.3 ± 3.9 mm. The total range of the average contact in the mediolateral direction was 4.8 mm from full extension to 90° of flexion.

4.3.3 Tibiofemoral contact location change from 90° to maximal flexion

Medial compartment The average medial tibiofemoral contact point translated posteriorly from 90° to maximal flexion ($p=0.038$, Figs. 4.3B and 4.3C).

It changed from -3.4 ± 5.6 mm at 90° to -5.8 ± 5.1 mm at maximal flexion. The range of motion in the anteroposterior direction was about 3.4 mm from full extension to maximal flexion.

However, the change in the contact location in the mediolateral direction after 90° was statistically insignificant, translating laterally from -2.8 ± 4.7 mm at 90° to -3.3 ± 6.1 mm at maximal flexion. The total range of the average contact in the mediolateral direction remained at 3.7 mm from full extension to maximal flexion.

Lateral compartment The average lateral tibiofemoral contact point showed significant posterior translation from 90° to maximal flexion (p=0.008, Figs. 4.3B and 4.3C). It changed from -8.2 ± 3.6 mm at 90° to -11.9 ± 3.9 mm at maximal flexion. The total range of the average contact in the anteroposterior direction was 9.3 mm from full extension to maximal flexion.

However, the motion of the average contact in the mediolateral direction after 90° was again insignificant. Contact was observed at -2.3 ± 3.9 mm at 90° and -1.9 ± 7.2 mm at maximal flexion. The total range of the average contact in the mediolateral direction was still 4.8 mm from full extension to maximal flexion.

4.3.4 Observation of tibiofemoral contact at maximal flexion

At maximal flexion, 7 patients had their lateral femoral condyle positioned posteriorly to the medial compartment on the tibial polyethylene component surface, indicating internal tibial rotation. In all patients, at least one of the femoral condyles showed posterior translation when reaching maximal flexion. The tibiofemoral articular contact locations were at the posterior portion of the tibial polyethylene component, but the femoral condyles did not reach the posterior edge of the polyethylene surface. One patient showed lateral condyle lift-off at 45°of flexion (with a gap of 0.32 mm detected between the femoral condyle and the tibial polyethylene surface). Another patient showed lateral femoral condyle lift-off at both full extension and maximal flexion (with a gap of 0.65 and 0.64 mm detected between the femoral condyle and the tibial polyethylene surface, respectively). Component positions at maximum flexion are shown for two patients in which one patient has a low maximal flexion angle of 96°while the other has a high maximal flexion angle of 138° (Fig. 4.4A and 4.4B).

4.4 Discussion

The data of this paper demonstrated that the dual orthogonal fluoroscopic system has sufficient reproducibility when measuring 6DOF positions of the TKA components in space. The in vivo kinematics of the CR patients investigated in this study showed that femoral translation in the anterior direction was observed through 45° of flexion before moving posteriorly through maximum flexion, which is consistent with the observation of in vitro robotic measurement (Li, Zayontz et al. 2001). Consistent proximal translation was also observed throughout flexion. Translation was detected in the medial/lateral direction, though approximately a magnitude lower than the translation in the anterior/posterior direction. While internal tibial rotation consistently increased with flexion (a trend similar to normal tibial rotation), a lower magnitude was observed than that reported for the normal knee (Asano, Akagi et al. 2001; Andriacchi, Dyrby et al. 2003; Komistek, Dennis et al. 2003; Li, Zayontz et al. 2004). However, the magnitude is similar to the CR TKA rotation simulated in in vitro robotic experiments (Li, Zayontz et al. 2001; Most, Zayontz et al. 2003). The varus rotation was also detected to be small throughout flexion, with mean values between -0.03° and 1.48°.

Accurate knowledge of three-dimensional tibiofemoral articular contact kinematics is important for understanding the mechanism of polyethylene component failure and biomechanical factors, such as articular tibiofemoral maltracking, that prevent high flexion of the knee. Even though several studies have reported one-dimensional tibiofemoral contact positions in the anteroposterior direction during knee flexion (Banks, Markovich et al. 1997; Bertin, Komistek et al. 2002; Watanabe, Yamazaki et al. 2004), the actual tibiofemoral contact locations on the three-dimensional tibial articular surface during knee flexion are still not known. This study investigated the three-dimensional contact kinematics of the knee after a posterior cruciate ligament-retaining total knee arthroplasty using a dual-orthogonal fluoroscopic imaging technique (Li, Wuerz et al. 2004). The change in tibiofemoral contact locations with respect to flexion on the tibial polyethylene surface was determined in patients after cruciate-retaining total knee arthroplasty when performing weight-bearing flexion from full extension to maximal flexion.

Previous studies have used image matching techniques to investigate in-vivo knee kinematics by taking single plane fluoroscopic images of the knee in the sagittal plane (Dennis, Komistek et al. 1996; Banks, Markovich et al. 1997; Nozaki, Banks et al. 2002). These fluoroscopic studies only reported tibiofemoral contact locations in the anteroposterior direction in the medial and lateral compartments. Banks et al. (Banks, Markovich et al. 1997) showed a reduced, but notable, posterior femoral translation in a posterior cruciate ligament-retaining knee prosthetic (AMK, DePuy). Dennis et al. (Dennis, Komistek et al. 1996) showed that the femur in another posterior cruciate ligament-retaining design (Press-Fit Condylar Designs, J&J) tended to translate anteriorly in midflexion during deep knee bends. Nozaki et al. (Nozaki, Banks et al. 2002) showed that the anteroposterior translation contact pattern during stair climbing could change substantially due to varying surgical techniques between two subject groups with the same posterior cruciate ligament-retaining total knee arthropalsty (Advantim, Wright Medical Technology).

It is always difficult to make a direct comparison between studies due to various factors, including the different geometrics of the components, surgical technique and loading conditions. Therefore, comparisons were made only to a study by Bertin et al. that involved the anteroposterior contact analysis of the same cruciate-retaining total knee arthroplasty design (Bertin, Komistek et al. 2002). For both the medial and lateral compartments, both studies reported similar contact starting positions, anterior translations in mid-flexion and had similar overall posterior translation. Bertin et al. reported that the tibiofemoral contact motion in the medial compartment started at 4.0 mm posterior to the midline, moved posteriorly through 60°, then had an anterior motion occurring from 60-80° of flexion and had an overall posterior translation of 3.0 mm (Bertin, Komistek et al. 2002). Bertin et al. also reported that tibiofemoral contact in the lateral compartment started at 3.4 mm posterior to the midline, showed an anterior translation of 0.1 mm from 20-40° of flexion, then showed posterior translation through 100° of flexion and had an overall translation of 4.4 mm (Bertin, Komistek et al. 2002). Similar trends were observed in this current study for both compartments in the anteroposterior direction (Fig 4.3C).

However, our data indicated that the tibiofemoral contact points also shifted along the mediolateral direction. As a result, the design of the articular surface geometry in the coronal direction may have a direct effect on contact, since the concave geometry of the polyethylene insert will force the femoral condyles to move in the proximodistal direction as they translate in the mediolateral direction. When either the mediolateral motion or the articular geometry is neglected in contact analysis, proximodistal motion may be mistaken for lift-off or values of lift-off may be artificially inflated. For example, in one instance of patient lift-off, a gap of 0.64 mm was measured using the femoral condyle and polyethylene tibial insert surface. However, if the difference in distances between the medial and lateral femoral condyles to the tibial plate was used to determine the presence of lift-off (Dennis, Komistek et al. 2003), a 2.4 mm difference would be detected for this same patient. By neglecting the curved geometry of the polyethylene surfaces, this method of lift-off determination may not accurately detect femoral condylar lift-off. Similar observations have also been noted by Taylor and Barrett (Taylor and Barrett 2003). It should be noted that the femoral condylar lift-off discussed in this paper was for patients performing a single-leg lunge activity. For other activities, such as a double-leg deep knee bend, the tibiofemoral contact might show different contact patterns due to the different physiological loads.

In a recent in-vivo investigation of 5 normal living subjects from a different patient polulation (DeFrate, Sun et al. 2004; Li, DeFrate et al. 2005), we found that the medial tibiofemoral articular contact points were located in the central part of the tibial plateau in the anteroposterior direction, while showing movement in the mediolateral direction as the knee flexed from full extension to 90° of flexion (Fig. 4.5B). The change in posterior location in the lateral compartment was larger at low flexion angles than at high flexion angles. The posterior cruciate ligament-retaining total knee arthroplasty design in this study also showed contact on the inner half of the tibial compartments, but the contact shifted posteriorly relative to the normal knee from full extension to 90° of flexion (Fig. 4.5A). However, it must be noted that the normal subjects (Li, DeFrate et al. 2005) were young and healthy, while the arthroplasty patients in this study were, on average, 67.5 years old. Thus, comparison of the findings between the two studies is made with caution. In the future, the kinematics of the knee before and after total knee arthroplasty should be compared.

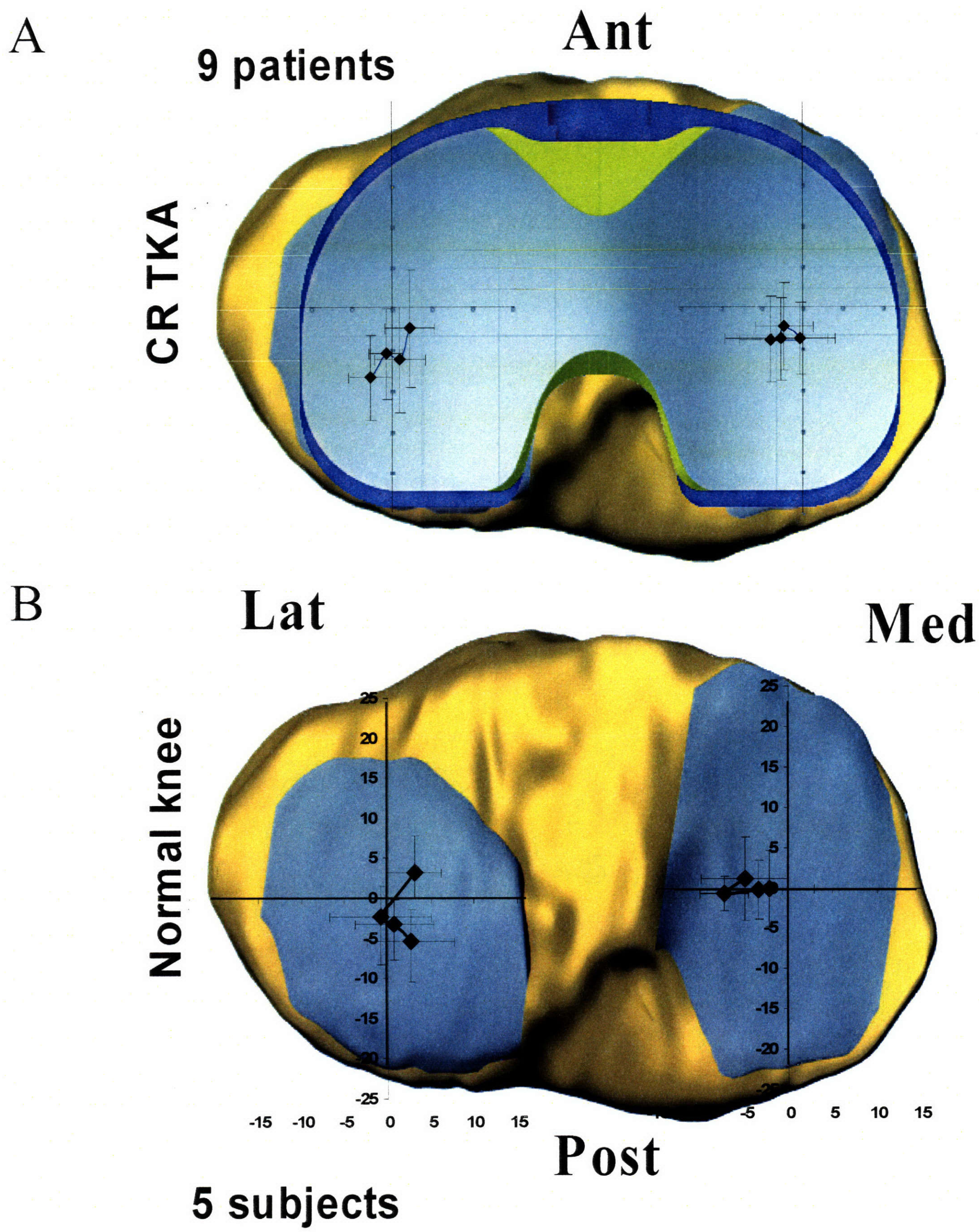

Fig. 4.5 Comparison of tibiofemoral contact locations at 0, 30, 60, and 90° of flexion of the cruciate-retaining total knee arthroplasty and normal subjects.

In the present study, patients achieved different amounts of maximal flexion. Therefore, the tibiofemoral articular kinematics at maximal flexion was averaged and presented separately from the data before 90° of flexion. Beyond 90°, both medial and lateral contact points were found to move posteriorly in our experimental data. Although maximal flexion angles varied among patients, a consistent pattern of the tibiofemoral articulation was observed. In 7 of the 9 patients, the contact at maximum flexion was at least 6 mm away from the posterior edge of the polyethylene insert (Fig. 4.4B). On average, the contact in the lateral compartment was more posterior than in the medial compartment. This is consistent with the internal tibial rotation of the knee with flexion, as previously observed (Li, Wuerz et al. 2004). Only two knees showed more posterior contact points in the medial compartment (Fig. 4.4A).

At maximal weight-bearing flexion, patients of this study felt that the knee was too tight to flex further. One possible explanation is based on the concave nature of the tibial articular surfaces (Fig. 4.4C). At high flexion, the femur must translate posteriorly to avoid impingement between the posterior surfaces of the femur and tibia with increasing flexion. The concave curvature of the tibial articular surfaces requires the femoral condyles to move proximally to further translate posteriorly for additional flexion, causing additional stretching of the extensor mechanism. The extensor mechanism could become highly stretched before the knee reaches what would otherwise be maximal flexion (Fig. 4.4C). In addition, any further posterior femoral translation might cause the femoral condyle to roll onto the posterior edge of the tibial polyethylene component, resulting in unstable edge-loading. As noted in our previous investigations of the normal knee, the femoral condyle was shown to roll off the tibial plateau in high flexion and remained stable due to the posterior motion of the menisci, especially on the lateral side of the femoral condyles (Fig. 4.4D) (Li, Wuerz et al. 2004; Li, Zayontz et al. 2004). The contact mechanism of the total knee implant is constricted to the tibial articulating surface, and as a result, the femoral condyles are unable to roll off the tibial plateau at high flexion.

In conclusion, this in-vivo study suggests that the tibiofemoral articular contact kinematics of the NexGen posterior cruciate ligament-retaining total knee arthroplasty moves in the mediolateral direction as also observed in the normal knee from full extension to 90°. At maximal flexion, the tibiofemoral contact, especially on the lateral side, approached the posterior edge of the polyethylene component but did not reach the edge. This three-dimensional tibiofemoral contact data may provide new insight for determining wear patterns in-vivo and designing the articulating surfaces by accounting for contact location in both the anterioposterior and mediolateral directions. Finally, it should be noted that this study only tested a single posterior cruciate ligament-retaining total knee arthroplasty design. The testing protocol established in this paper, however, is applicable to all other knee arthroplasty designs including unicondylar knee arthroplasty designs. In future research, information obtained with this methodology will be used to establish boundary conditions for three-dimensional finite element analysis of the polyethylene stress-strain distribution under in-vivo loading conditions, potentially providing quantitative insights into the polyethylene wear and failure in patients.

Chapter 5. In-vivo Flexoin and Kinematics of the Knee after TKA – Comparison of a Conventional and a High Flexion Cruciate-Retaining Total Knee Arthroplasty Design

5.1 Introduction

Restoration of the full range of knee flexion for patients after total knee arthroplasty (TKA) is important for maintaining various life style activities, such as sports, gardening, stair ascent/descent, and taking a bath (Laubenthal, Smidt et al. 1972; Rowe, Myles et al. 2000; Hemmerich, Brown et al. 2006). It is believed that contemporary TKA patients are more active than patients in the past and have a greater desire to participate in activities that require high flexion. Consequently, many new TKA components have been designed to better accommodate high knee flexion after surgery. It has been suggested that the mechanical environment experienced by the polyethylene insert at high flexion may be highly unfavorable and that participation in high flexion activities could accelerate wear of the polyethylene component (Nagura, Otani et al. 2005; Ritter 2006).

Several studies have evaluated high flexion TKA designs using either clinical examination or single-plane fluoroscopic techniques (Argenson, Komistek et al. 2004;

Huang, Su et al. 2005; Kim, Sohn et al. 2005; Seon, Song et al. 2005; Gupta, Ranawat et al. 2006; Bin and Nam 2007). These in-vivo studies have only dealt with posterior-substituting designs. No study has reported on the biomechanics of high flexion posterior cruciate-retaining TKA designs. Further, no study has compared the in-vivo contact biomechanics of high flexion TKAs with those of conventional TKA designs.

The objective of this study was to compare the in-vivo kinematics of two cruciate retaining total knee arthroplasty designs, one conventional (NexGen CR, Zimmer, Warsaw, IN) and one high flexion design (NexGen CR-Flex, Zimmer, Warsaw, IN). We hypothesized that the CR-Flex design would enhance knee flexion compared to the conventional CR design. Six degree-of-freedom kinematics were obtained from patients implanted with either the conventional component or the high flexion component using a dual fluoroscopic imaging system. Information on maximum knee flexion and the contact location between the femoral component and the polyethylene insert were also compared between the two designs.

5.2 Materials and Methods

5.2.1 Experimental Setup

Twenty-nine knees (15 NexGen CR, 14 NexGen CR-Flex, Zimmer, Warsaw, IN) were analyzed in this study under IRB approval. Patients were recruited from the practice of a senior surgeon (AAF), and each patient gave informed consent. There was no difference in age, body weight, height, gender, or knee scores between the group with conventional TKA components and the group with high flexion components

(Table 5.1). All patients had their knees replaced at least six months prior to participation in this study, demonstrated passive range of motion greater than 90°, and were evaluated to be clinically successful.

Table 5.1: Demographics for CR and CR-Flex groups

	CR	CR-Flex
Age (yrs)	69.1 ± 10.9	64.1 ± 10.3
Weight (lbs)	195.1 ± 31.0	189.8 ± 40.5
Height (in)	69.6 ± 3.0	68.5 ± 3.4
Gender (F/M)	3 / 12	3 / 11
Side (L/R)	5 / 10	5 / 9
Max Passive Extension (deg)	1.5 ± 3.5	0.7 ± 3.0
Max Passive Flexion (deg)	122.1 ± 8.9	118.0 ± 9.7
Max Weightbearing Flexion (deg)	110.1 ± 13.4	109.1 ± 12.5
Knee Society Knee Score	91.9 ± 13.4	90.8 ± 10.5
Knee Society Functional Score	86.0 ± 15.1	86.4 ± 13.8

The maximum passive flexion of each patient was assessed using a goniometer (Table 5.1). During the experiment, the patient was asked to perform a weightbearing single leg lunge from full extension to maximum flexion while the knee was imaged using a dual fluoroscopic imaging system (Hanson, Suggs et al. 2006; Li, Suggs et al. 2006). Pairs of fluoroscopic images were captured simultaneously at intervals of approximately 15° of flexion.

The positions of the total knee components during the weightbearing flexion were deduced with the use of a virtual dual fluoroscopic imaging system created in solid modeling software (Rhinoceros, Robert McNeel and Associates, Seattle, WA), where the image intensifiers were represented by the acquired fluoroscopic images, and the x-ray sources were represented by two virtual cameras (Li, Suggs et al. 2006). Solid models of the TKA components were imported into the virtual fluoroscopic system. The component models were manipulated in 6 DOF until they overlapped their silhouettes on both fluoroscopic images, as seen from their respective cameras. When the models overlapped their silhouettes, the in-vivo pose at the time of image acquisition was recreated. Therefore, the in-vivo positions of the total knee components along the flexion path were represented by a series of 3D total knee models.

After the in-vivo positions were determined, the 6 DOF kinematics were calculated relative to a reference pose (Fig 5.1). This reference position was defined by orienting the pegs of the femoral component perpendicular to the tibial plate and placing the most distal points of the femoral condyles at the lowest points on the polyethylene articular surface. A fixed coordinate system was created for both the tibial and femoral components at the reference position. Using this coordinate system, we determined anterior-posterior, medial-lateral, and proximal-distal femoral translations as well as internal-external and varus-valgus tibial rotations (Li, Most et al. 2004; Li, Zayontz et al. 2004; Hanson, Suggs et al. 2006).

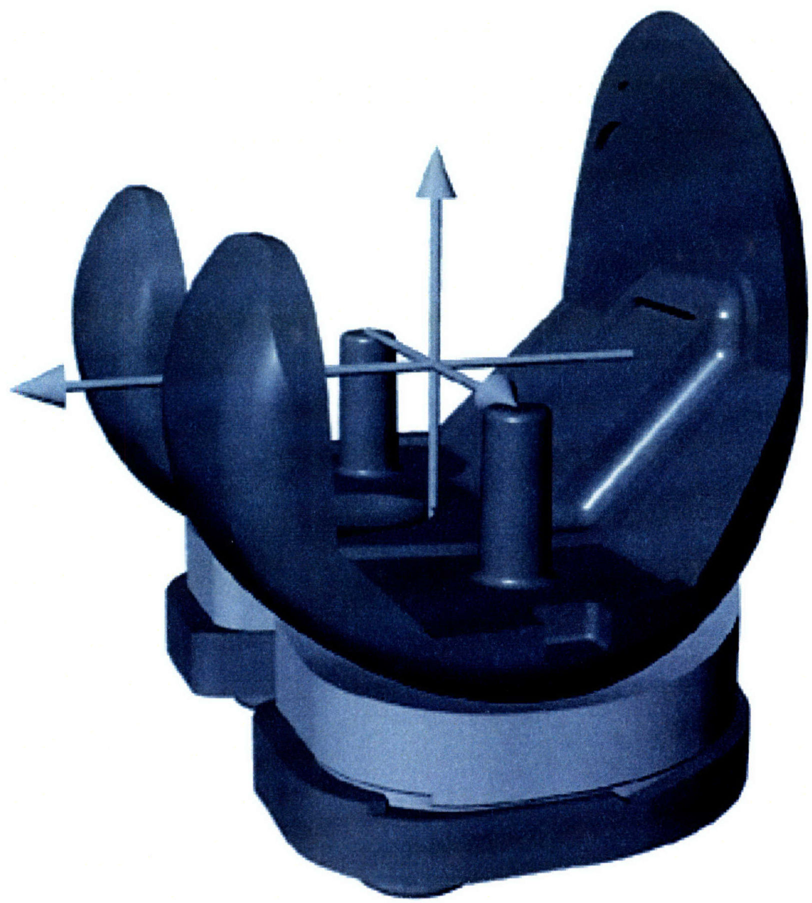

Fig. 5.1 TKA components in their reference position. Femoral translations were measured from the point midway between the peg tips.

The tibiofemoral contact location was determined by calculating the centroid of the overlap between the femoral component and the polyethylene surfaces in the medial and lateral compartments (Li, Suggs et al. 2006). If no overlap was present, the point on the polyethylene surface nearest to the femoral condyle was used as the contact location. A previous study has shown that the imaging system has an accuracy of 0.16mm for the femoral component and 0.13mm for the tibial component, so lift-off was defined as the closest distance between the polyethylene and the femoral condyle being greater than 0.29mm (Hanson, Suggs et al. 2006).

To quantitatively describe the contact locations, two coordinate systems were created for the articular contact in the medial and lateral compartments. The origins were midway between the anterior-posterior extremes of the polyethylene and 25% of the insert's medial-lateral dimension from the medial-lateral extremes.

5.2.2 Component geometry and surgical technique

The geometry and surgical technique used for the conventional CR component have been discussed previously (Li, Suggs et al. 2006; Most, Sultan et al. 2006). The CR-Flex femoral component has a thicker posterior condyle than the conventional CR component (Fig 5.2). An additional 2mm of bone is removed from the posterior condyles to allow this increase in thickness without overstuffing the joint. This modification was made in order to increase the contact area between the femoral component and polyethylene articular surface at high flexion (Li, Most et al. 2004; Most, Sultan et al. 2006). Both designs were implanted through a medial arthrotomy. The femoral component was placed in 5° of valgus and 3° of external rotation using intramedullary alignment and the epicondylar axis. The posterior condyles and Whiteside's line were used as secondary references. The tibial component was placed in 7° of posterior slope using an extramedullary guide. The tibial component was also externally rotated with the center of the tibial plateau, the junction of the medial and middle thirds of the tibial turberosity, and the tibial crest as references. Tension in the posterior cruciate ligament was assessed by manual palpation and by flexing the knee while checking for anterior lift-off of the tibial tray. The patella was surfaced in all the patients, and all the components were cemented. Interrupted absorbable sutures were used to close the extensor mechanism and skin.

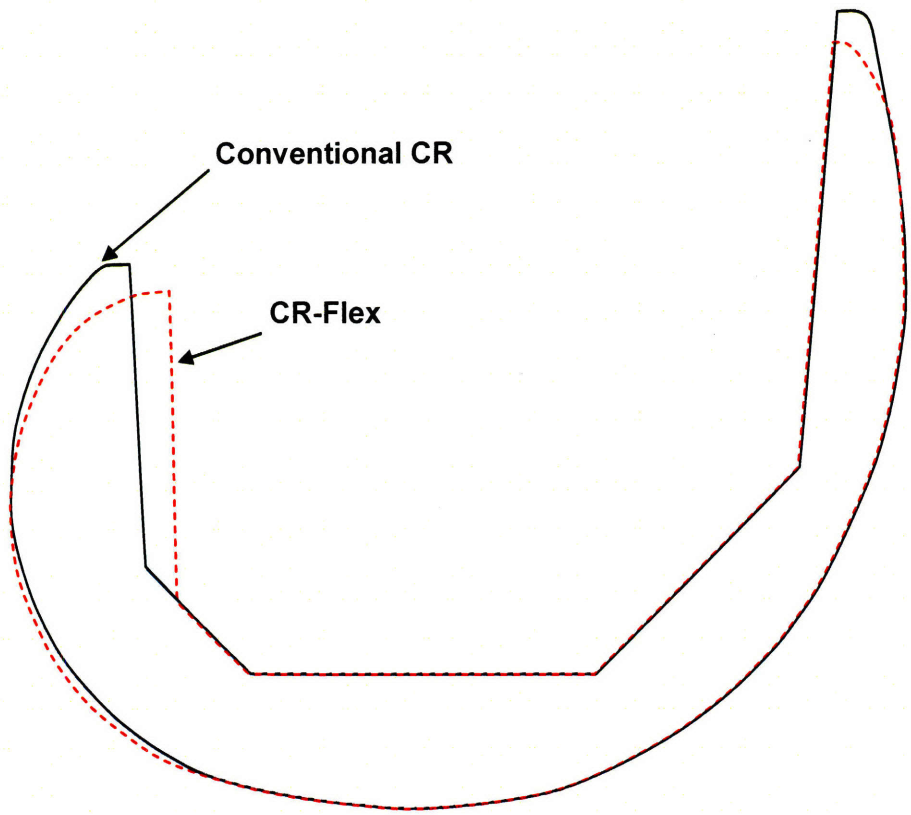

Fig. 5.2 Sagittal profile of NexGen's conventional (solid) and high flexion (dashed) designs. By removing an additional 2mm of bone from the posterior cut, the high flexion design maintains a smooth curvature through higher flexion.

5.2.3 Data analysis

Patients in each group were averaged at hyperextension, in 15° intervals from 0° to 90° of flexion, and at maximum flexion of the implant (Li, Suggs et al. 2006). The reported data at hyperextension and maximum flexion only included patients who achieved greater than 3° of hyperextension or 100° of flexion, respectively. A student's t-test with Bonferroni correction was used to compare the maximum flexion, 6 DOF kinematics data, and the contact locations in the medial and lateral compartments between the patient groups with the conventional component or high flexion component. Differences were considered significant when $p < 0.05$.

5.3 Results

5.3.1 Flexion Range

Maximum passive flexion averaged 122.1±8.9° for all the CR patients and 118.0±9.7° for all the CR-Flex patients (Table 5.1). There was no significant difference between the two patient groups in maximum passive flexion. During weightbearing flexion, the average maximum flexion for all the CR patients was 110.1±13.4°, and the average maximum flexion for all the CR-Flex patients was 109.1±12.5°. There was no difference in maximum flexion between the two patient groups during the weightbearing flexion. However, the maximum passive flexion was significantly higher than that under weightbearing flexion for both the conventional or the high flexion component patients ($p < 0.02$).

5.3.2 Six DOF kinematics of CR and CR Flex TKA patients

Patients demonstrated similar posterior femoral translation throughout the flexion range (Fig 5.3). The femoral component of the CR patients translated anteriorly from 1.1±1.7mm at hyperextension to -4.9±2.5mm at 45° of flexion, and then translated posteriorly to 8.5±5.3mm at maximum flexion. In the CR-Flex group, the femoral component translated anteriorly from 1.8±2.0mm at hyperextension to -4.0±2.4mm at 45° of flexion, and then translated posteriorly to 9.1±4.5mm at maximum flexion. No statistical difference was detected between the two patient groups in posterior femoral translation.

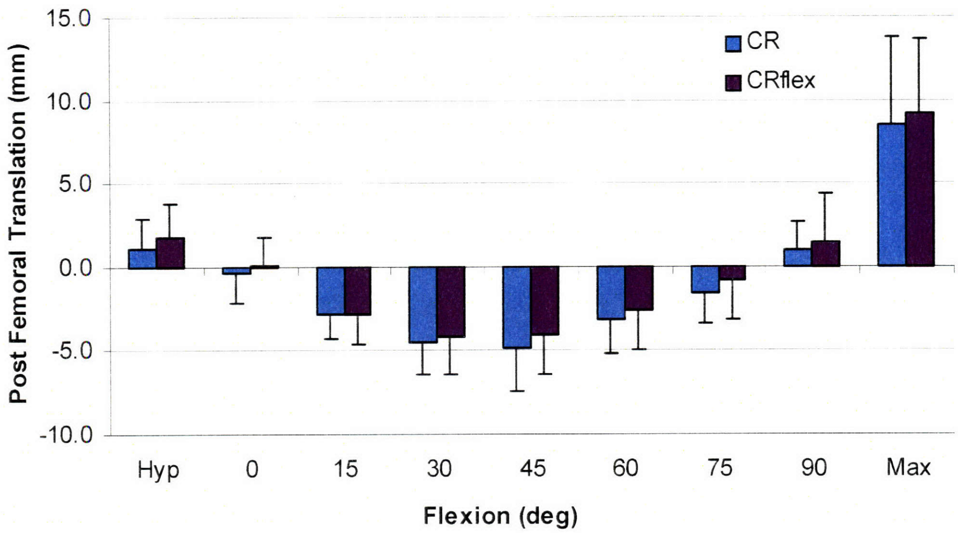

Fig. 5.3 Posterior Femoral Translation.

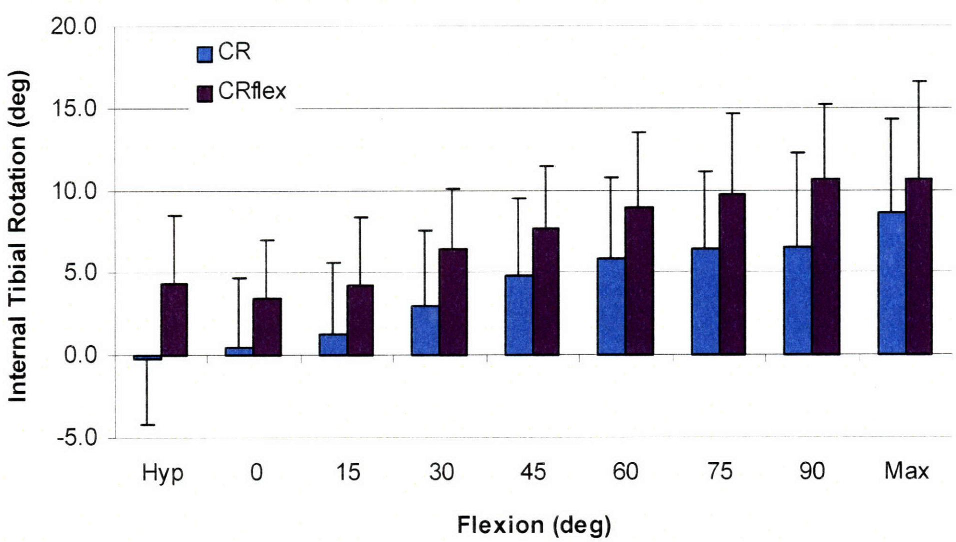

Fig. 5.4 Internal Tibial Rotation.

The two patient groups exhibited similar patterns of medial-lateral femoral translation. In the CR patients, the femoral component moved laterally from 0.5±0.7mm at hyperextension to -0.8±0.9mm at 45° of flexion and then medially to 0.1±1.7mm at maximum flexion. In the CR-Flex group, the femoral component moved laterally from 0.1±0.7mm at full extension to -1.4±0.9mm at 45° of flexion and then medially to 0.4±1.5mm at maximum flexion. Statistically, the CR-Flex femurs were more lateral than the CR femurs at 15° of flexion ($p < 0.0054$), but the difference was less than 1.0 mm.

The two groups showed similar varus-valgus patterns, starting from around 0.1±0.6° at hyperextension, rotating varus to about 1.6±0.5° at 30° of flexion, and then rotating valgus to 0.0±1.5° at maximum flexion. The two groups also demonstrated similar patterns of internal tibial rotation (Fig 5.4). In the CR patients, the tibia rotated internally from -0.2±4.0° at hyperextension to 8.6±5.8° at maximum flexion, and in the CR-Flex patients, the tibia rotated internally from 4.4±4.1° at hyperextension to 10.6±6.0° at maximum flexion. The CR-Flex patients generally demonstrated more internal tibial rotation compared to the CR patients. However, no difference was detected in varus-valgus or internal tibial rotation between the groups.

5.3.3 Tibiofemoral contact kinematics of CR and CR Flex patients

In the lateral compartment of the CR patients, the contact location moved posterior from -2.1±5.4mm to -8.1±4.4mm at early flexion and remained constant until maximum flexion, where it moved farther posterior to -15.2±4.0mm (Fig 5.5). In the CR-Flex patients, the contact also moved posteriorly in early flexion, but moved anteriorly through mid flexion, and then posteriorly again to -13.6±3.9mm at maximum flexion. No statistical difference was detected between the two patient groups.

In the medial-lateral direction, the lateral compartment contact of the CR group gradually moved laterally from -3.5±3.6mm at hyperextension to -7.9±6.3mm at maximum flexion. For the CR-Flex patients, the contact also moved laterally from -3.7±6.9mm at hyperextension to -7.7±8.1mm at maximum flexion. There was no difference in lateral compartment contact location between the two patient groups.

In the medial compartment, the contact location in the anterior-posterior direction remained relatively constant with flexion until maximum flexion for both groups. In the CR group, the medial compartment contact occurred at -2.0±4.0mm throughout the flexion range until maximum flexion, where the contact moved to -5.4±9.1mm. The medial compartment contact in the CR-Flex group remained at 0.0±4.0mm through early and mid flexion and reached -3.8±7.3mm at maximum flexion. There was no difference between the groups in the AP location of the medial compartment contact.

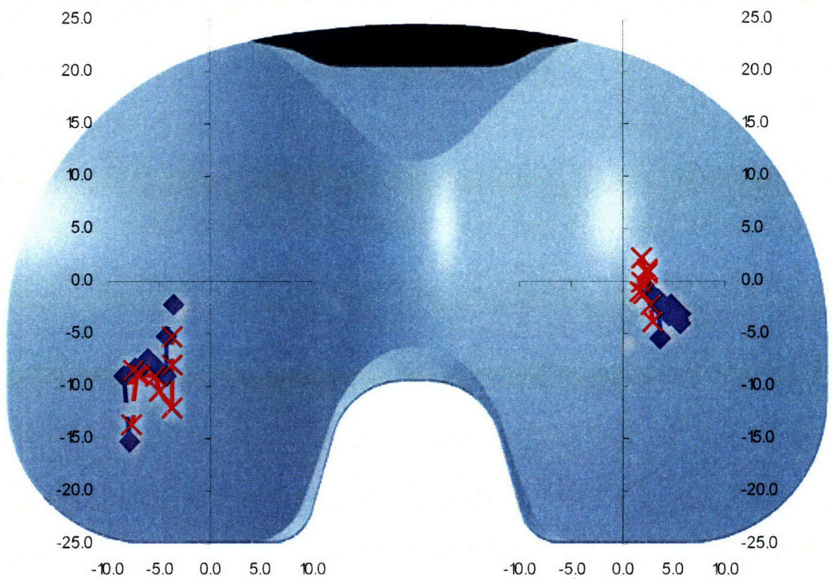

Fig. 5.5 Tibiofemoral contact on the polyethylene for the CR (diamonds) and CR-Flex (crosses) components.

The medial compartment contact location was also relatively constant in the medial-lateral direction throughout the entire flexion range for both groups. In the CR group, the contact remained around 4.5±4.5mm throughout the range of flexion. In the CR-Flex group, the contact was around 2.3±5.0mm. Again, no difference was found between the CR and CR-Flex knees.

5.3.4 Observation of tibiofemoral contact patterns of CR and CR Flex patients

Lift-off occurred at maximum flexion in 5 patients of each group. In the CR group, there were 3 patients with lift-off only in the lateral compartment, 1 patient with lift-off only in the medial compartment, and one patient with lift-off in both compartments. In the CR-Flex group, there were also 3 patients with lift-off only in the lateral compartment, 1 patient with lift-off in the medial compartment, and 1 patient with lift-off in both compartments. The average maximum flexion for these 10 patients with lift-off was 113.7 ± 12.8, which was 6° greater but not statistically different from that of patients with no lift-off (107.5 ± 12.6).

At low flexion angles, the tibiofemoral articulation was similar for both the CR and CR-Flex patients. For example, at 75° of flexion, the articulating surfaces around the contact location were very conforming for both the CR and CR-Flex components. However, at maximum flexion angles, the CR components had a different articulation compared to that of the CR-Flex components. This observation is illustrated in Figure 5.6, which shows the articulation of a CR patient and a CR-Flex patient at 131.4° and 131.1°, respectively. In the CR TKA, the femoral condyle tip came into contact with the polyethylene surface. In the CR-Flex TKA, the femoral surface in contact with polyethylene surface is much more conforming than in the conventional design.

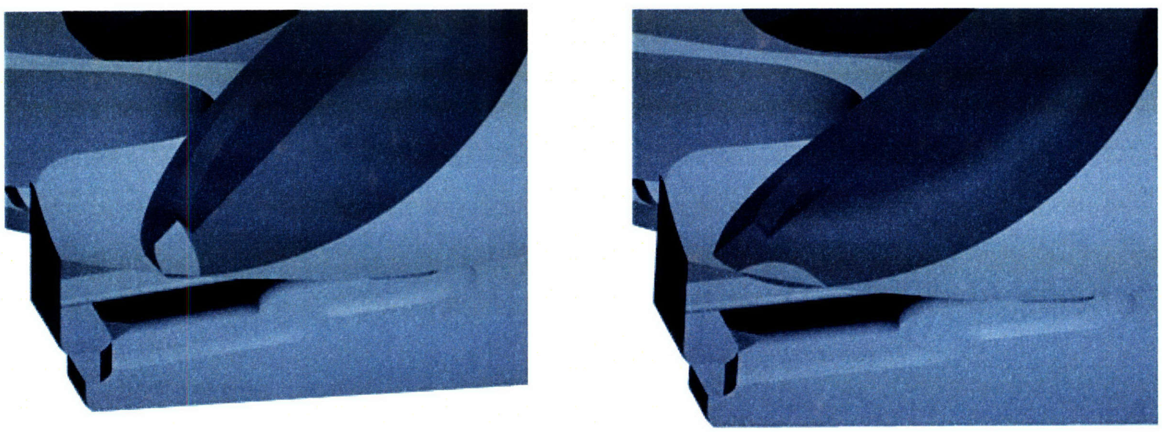

A B

Fig. 5.6 Cross-sections of the tibiofemoral articulation at 130° of flexion in a **A)** CR and **B)** CR-Flex patient. With the CR design, the tip of the femoral component is contacting the polyethylene. With the CR-Flex design, the smooth articular surface of the femoral component remains in contact with the polyethylene.

5.4 Discussion

Despite the debate over the need and efficacy of high flexion components (Ranawat 2003; Nagura, Otani et al. 2005; Ranawat, Gupta et al. 2006; Ritter 2006), many new components have been used clinically with the aim of enhancing the flexion capability of the knee after TKA (Sultan, Most et al. 2003). However, previous studies have only compared high flexion TKA designs to conventional designs in a posterior substituting knee (Argenson, Komistek et al. 2004; Huang, Su et al. 2005; Kim, Sohn et al. 2005; Seon, Song et al. 2005; Gupta, Ranawat et al. 2006; Bin and Nam 2007). This study investigated the 6DOF knee kinematics of patients after total knee arthroplasty using either a conventional cruciate retaining component (NexGen, CR) or a high flexion cruciate retaining component (NexGen, CR Flex).

In this study, patients with specially designed high flexion components behaved similarly to those with conventional implants kinematically. There was no difference in posterior femoral translation throughout the entire flexion range. For the CR patients, the tibiofemoral contact moved 4.5 mm posteriorly in the medial compartment and 13.0 mm in the lateral compartment during the weightbearing lunge. For the CR-Flex patients, the tibiofemoral contact moved 6.2 mm posteriorly in the medial compartment and 8.3 mm in the lateral compartment. There were no dramatic differences in the contact positions during knee flexion between the two patient groups. The CR-Flex knees showed approximately 3° greater internal tibial rotation than the CR knees throughout the flexion range, although this difference was not statistically significant.

Besides the similarity in kinematics, the two patient groups had similar maximum flexion under both passive and weightbearing conditions. However, the tibiofemoral contact behavior was different between the components at high flexion angles (>120°). Figure 10 showed the tibiofemoral contact patterns of a CR patient and a CR Flex patient at 130° of flexion. At this flexion angle, the condylar tip of the conventional CR TKA was in contact with the polyethylene surface. This could cause a stress concentration on the polyethylene surface and lead to increased wear in patients who attain high flexion. However, at the same flexion angle, the articulating surface of the CR Flex component was much more conforming compared to the conventional CR design. The increased conformity would help reduce any potential high stresses experienced by the polyethylene at high flexion. This improvement in contact can be explained by the thicker posterior femoral condyle of the CR-Flex design (Figure 2). The increased thickness of the femoral condyle allows for a larger radius of curvature at higher flexion angles, which translates into more conforming surfaces between femoral and polyethylene components at high flexion. Therefore, this high flexion total knee design seems to have improved the articular contact mechanics when the knee is able to achieve high flexion. This observation confirmed a previous prediction based on radiographs at full flexion which suggested that the high flex designs had better contact area (Kim, Sohn et al. 2005).

It should be noted that the data obtained in the present study for the conventional implant is similar to published data for other cruciate-retaining components. Previous studies have reported passive maximum flexion values between 100° and 120° (Bellemans, Banks et al. 2002; Banks, Bellemans et al. 2003; Aglietti, Baldini et al.

2005; Bertin 2005; Victor, Banks et al. 2005). The current study found an average weightbearing maximum flexion of 110°, and a mean passive maximum flexion around 120°.

In the literature, most studies on high flexion TKA patients consist of Asian cohorts and focus on the passive range of motion of PS TKA designs (Huang, Su et al. 2005; Kim, Sohn et al. 2005; Seon, Song et al. 2005; Gupta, Ranawat et al. 2006; Bin and Nam 2007). There are inconsistent conclusions when comparing the flexion capability of patients with conventional implants and high flexion implants. For example, Bin et al compared 90 conventional LPS knees to 90 matched LPS-Flex (Zimmer) knees at one year postoperatively (Bin and Nam 2007). They found the LPS-Flex knees to have more ROM (129.8±5.2°) than the conventional knees (124.3±9.2°). Huang et al also found LPS-Flex knees to have about 10° more flexion than LPS knees at 2 years follow-up (Huang, Su et al. 2005). Gupta et al compared a conventional rotating platform posterior stabilized design (P.F.C. Sigma RP, Depuy) to high flexion version of the same component (P.F.C. Sigma RP-F) (Gupta, Ranawat et al. 2006). They reported that the patients with a high flexion design gained significantly more ROM from preop to postop (110° to 125°) than the patients with the conventional design (110° to 116°). Kim et al compared LPS-Flex to LPS in 50 bilateral patients and did not find a difference in ROM between the components (139° vs. 136°) (Kim, Sohn et al. 2005). Seon et al compared LPS-Flex to a mobile bearing CR design (e-motion, B. Braun-Aesculap) and found no difference in maximum flexion (131° vs 129°) (Seon, Song et al. 2005).

Even though our data did not reveal a difference in maximum flexion between the two cruciate retaining implants, we did notice that the passive maximum flexion was significantly higher than that measured during weightbearing flexion. This indicates that when evaluating knee flexion, it is important to clearly define the loading conditions used during the experiment. Comparisons between studies reported in literature should only be made when the data was collected under similar conditions.

One limitation of the current study is that the condition of the polyethylene surface could not be directly analyzed due to the in-vivo nature of the experiment. As contact behavior was revealed to be different between the two implant designs at high flexion, it would be clinically interesting to examine the wear modes and patterns of their polyethylene components. In the future, this can be studied using retrieved polyethylene components from revision patients who used one of the two implants.

In conclusion, the kinematics of the CR-Flex patients analyzed in this study were similar to those of the patients with a conventional CR component. No difference was seen in the maximum flexion achieved by the patients, and the kinematics demonstrated by the groups were quite comparable. Use of this high flexion component did appear to improve tibiofemoral conformity at high flexion in patients that could achieve high flexion. Further analysis is necessary to determine if the longevity of the polyethylene is indeed improved through the use of a high flexion component.

Chapter 6. Patient Function after a Posterior Stabilizing Total Knee Arthroplasty – Knee Kinematics and Cam-Post Engagement

6.1 Introduction

The ability to participate in activities requiring deep flexion is of increasing importance to patients receiving total knee arthroplasties (TKA), especially in Asian cultures. In posterior substituting total knee arthroplasty, a cam-post mechanism was implemented to substitute for the function of the posterior cruciate ligament. The cam-post mechanism was designed to induce posterior femoral translation during knee flexion in hopes of increasing maximum knee flexion. Biomechanical studies have reported kinematics of posterior substituting total knee arthroplasties for several activities (Banks, Markovich et al. 1997; Dennis, Komistek et al. 1998; Dennis, Komistek et al. 2003; Lee, Matsui et al. 2005; Victor, Banks et al. 2005; Catani, Fantozzi et al. 2006; Fantozzi, Catani et al. 2006). Clinical outcome studies have reported similar maximal knee flexion values for various posterior substituting designs (Anouchi, McShane et al. 1996; Emmerson, Moran et al. 1996; Ranawat, Luessenhop et al. 1997; Ritter, Harty et al. 2003; Aglietti, Baldini et al. 2005; Capeci, Brown et al. 2006) with studies of Asian cohorts typically reporting higher maximum flexion than Western cohorts (Kim, Sohn et al. 2005; Seon, Song et al. 2005).

Despite the number of studies of posterior-substituting TKA, few quantitative data, however, have been reported on the effect of the cam-post mechanism on knee kinematics and on knee flexion capability (Delp, Kocmond et al. 1995; Piazza, Delp et al. 1998; Li, Most et al. 2002).In the literature, two dimensional computerized models have been used to investigate the effect of position and height of the tibial post on the tibiofemoral translation of the knee (Delp, Kocmond et al. 1995; Piazza, Delp et al. 1998). Recently, cam-post contact forces were measured using cadaveric knee specimens and compared to the forces of the posterior cruciate ligament (Li, Most et al. 2002). However, cam-post interaction in patients after posterior substituting total knee arthroplasties and its effect on knee joint kinematics are still not clearly described, especially under physiological weight-bearing conditions. Information on how cam-post engagement affects knee kinematics and flexion in-vivo would be instrumental in improving component designs as well as surgical implantation of the components in order to restore full range of motion after total knee arthroplasty.

We therefore hypothesized that cam-post engagement improved maximum flexion of the knee after total knee arthroplasty and that earlier engagement may result in larger posterior femoral translation and higher knee flexion. The objective of this study was to determine the tibiofemoral kinematics and timing of the cam-post engagement in patients after posterior substituting total knee replacement (NexGen, Zimmer, Warsaw, IN) during a single leg, weightbearing flexion using a dual-orthogonal fluoroscopic system (Hanson, Suggs et al. 2006; Li, Suggs et al. 2006). Because Asian patient populations seem to perform better than Western populations, data was collected from a U. S. population and a South Korean population. Posterior femoral translation, internal tibial rotation, and tibiofemoral articular contact locations in the medial and lateral compartments were determined. The flexion angle where cam-post engagement occurred during knee flexion was also estimated for each patient.

6.2 Materials and Methods

Forty-two knees were included in this study. Sixteen patients (14 unilateral, 2 bilateral) were from an U. S. population, and 17 patients (10 unilateral, 7 bilateral) were from a South Korean population. Each patient was randomly recruited with IRB approval and gave informed consent before testing. All patients were found to have clinically acceptable function. Each knee included in the study was tested no less than 6 months after surgery and demonstrated at least 90° passive range of motion (ROM). For the U. S. patients, the average age, weight, and height was 66.7 ± 7.5 yrs, 94.5 ± 16.1 kg, and 1.76 ± 0.12 m, respectively (Table 6.1). There were 10 males and 7 females with an average postoperative time of 20.8 months. Twelve knees received a NexGen LPS implant (Zimmer, Inc, Warsaw, IN), and 6 knees received a NexGen LPS-Flex implant. All of the South Korean patients were female, and all of them received a NexGen LPS-Flex implant. Their average age, weight, and height was 70.4 ± 5.2 yrs, 60.5 ± 8.0 kg, and 1.52 ± 0.06 m, respectively. The U. S. patients were significantly heavier and taller than the South Korean patients ($p < 0.0001$), but no difference in age was detected ($p = 0.055$, power = 64%). The surgical technique and component geometry have been described in our previous publications (Li, Most et al. 2002)

Table 6.1: Patient Demographics

	U. S.	S. K.
Age (yrs)	66.7 ± 7.5	70.4 ± 5.2
Weight (kg)	94.5 ± 16.1	60.5 ± 8.0
Height (m)	1.76 ± 0.12	1.52 ± 0.06
Gender (F/M)	8/12	24/0
Side (L/R)	9/9	10/14
Passive ROM (deg)	118.6 ± 14.0	142.5 ± 9.2
Minimum Active Flexion (deg)	-4.1 ± 7.5	-5.0 ± 6.7
Maximum Active Flexion (deg)	113.3 ± 19.4	112.5 ± 13.1
Active ROM (deg)	117.4 ± 23.9	117.5 ± 15.3

Before imaging, the patient's maximum passive flexion and extension were measured using a goniometer. During the experiment, each subject performed a single leg, weightbearing lunge with the contralateral leg helping to balance the body (Li, Suggs et al. 2006). The target knee joint was positioned inside the common imaging zone of two fluoroscopes (BV Pulsera, Philips, Netherlands). As the patient flexed the knee, the fluoroscopes simultaneously imaged the knee from two orthogonal directions from full extension to maximal flexion in approximately 15° increments. The maximum active flexion angle was achieved when the patients felt that they could not flex their knee any farther.

Therefore, the in-vivo knee kinematics along the flexion path was recorded using a series of dual fluoroscopic images.

The pair of fluoroscopic images taken at each flexion angle and three-dimensional CAD models of the TKA components were input into a virtual dual fluoroscopic system constructed in a solid modeling software (Rhinoceros, Robert McNeel, Seattle, WA) using our previously published methodology (Hanson, Suggs et al. 2006; Li, Suggs et al. 2006). The virtual fluoroscopic system recreated the geometric positions of the two fluoroscopes. The two fluoroscopic images were placed in the same relative positions as the image intensifiers of the two fluoroscopes, and two virtual cameras were positioned at the same locations as the X-ray sources using the manufacturer's specifications. The three-dimensional models of the femoral and tibial tray components were then manipulated in the virtual fluoroscopic system in 6 degrees-of-freedom, and the two virtual cameras projected the components onto the virtual image intensifires. The polyethylene tibial insert was fixed to the tibial tray and hidden from view during the matching procedure. Once the projections of the components were matched to the images of the actual component positions, the in-vivo position of the total knee arthroplasty at the target flexion angle was reproduced using the three-dimensional models. Figure 6.1 shows 3D knee models representing two in-vivo positions of the knee along the flexion path.

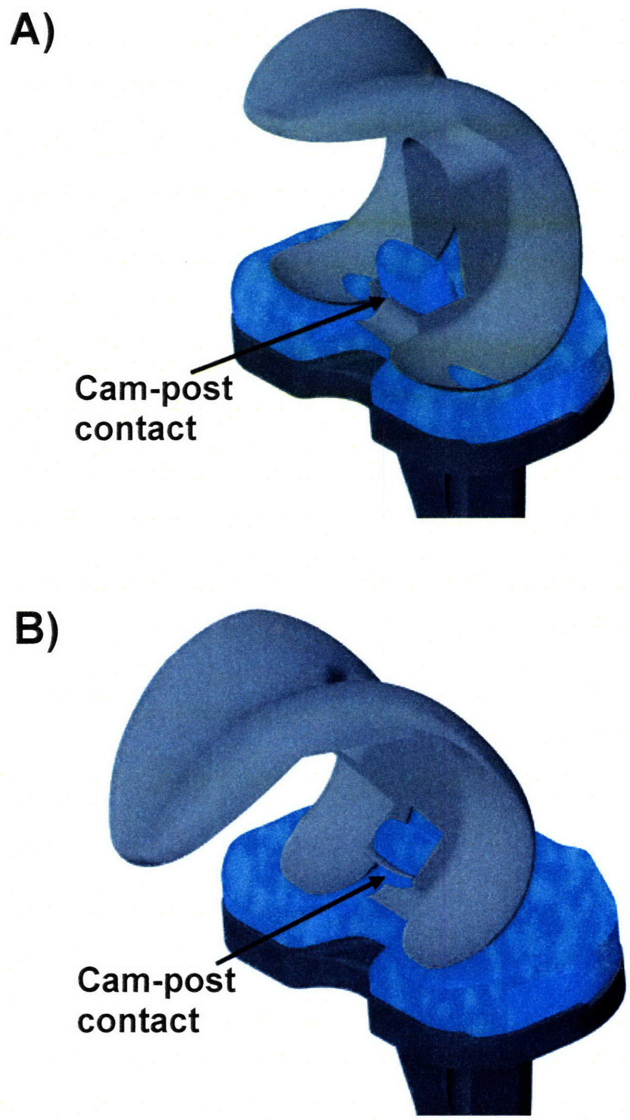

Fig. 6.1 A) Initial cam-post engagement of a patient with cam-post engagement medial post corner; **B)** cam-post engagement at 120° of the same patient.

Since bony geometry was not available, a flexion axis was defined by a line connecting the two femoral component peg tips (Fig 6.2). Anterior-posterior femoral translation was measured at the center of the flexion axis. Internal-external rotation was defined as the rotation of the flexion axis when projected onto the tibial plateau. Tibiofemoral contact was defined as the overlapping of the femoral component surface with the polyethylene articular surface (Li, Suggs et al. 2006). The center of the overlapping area was defined as the contact point. The locations of the contact point at the medial and lateral compartments along the flexion path defined the tibiofemoral articular contact kinematics.

The in-vivo three-dimensional cam-post contact was then determined by directly analyzing the overlap of the surface models of the cam and post (Li, Suggs et al. 2006). Figure 6.1 shows the cam-post contact for two in-vivo positions of a patient. The flexion angle where the cam-post contact was first detected did not represent the true cam-post engagement angle since the knee was imaged at discrete flexion positions. Therefore, in this paper, the cam-post engagement angle was defined as the flexion angle midway between two positions, one at the first detected cam-post contact and the one immediately before the initial cam-post contact.

Standing X-rays of the operated knee in the sagittal plane were obtained from the patient's clinical records. These X-rays were used to determine the tibial component slope and femoral component flexion relative to the corresponding tibial and femoral shafts (Hanson, Suggs et al. 2007). Femoral components placed in flexion and posterior tibial slope were defined as positive (Figure 6.3).

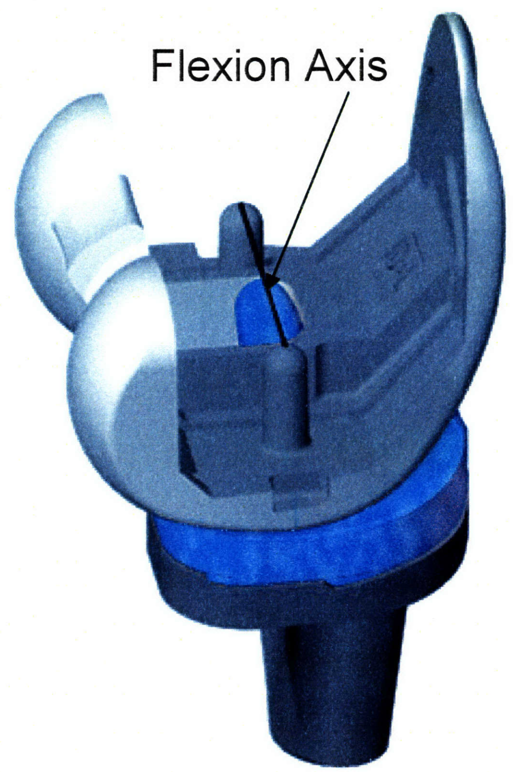

Fig. 6.2 Definition of the flexion axis of the femoral component.

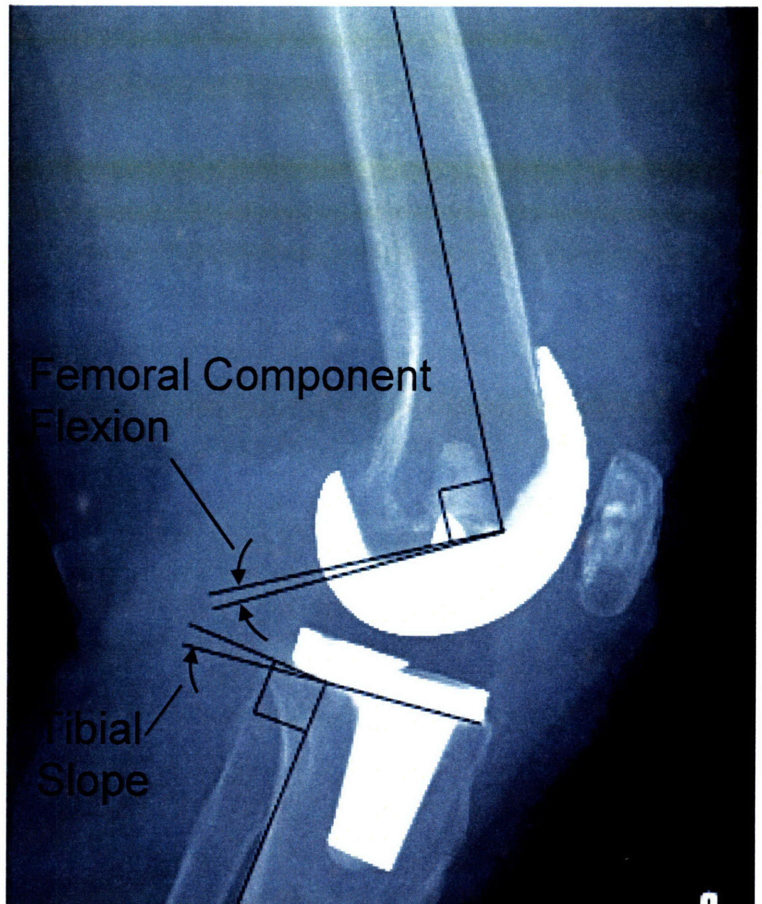

Fig. 6.3 Sagittal plane image of a patient was used to define femoral component flexion angle and tibial slope.

Statistical Methods

For this study, we reported posterior femoral translation, internal tibial rotation, tibiofemoral articular contact kinematics, and the flexion angle where cam-post engagement was observed. The maximum passive and active flexion angles were also reported. Kinematic data under weight-bearing was reported at hyperextension, 0° through 90° in 15° intervals, and at maximum flexion. Only patients having more than 3° of hyperextension were included in the values reported at hyperextension. Similarly, only patients who achieved flexion beyond 100° were included in the values reported at maximum flexion. Anterior-posterior (AP) and medial-lateral (ML) translations were normalized to the AP and ML dimensions of the polyethylene tibial insert. The Pearson product-moment was used to examine possible correlations between the cam-post engagement angle and maximal flexion angle and to evaluate what kinematic factors may affect the timing of cam-post engagement. Differences between groups were examined using the Independent T-test. Differences between values within a group were evaluated using the Dependent T-test. Statistically significant differences were indicated when $p < 0.05$.

6.3 Results

6.3.1 Flexion Range

The minimum and maximum passive flexion for all the U. S. patients was 0.6 ± 1.7° and 118.1 ± 14.2°, respectively. The minimum and maximum component flexion under weight-bearing averaged -3.6 ± 7.5° and 111.0 ± 19.2° (Table 6.1). These patients did not demonstrate a statistical difference between passive ROM (118.6 ± 14.0°) and active ROM (113.3 ± 19.4°, p = 0.7, power = 14%). Twelve knees demonstrated more than 3° of hyperextension under weight-bearing. The South Korean patients demonstrated a minimum and maximum passive flexion of 0.0 ± 4.2° and 142.5 ± 6.4°, respectively. The average minimum weight-bearing flexion angle for these patients was -5.0 ± 6.7°, and the average maximum weight-bearing flexion angle was 112.5 ± 13.1°. The passive ROM was significantly greater than the weight-bearing ROM (p < 0.0001). The South Korean patients demonstrated a significantly greater passive ROM than the U. S. patients (p < 0.0001), but no difference was detected in active ROM (p = 0.64, power = 12%).

6.3.2 Six Degree-of-Freedom Kinematics

At hyperextension in the U. S. patients, the femoral component center was 2.1 ± 1.7 mm anterior to its reference position (Fig 6.4A). As the knee flexed, the femur moved anteriorly and reached a peak anterior position of -6.9 ± 1.5 mm at

30° of flexion. Beyond 30° of flexion the femoral component consistently translated posteriorly. From 30° to 90° of flexion, the femoral component translated posteriorly by about 7 mm to a position of -0.2 ± 1.6 mm. From 90° to maximal flexion, the femoral component translated posteriorly to 13.0 ± 4.3 mm. At hyperextension, the tibia was externally rotated by 3.0 ± 4.3° (Fig 6.4B). As the knee flexed, the tibia consistently rotated internally and reached peak internal tibial rotation of 5.3 ± 5.1° at 90° of flexion. Beyond 90° of flexion, the internal tibial rotation was slightly reduced to 3.3 ± 4.2° at maximal flexion.

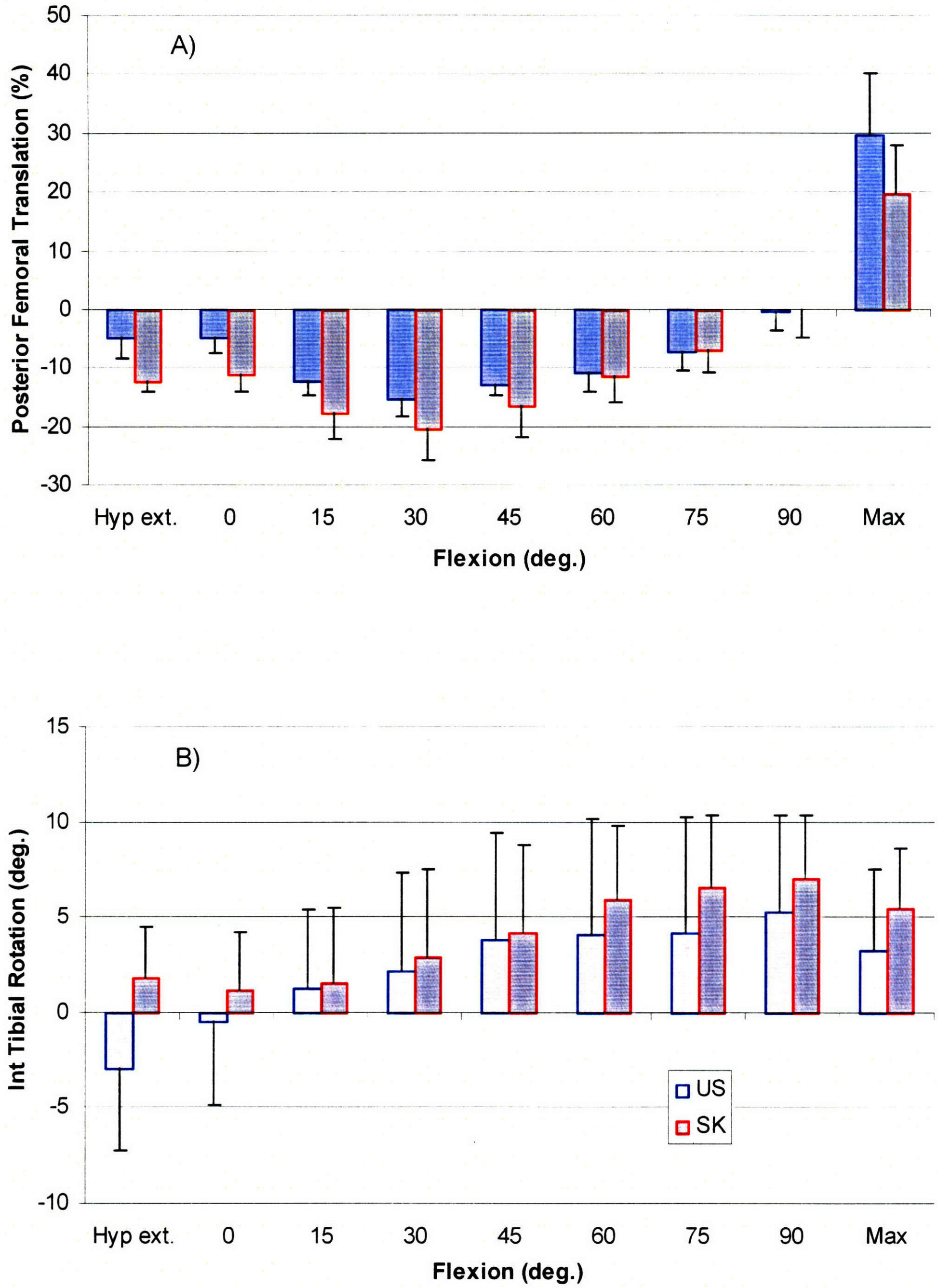

Fig. 6.4 A) Posterior femoral translation and **B)** internal tibial rotation of the knee during active flexion.

In the South Korean patients, the femur moved anteriorly from -5.1 ± 0.7 mm at hyperextension to -8.5 ± 2.3 mm at 30° of flexion. The femur then steadily moved posteriorly throughout the rest of flexion, reaching -0.1 ± 2.1 mm at 90° of flexion and 8.2 ± 3.2 mm at maximum flexion. The tibia of the South Korean patients internally rotated approximately 1.5° at early flexion. The tibia rotated internally with flexion to 7.0 ± 3.3° of internal rotation at 90° of flexion. The internal rotation was 5.4 ± 3.2° at maximum flexion.

The femur in the South Korean patients was more anterior than in the U. S. patients from hyperextension to 30° of flexion ($p < 0.02$). No difference was detected in anterior-posterior position of the femur throughout the rest of flexion. The South Korean patients tended to exhibit greater internal tibial rotation than the U. S. patients throughout the flexion range, but this difference was not statistically significant.

6.3.3 Tibiofemoral contact kinematics

In the medial compartment of the U. S. patients, the contact location was near the center of the medial tibial surface at hyperextension of the knee (Fig 6.5, Table 6.2). Along the anterior-posterior direction, the contact location was slightly posterior to the midline at -0.4 ± 6.2 mm. The contact location moved posteriorly with flexion until 30° (-4.4 ± 3.3 mm) and then anteriorly until 75° of flexion (-1.0 ± 3.4 mm). The contact point then moved posteriorly again to -2.8 ± 3.5 mm at 90° of flexion. At maximal flexion, the contact location sharply moved posteriorly to

-15.0 ± 2.4 mm. In the medial-lateral direction, the contact location moved from an initial position on the half closer to tibial spine (-2.2 ± 4.5 mm) towards the center of the medial tibial surface and reached 1.0 ± 3.9 mm at 15° of flexion. It stayed close to the center of the medial tibial surface through 90° of flexion (1.1 ± 4.6 mm). It then moved towards the outer half and reached 2.6 ± 5.1 mm at maximal flexion.

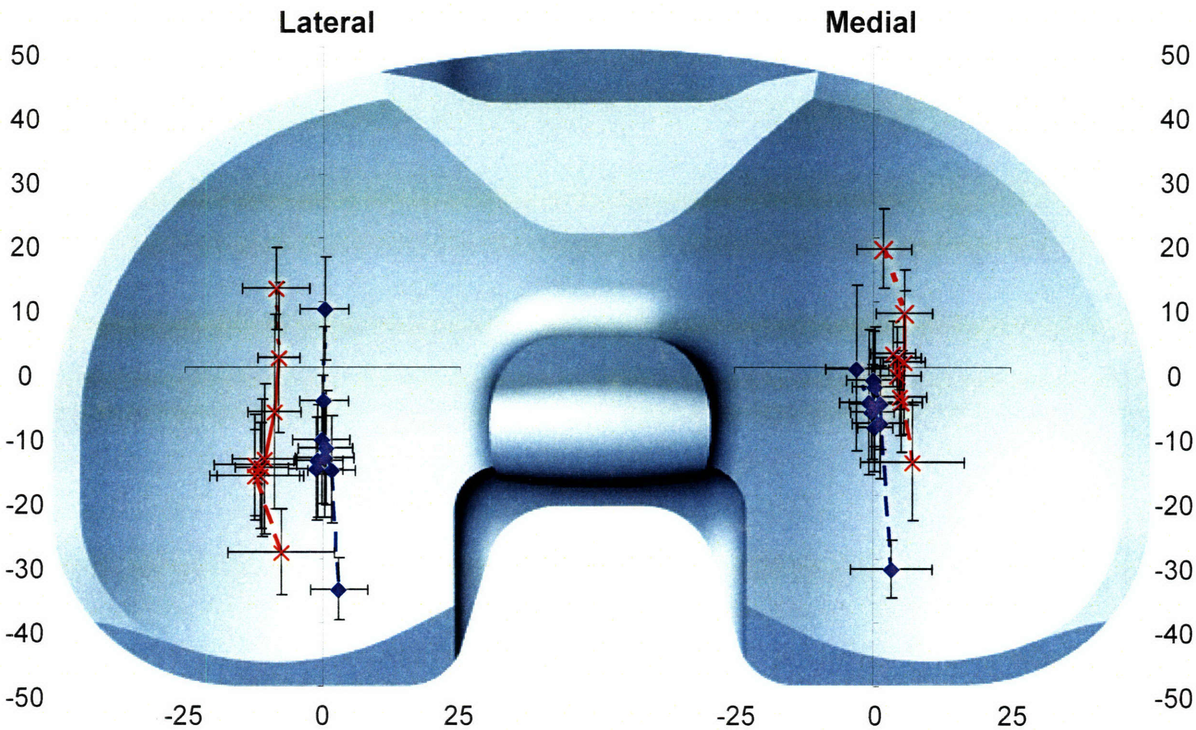

Fig. 6.5 Graphic of normalized tibiofemoral articular contact kinematics (%) in the medial and lateral compartments during weightbearing flexion for U.S. and South Korean knees.

Table 6.2: Tibiofemoral Contact Location in U. S. patients

Flexion	Lateral Compartment Medial	Lateral Compartment Anterior	Medial Compartment Medial	Medial Compartment Anterior
Hyperextension	0.4 ± 4.5	9.0 ± 8.0	-2.8 ± -5.7	-0.2 ± -12.9
0	0.2 ± 4.4	-5.3 ± -11.6	-0.6 ± -5.4	-5.5 ± -11.2
15	0.3 ± 5.3	-14.3 ± -9.2	1.3 ± 5.1	-8.7 ± -8.8
30	-0.8 ± -4.4	-14.7 ± -8.8	0.5 ± 3.1	-9.4 ± -7.0
45	-1.2 ± -4.9	-16.0 ± -7.9	0.0 ± -3.9	-7.1 ± -7.4
60	0.6 ± 5.0	-12.6 ± -8.9	0.4 ± 4.1	-3.2 ± -9.4
75	-0.2 ± -5.1	-11.4 ± -10.0	0.2 ± 4.9	-2.1 ± -7.5
90	1.6 ± 4.3	-16.1 ± -8.3	1.4 ± 5.7	-5.8 ± -7.1
Max Flexion	3.0 ± 5.1	-34.7 ± -5.0	3.4 ± 7.4	-31.6 ± -4.5

Table 6.3: Tibiofemoral Contact Location in S. K. patients

Flexion	Lateral Compartment Medial	Lateral Compartment Anterior	Medial Compartment Medial	Medial Compartment Anterior
Hyperextension	-8.4 ± -6.1	12.2 ± 6.5	1.9 ± 5.0	18.4 ± 6.2
0	-8.0 ± -3.7	1.3 ± 11.7	5.7 ± 5.0	8.3 ± 6.8
15	-8.8 ± -4.8	-7.0 ± -15.1	5.8 ± 3.8	0.7 ± 11.2
30	-10.6 ± -5.8	-14.5 ± -11.7	5.3 ± 3.7	-5.5 ± -8.0
45	-11.0 ± -4.8	-15.8 ± -10.8	4.9 ± 4.8	-4.7 ± -6.1
60	-11.2 ± -7.8	-17.0 ± -8.2	4.5 ± 4.2	-1.4 ± -5.2
75	-12.2 ± -7.5	-15.4 ± -8.0	3.7 ± 4.1	2.0 ± 5.0
90	-12.3 ± -8.0	-17.0 ± -7.0	4.4 ± 4.3	1.4 ± 4.8
Max Flexion	-7.5 ± -9.6	-29.0 ± -6.7	7.3 ± 9.3	-15.0 ± -9.0

In the lateral compartment, the contact point was anterior to the center of the lateral tibial surface at hyperextension of the knee (Fig 6.5). Along the anterior-posterior direction, the contact location was at 4.2 ± 3.6 mm. The contact location moved posteriorly with flexion until 45° (-7.4 ± 3.7 mm) and then anteriorly until 75° of flexion (-5.2 ± 4.7 mm). The contact point then moved posteriorly again to -7.5 ± 3.9 mm at 90° of flexion. At maximal flexion, the contact location sharply moved posteriorly to -16.5 ± 1.9 mm. In the medial-lateral direction, the contact location stayed close to the center of the lateral tibial surface from hyperextension (0.2 ± 3.0) through 90° of flexion (1.2 ± 3.3 mm). It then moved towards the inner half to 2.3 ± 4.0 mm at maximal flexion.

The contact in the medial compartment of the South Korean patients started 8.9 ± 2.5 mm anterior to the midline at hyperextension (Table 6.3). The contact moved posteriorly with flexion until 30° of flexion where it reached -1.0 ± 3.3 mm. The contact point then stayed close the center of poly through 90° where the contact was at 1.8 ± 2.1 mm. After 90°, the contact moved posteriorly to -5.0 ± 3.8 mm at maximum flexion. The contact position in the medial compartment was relatively constant in the medial-lateral direction. At hyperextension, the contact was 1.1 ±3.1 medial to the centerline and remained approximately 3.0 mm medial to the center line from 0° to 90° of flexion. At maximum flexion, the contact was 4.6 ± 5.9 mm medial to the center line.

The contact in the lateral compartment moved posteriorly from 6.3 ± 2.6 mm at hyperextension to -5.8 ± 3.4 mm at 60° of flexion. The contact remained there until 90° of flexion and then moved farther posterior to -10.7 ± 2.8 mm. Similar to the contact in the medial compartment, the contact in the lateral compartment was relatively constant in the medial-lateral direction, starting approximately 5 mm lateral to the center line at early flexion, moving slightly more lateral to -7.6 ± 4.8 mm at 90° of flexion, and then moving slightly medial to -4.6 ± 6.3 mm at maximum flexion.

The contact point in the medial compartment was more anterior in the South Korean patients throughout the entire flexion range. It was also more medial in the South Korean patients from 0° to 90° of flexion. In the lateral compartment, the South Korean patients exhibited more anterior contact only at early flexion ($p < 0.023$). The contact in the lateral compartment was more lateral in South Korean patients throughout flexion ($p < 0.0001$).

6.3.4 Cam-Post Engagement

Seventeen of the eighteen U. S. knees demonstrated cam-post engagement. The one patient who did not have cam-post engagement had a maximum flexion angle of 90°. For the 17 knees with engagement, initial cam-post contact occurred between 69° and 98°. The mean flexion angle where the cam-post engagement was observed was 86.2 ± 8.6°. For the South Korean patients, 21 of the 24 patients demonstrated cam-post engagement. The 3 patients that did not have cam-post engagement achieved maximum flexion angles of 78°, 85° and 116°. In the other 21 patients, cam-post engagement occurred between 69° and 114°. Post-cam engagement was observed at an average of 91.1 ± 10.9in these patients. For all patients, the cam-post contact was first observed at the posterior-medial corner of the tibial post (Fig 6.2A). At higher flexion after cam-post engagement, the contact began to cover more of the posterior aspect of the post (Fig 6.2B). The subject with the greatest maximal flexion, which was 135°, showed cam-post disengagement at the maximal flexion position.

The data suggested a possible correlation between the initial cam-post contact angle and the maximum flexion angle (Figure 6.6). When including all the U. S. patients, the correlation between maximum flexion and cam-post engagement is $r = 0.362$ ($p = 0.153$). After removing one outlier, the correlation coefficient increases to $r = 0.512$ ($p = 0.043$). When looking at just the South Korean patients, the correlation was $r = 0.505$ ($p = 0.019$). When combining the two groups, the correlation was $r = 0.378$ ($p = 0.019$). The correlation curve indicated that patients might have lower maximal flexion if the cam-post engaged at a lower flexion angle.

On average, the femoral component was placed in $0.9 \pm 3.1°$ of flexion. The slope of tibial component was $3.4 \pm 2.5°$. Flexion of the femoral component was not shown to correlate to the initial cam-post contact angle ($R = 0.35$, $p = 0.32$). The tibial slope was also not found to affect the cam-post contact ($R = 0.39$, $p = 0.27$).

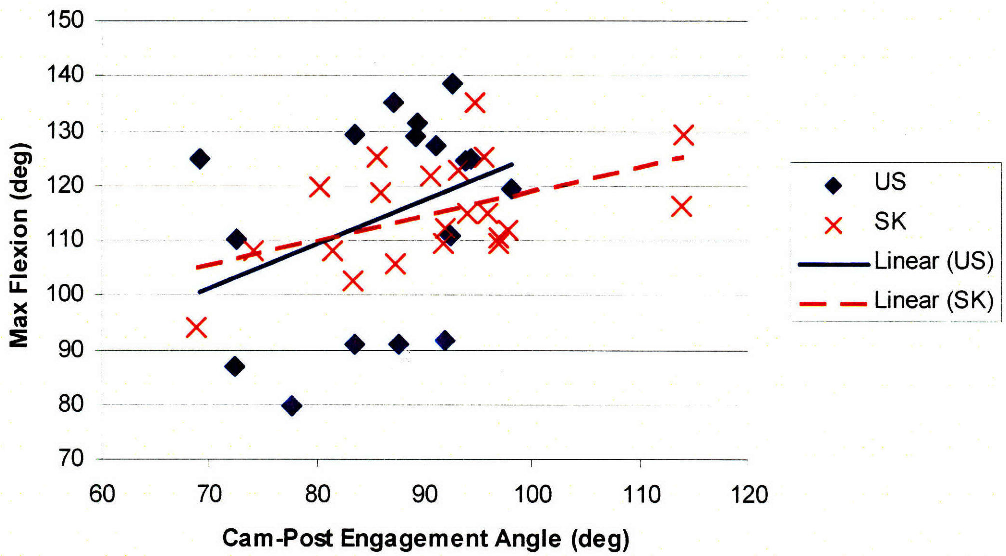

Fig. 6.6 Correlation between cam-post engagement angle and maximum knee flexion angle for U. S. and South Korean patients.

6.4 Discussion

This study investigated the in-vivo kinematics of posterior substituting total knee arthroplasty during a weightbearing flexion. Posterior femoral translation, internal tibial rotation, and tibiofemoral articular contact kinematics as well as the timing of cam-post engagement were determined. A mean maximum active flexion angle of 113.3° and 112.5° was measured for these groups of U. S. and South Korean patients, which is similar to those reported in the literature (Anouchi, McShane et al. 1996; Emmerson, Moran et al. 1996; Ranawat, Luessenhop et al. 1997; Ritter, Harty et al. 2003; Aglietti, Baldini et al. 2005; Capeci, Brown et al. 2006). However, our data on cam-post engagement did not prove our hypothesis that earlier engagement of cam-post would enhance flexion of the posterior substituting total knee arthroplasty. Rather, the data suggested that later cam-post engagement might be beneficial to flexion.

Most biomechanical investigations of posterior substituting total knee arthroplasties have focused on anterior-posterior translation of the medial and lateral femoral condyles (Banks, Markovich et al. 1997; Dennis, Komistek et al. 1998; Dennis, Komistek et al. 2003; Lee, Matsui et al. 2005; Victor, Banks et al. 2005; Catani, Fantozzi et al. 2006; Fantozzi, Catani et al. 2006). These studies involved different activities, such as sitting and rising from a chair (Fantozzi, Catani et al. 2006), knee bends (Dennis, Komistek et al. 1998), and step-up maneuvers (Banks, Markovich et al. 1997). Our data indicated that up to 90° of flexion, the contact point in the lateral compartment had a larger excursion than that in the medial compartment (Fig 6.5). This may be indicative of a "medial pivot" during knee flexion and is consistent with previous studies. However, both compartments showed large posterior translation beyond 90° of flexion. In addition, our data showed that the contact points also moved in the medial-lateral direction during flexion.

Even though the kinematics of posterior substituting total knee arthroplasty has been studied extensively, no data has been reported on the timing of in-vivo cam-post engagement. Previous in-vitro robotic tests using cadaveric knees measured cam-post contact forces during knee flexion under simulated muscle loads (Li, Most et al. 2002). The in-vitro data showed that cam-post engagement occurred between 60° and 90°. On average, our in-vivo data showed that cam-post engagement occurred at 85° and 91° in these groups of patients. Despite the fact that the in-vivo loading conditions of this study were different from those simulated in the robotic experiment, the ranges of knee flexion at which cam-post engagement was observed were similar between the in-vitro study and the U. S. patients in the current study. The South Korean patients tended to have cam-post engagement later in flexion than the U. S. patients, although a statistical difference could not be detected ($p = 0.12$, power = 30%)

Cam-post engagement has been widely thought to be a factor in increasing posterior femoral translation and thus enhancing knee flexion (Argenson, Scuderi et al. 2005). Our data showed a sharp increase in posterior translation of the femur and tibiofemoral contact locations beyond 90° of flexion, right after the cam-post engagement. The data also indicated that cam-post engagement corresponded to a reduction in internal tibial rotation at high flexion. Initial cam-post contact was always observed at the medial corner of the post in this study (Fig 6.2). The cam-post contact at the medial corner of the post might cause an external rotational moment on the tibia. After the initial cam-post engagement, the cam-post contact tended to cover more of the posterior aspect of the post with further flexion of the knee, which corresponds to the reduced internal tibial rotation at flexion angles after 90°. This phenomenon was similar to our previous observation in normal knees where internal tibial rotation was noted to be slightly reduced at high flexion angles (Li, Papannagari et al. Accepted). These data showed that cam-post engagement did alter joint kinematics at high flexion of the knee. However, no articular contact reached the posterior edge of the tibial component at maximal flexion angles in this group of patients.

Even though the timing of cam-post engagement did provide posterior femoral translation, it is interesting to note that the *timing* of the cam-post engagement did not have a strong effect on maximal flexion. As demonstrated in Fig 6.6, the data suggested a mild, positive correlation between the cam-post engagement flexion angle and the maximal flexion angle of the knee. This implied that later cam-post engagement might indicate a more conducive environment for greater flexion of the knee. A power analysis showed that the current subject number only had 40% power to detect a correlation with $R = .50$ between cam-post engagement and maximal flexion angles. To enhance the statistical power to 80%, 28 subjects will be needed.

The data on cam-post engagement and knee kinematics implied the importance of controlling the timing of cam-post engagement in the posterior substituting total knee arthroplasty. In general, component positioning during implantation, as well as the geometry of the component, has been thought to affect cam-post engagement. The flexion of the femoral component and the tibial slope were not found to affect the cam-post engagement timing in this study. A power analysis demonstrated that the subject number of this study only has 27% power to analyze the effect of femoral component flexion and tibial slope on the timing of cam-post engagement. More subjects need to be recruited to reach a conclusion on the effect of component orientations on initial cam-post engagement flexion angle. Other parameters that might also influence cam-post engagement timing include the components' anteroposterior translation and internal/external rotation relative to the bone during surgical implantation. These parameters, however, are difficult to obtain in post-operative total knee arthroplasty patients. A CT scan to determine the relative component positions inside the knee joint is necessary to define the relevant parameters that may affect the timing of the cam-post engagement.

Cam-post disengagement was observed in two knees in the U. S population and 3 knees in the South Korean population. Generally, the disengagement occurred between 120° and 135° of flexion. This phenomenon was consistent with a previous in-vitro cadaveric study (Li, Most et al. 2004), where consistent disengagement of the cam-post mechanism was observed when the knee flexed beyond 135° on a robotic testing system. An explanation for this phenomenon was that the compression of posterior soft tissue pushed the tibia anteriorly and separated the femoral component from the tibial component, thus causing disengagement of the cam-post mechanism. The compression of posterior soft tissues may play an important role in knee joint stability at high flexion angles.

There are some limitations to the current study. Only a single total knee arthroplasty design was investigated. Also, the knee flexion was imaged in discrete flexion angles. Therefore, the determined angles of cam-post engagement did not represent the exact beginning of the cam-post contact. Employing continuous imaging with the dual-orthogonal fluoroscopic imaging system would allow more accurate determination of the cam-post engagement angle. However, this would also increase the radiation dosage to the patients. Another limitation is that the component positions and rotations were not known relative to the tibial and femoral bones in 3 dimensions, so an accurate explanation of the mechanism of cam-post contact timing is difficult to obtain. Despite these potential limitations, our study provided the first quantitative data on the in-vivo cam-post engagement timing during weightbearing flexion.

In conclusion, this study investigated the in-vivo kinematics and cam-post engagement of a posterior substituting total knee arthroplasty in a U. S. cohort and a South Korean cohort of patients. The South Korean patients had significantly greater passive ROM, but no difference was detected in active ROM between the populations. This suggests that muscle activity, especially in the extensor mechanism, may play a significant role in limiting knee flexion. The kinematic data indicated that the cam-post did engage during in-vivo knee flexion and that cam-post engagement affected the kinematics of the knee during flexion. The timing of the cam-post engagement was suggested to have a mild correlation with the maximal flexion angle of the knee. In the future, the factors that affect cam-post engagement timing should be established in hopes of improving the flexion capability of the knee after posterior substituting total knee arthroplasty.

Chapter 7. Distribution of Maximum Flexion Following Total Knee Arthroplasty

7.1 Introduction

Total knee arthroplasty has been a successful treatment for alleviating pain and dysfunction resulting from severe cartilage degeneration (March, Cross et al. 1999; Bachmeier, March et al. 2001; Mahomed, Liang et al. 2002). However, TKA patients have not reached the same level of function as their peers (Finch, Walsh et al. 1998; March, Cross et al. 1999; Mizner, Petterson et al. 2005; Noble, Gordon et al. 2005). Achieving full range of flexion has been one of the major goals in total knee arthroplasty. It has been reported that 50% or more of TKA patients participate in activities such as kneeling and gardening or feel such activities are important but have difficulty performing them (Weiss, Noble et al. 2002). Even though there are several activities that require higher flexion (Laubenthal, Smidt et al. 1972; Szabo, Lovasz et al. 2000), it has been suggested that 110° of flexion is an appropriate goal for rehabilitation following TKA (Rowe, Myles et al. 2000).

Over the years, many studies have reported on the average maximum flexion for various patient cohorts (Table 7.1) (Insall, Hood et al. 1983; Aglietti, Buzzi et al. 1988; Goldberg, Figgie et al. 1988; Lee, Keating et al. 1990; Rosenberg, Barden et al. 1990; Malkani, Rand et al. 1995; Anouchi, McShane et al. 1996; Emmerson, Moran et al. 1996; Ranawat, Luessenhop et al. 1997; Dennis, Komistek et al. 1998; Kawamura and Bourne 2001; Bellemans, Banks et al. 2002; Banks, Bellemans et al. 2003; Kotani, Yonekura et al. 2005; Matsumoto, Tsumura et al. 2005; Victor, Banks et al. 2005). The average maximum flexion angle for TKA patients remains between 100° and 115°, regardless of the type of components used. While the average maximal flexion is getting close to meet the requirement of most daily activities, all these data have showed either a large standard deviation or a wide range of the maximal flexion angles existing among the patients. This indicated that half of the patients could flex beyond the averaged maximal flexion angle, and the other half could not reach the averaged maximal flexion angle and might not achieve the goal of rehabilitation. The distribution of the maximal flexion angles of the patient population has not been investigated in literature, even though numerous studies examining high flexion of the knee after TKA have sought to correlate various surgical and kinematic factors with flexion (Parsley, Engh et al. 1992; Harvey, Barry et al. 1993; Anouchi, McShane et al. 1996; Lizaur, Marco et al. 1997; Schurman, Matityahu et al. 1998; Bellemans, Banks et al. 2002; Kurosaka, Yoshiya et al. 2002; Matsumoto, Tsumura et al. 2005; Evans, Parsons et al. 2006). Information about the distribution of maximum flexion may be invaluable for improving surgical technique for the purpose of enhancing knee flexion after TKA.

In this study we hypothesized that the maximal flexion angles of TKA patients follow a normal distribution. Further, the averaged maximal flexion angle cannot be used to represent the flexion capability of a patient cohort. The objective of this study was to investigate the distribution of maximum flexion after TKA using various cruciate retaining (CR) and posterior substituting (PS) designs. Knee scores were also analyzed to help assess the degree of functional limitation experienced by patients with lower flexion.

Table 7.1: Reported Range of Motion for Various Types of Total Knee Designs

Authors	Follow-Up	Design	No. of Knees	Flexion
		Crucitate-Sacrificing		
Bhan, Malhotra et al. 2006	6 years	LCS (Depuy)	32	105.6±7.7°
Goldberg, Figgie et al. 1988	9 years	Total Condylar	109	101° (15° - 115°)
Insall, Hood et al. 1983	6.5 years	Total Condylar	100	89° (no range)
Myles, Rowe et al. 2002	1.7 years	LCS (Depuy)	42	96.9±13.2°
Ranawat, Flynn et al. 1993	13.2 years	Total Condylar	62	99° (65° - 120°)
		Cruciate-Substituting		
Aglietti, Baldini et al. 2005	3 yrs	LPS	107	112°(93° - 130°)
Aglietti, Buzzi et al. 1988	5.5 years	Insall-Burstein	73	96° (70° - 120°)
Anouchi, McShane et al. 1996	2 years	Advantim	86	107±10°
Banks, Bellemans et al. 2003	1 year	Duracon, Genesis 2, Scorpio	29	121±8°
Bhan, Malhotra et al. 2006	6 years	IB-II	32	106.9±7.8°
Capeci, Brown et al. 2006	2.8 yrs	IB-II, LPS, LPS-Flex	506 (253 bilaterals)	115° (no SD or range)
Dennis, Komistek et al. 1998		Press-fitCondylar	20	127° 113° Active
Emmerson, Moran et al. 1996	12.7 years	Kinematic Stabilizer	109	98±18° (25° - 130°)
Gupta, Ranawat et al. 2006	1 yr	PFC Sigma RP	50	116° (90-130)
	1 yr	PFC Sigma RP-F	50	125° (105-150)
	Early	PFC Sigma RP	24	118°(95-140)
	Early	PFC Sigma RP-F	24	128° (115-145)
Lee, Matsui et al. 2005	2.5 years	P.F.C Sigma	18	
Ranawat, Luessenhop et al. 1997	4.8 years	Press-fitCondylar	125	111° (75° - 135°)
Ritter, Harty et al. 2003	7 years	AGC	4727	113±12°
Teeny, York et al. 2005	1 yr	PFC Sigma (mostly)	110	118°

***All flexion values are for passive flexion unless otherwise noted**

Continued on next page

Table 7.1 cont'd: Reported Range of Motion for Various Types of Total Knee Designs

Authors	Follow-Up	Design	No. of Knees	Flexion
		Cruciate-Retaining		
Aglietti, Baldini et al. 2005	3 yrs	MBK	103	108°(75° - 130°)
Banks, Bellemans et al. 2003	1 year	Duracon, Foundation, Genesis 2, Profix, Scorpio	63	109±11°
Bellemans, Banks et al. 2002	2-5 years	Profix	150	106±17°
Bertin, Komistek et al. 2002		CR, NexGen	20	128°
Bertin, 2005	5-7 years	CR, NexGen	251	123°
Dennis, Clayton et al. 1992	11 years	CruciateCondylar	42	104° (76° - 120°)
Dennis, Komistek et al. 1998		Press-fitCondylar	20	123°
				103° Active
Evans, Parsons et al. 2006	2 years	PFC Sigma RP	97	116±15°(50-135)
	2 years	PFC Sigma FB	100	113±11°(85-140)
Leach, Reid et al. 2006	1 year	PFC CRRP	55	114°
Lee, Keating et al. 1990	9 years	CruciateCondylar	144	106° (no range)
Lee, Matsui et al. 2005	2.5 years	P.F.C Sigma	18	
Malkani, Rand et al. 1995	10 years	KinematicCondylar	119	105±11°
Moro-Oka, Muenchinger et al. 2006	6 yrs	Natural-Knee, Zimmer GmbH	5	128° (120-140)
				107±9° lunge 109±13° kneeling
Rosenberg, Barden et al. 1990	3.5 years	Miller-Galante	116	105° (45° - 140°)
		Bi Cruciate-Retaining		
Cloutier, Sabouret et al. 1999	10 years		107	107±12.6°(65 - 135)
Moro-Oka, Muenchinger et al. 2006	6 yrs	N2C, Zimmer GmbH	9	129° (120-135) 104±17° lunge 104±16° kneeling
		Unspecified		
Miner	1 yr		684	110.4±14.6°

***All flexion values are for passive flexion unless otherwise noted**

7.2 Methods

7.2.1 Patient recruitment

Fourty-six knees were randomly recruited among patients who underwent total knee arthroplasty with various components. (15 NexGen CR, 14 NexGen CR-Flex, 12 NexGen LPS, 5 NexGen LPS-Flex, Zimmer Warsaw, IN). The study was IRB approved from our institution, and informed consent was obtained from each patient before testing. The cohort consisted of 13 females and 33 males and included 19 left knees and 27 right knees. The average age at the time of testing was 66.6±9.5 years, the average weight was 201.2±37.8 lbs, and the average height was 69.2±3.9 inches. These patients were studied at a mean 15.1±10.3 months postoperatively.

7.2.2 TKA component and surgery

The NexGen CR implant is a posterior cruciate retaining design, and the NexGen LPS is a posterior-substituting design. The LPS design has a more conforming tibiofemoral articulation than the CR design. The Flex models of both the CR and LPS designs have femoral components very similar to their conventional models, but more bone is removed from the posterior condyle in order to improve the articular contact in deep flexion (Li, Most et al. 2004; Most, Sultan et al. 2006). The Flex models also have an anterior cutout in the polyethylene insert to reduce tension in the patellar tendon during deep flexion. The intent of these design modifications was not to induce greater flexion but rather to better accommodate greater flexion when the patient is able to achieve it.

All surgeries were performed by two senior orthopaedic surgeons. A medial arthrotomy was used in all knees. The femur was cut in 5° of valgus and 3° of external rotation using intramedullary alignment and the epicondylar axis as a reference. The posterior femoral condyles and Whiteside's line were used as secondary references. The tibia was cut with a 7° posterior slope using extramedullary alignment. The tibial plateau, the junction of the medial and middle thirds of the tibial tuberosity and visible part of the tibial crest were used as references. Flexion and extension gaps, stability, range of motion, and patellar tracking were assessed during trial reduction. In cruciate-retaining knees, PCL tension was assessed by manual palpation and by checking for anterior lift-off of the tibial tray while flexing the knee. All knees received a metal-backed tibial component and a resurfaced patella. The femoral, tibial, and patellar components were cemented, and the extensor mechanism and skin were closed with sutures in a standard fashion.

7.2.3 Measurement of ROM

Each patient performed a single leg lunge from full extension to maximum flexion while being imaged by a dual fluoroscopic imaging system. The imaging system consisted of two fluoroscopes placed in an orthogonal manner (Fig 7.1). Each fluoroscope had a 12-inch diameter image intensifier and source-to-image distance of 1m (9800 series, GE Medical, Milwaukee, WI). Patients placed the knee of interest within view of both fluoroscopes such that images were acquired from the posteromedial and posterolateral directions. Beginning at full extension, patients performed the lunge to 15, 30, 45, and so forth until they could not flex their knee any further. Passive range of motion and Knee society scores were also recorded at the same visit.

A virtual fluoroscopic imaging system was created in a 3D modeling software (Rhinoceros). The fluoroscopic images were imported into the software and arranged to mimic the relative orientation of the intensifiers during image acquisition. Virtual cameras were placed to replicate the x-ray sources of the fluoroscopes. Both fluoroscopic images could be viewed from its respective camera simultaneously. CAD models of the implant components were obtained from the manufacturer and imported into the virtual imaging system. For each flexion angle, the femoral component and tibial plate were manipulated independently in 6 degrees-of-freedom until their silhouettes matched their contours on both fluoroscopic images. When the components matched their image contours, the in-vivo position was reproduced. The series of matched poses represented the in-vivo kinematics.

7.2.4 Data Analysis

Shapiro-Wilk's W test, the Jarque-Bera test, and Q-Q plots were used to assess the normality of the distribution of maximum flexion angles. Differences between groups was analyzed using ANOVA. Differences were considered significant when $p<0.05$.

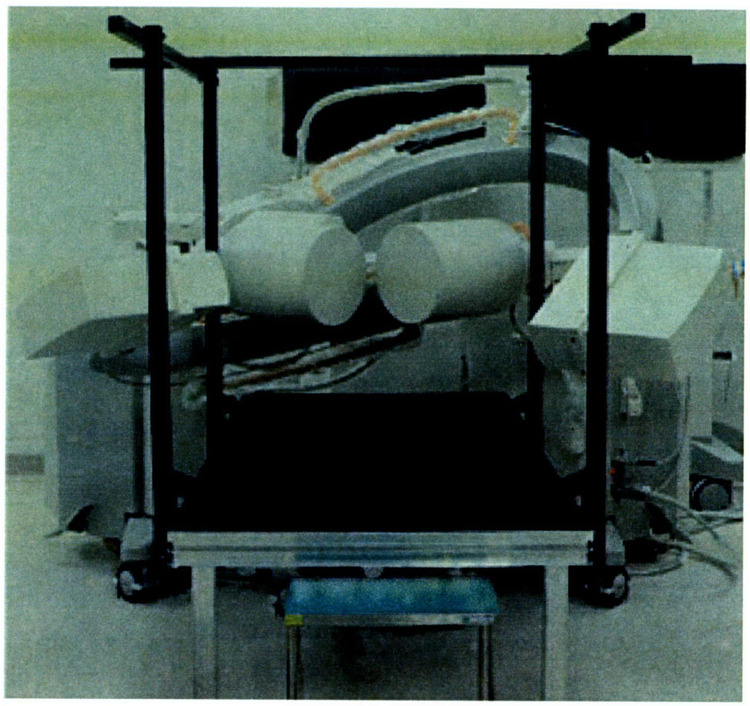

Fig. 7.1 Dual Orthogonal Fluoroscopic System

7.3 Results

7.3.1 Maximum Flexion

The CR patients reached an average maximum flexion angle of 110.1±13.4°. The maximum flexion for these patients ranged from 84.8° to 131.7°. The CR-Flex patients averaged a maximum flexion of 109.1±12.5° and ranged from 85.3° to 131.1°. The PS patients reached an average maximum flexion of 108.6±19.6° and ranged from 79.9° to 135.3°, while the PS-Flex patients had a mean maximum flexion of 113.0±19.5°, ranging from 90.2° to 129.1°. There was no difference in maximum flexion between component types.

When grouping all the knees together, the mean maximum flexion angle was 109.7±15.2° (Fig 7.2). Twenty-eight percent of all the knees reached maximum flexion below 100° with 11% not flexing past 90°. Twenty-two percent of the knees reached maximum flexion between 100° and 110°, and 24% reached their maximum between 110° and 120°. The remaining 26% were able to flex past 120° with 9% flexing past 130°. The Shapiro-Wilk's test yielded a W value of 0.95, and the Jarque-Bera test resulted in a JB statistic of 2.83, p=0.24. The QQ plot for the distribution of maximum flexion is shown in Fig 7.3. None of these tests suggest that the distribution of maximum flexion is not normally distributed.

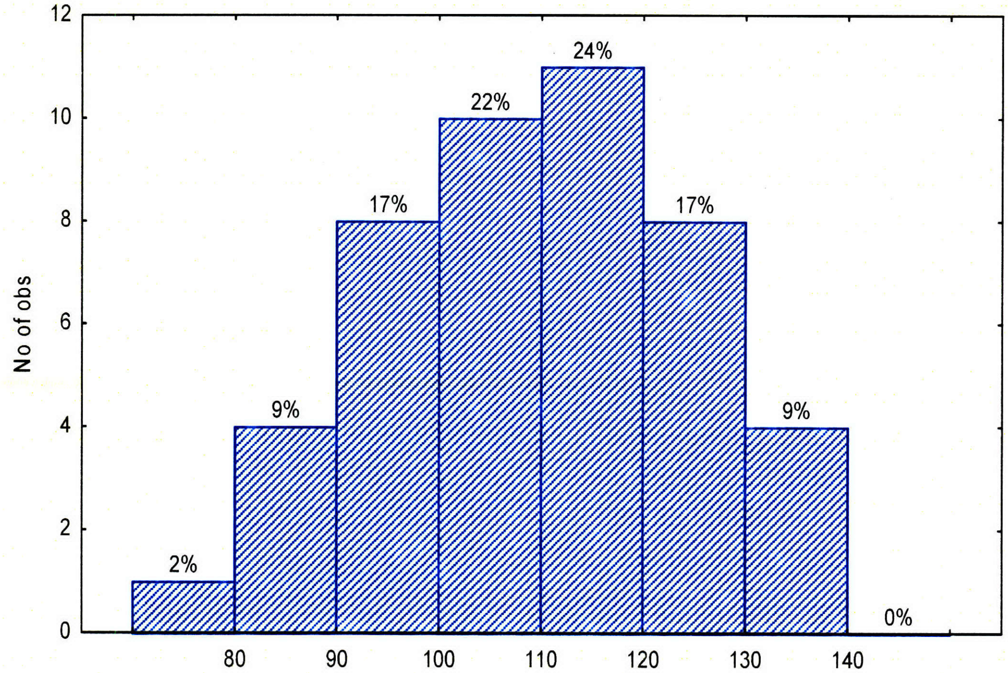

Fig. 7.2 Distribution of maximum flexion for all 46 patients

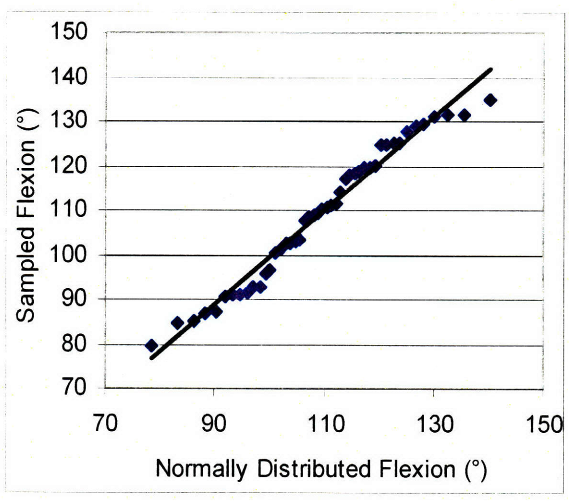

Fig. 7.3 Q-Q plot of maximum flexion

The average Knee score and functional score for all the knees was 89.5±12.6 and 85.4±13.6, respectively. The average knee score for the CR and CR-Flex knees was 91.4±13.2 and 91.2±10.8, respectively. The average Functional score was 84.9±14.4 and 86.9±14.2, respectively. The average knee score for the PS and PS-Flex knees was 86.2±15.9 and 87.3±7.3, while the average Functional score was 82.1±14.5 and 90.3±7.1, respectively. Knee score and Functional score did not vary between component types, but there was a correlation between Knee score and maximum flexion ($r = 0.51$, $p = 0.001$). No correlation was detected between Functional score and maximum flexion.

7.3.2 Lift-Off at Maximum Flexion

Out of the 46 knees, 18 demonstrated lift-off in either compartment with a maximum flexion of 117.5±13.0° and ROM of 124.9±15.9° (Table 7.2, Fig. 7.4). The remaining 28 knees demonstrated a significantly lower flexion and ROM of 104.8±14.3° and 109.8±18.5°, respectively. Knees that experienced lift-off in both the medial and lateral compartments or in the medial compartment alone demonstrated greater maximum flexion (122.5±8.3° and 120.4±13.9°, respectively) than knees with no lift-off ($p < 0.025$). Knees with lift-off only in the lateral compartment did not achieve any more flexion (112.7±15.2°) than knees with no lift-off ($p = 0.18$). No difference was detected in passive ROM between patients with lift-off and those without.

Table 7.2: Lift-Off and Maximum Flexion

	Lift-Off				
Compartment	Either	Both	Medial	Lateral	**No Lift-Off**
N	18	4	6	8	28
Max Flexion	117.5 ± 13.6° [a]	122.5 ± 8.3° [a]	120.4 ± 13.9° [a]	112.7 ± 15.2°	104.8 ± 14.3°
Active ROM	124.9 ± 15.9° [a]	126.9 ± 8.2°	126.5.1 ± 20.3°	122.7 ± 16.7°	109.8 ± 18.5°
Passive ROM	120.0 ± 13.7°	129.0 ± 5.3°	115.8.0 ± 20.2°	119.8 ± 8.9°	116.2 ± 12.4°

[a] Significantly different from all patients without lift-off

Fig. 7.4. In-vivo position of a patient exhibiting lift-off

7.4 Discussion

The range of motion after TKA has been an important index for clinical success of the surgery (Anouchi, McShane et al. 1996; Kawamura and Bourne 2001; Kim, Sohn et al. 2005; Rowe, Myles et al. 2005). Numerous studies have investaged the flexion capability of patients following TKA (Table 7.1). For example, Aglietti reported a mean range of motion of 96° in 73 patients after 5 and half years of follow-up (Aglietti, Buzzi et al. 1988). Lee et al reported that 144 knees had an average ROM of 106° at a mean of 9 years postoperatively (Lee, Keating et al. 1990). Malkani et al found a mean ROM of 105±11° in 119 knees at 10 years postop (Malkani, Rand et al. 1995). Emmerson reported that 109 knees had 98±18° at 12.7 years postop (Emmerson, Moran et al. 1996), and Anouchi et al reported that 86 knees had 107±10° of flexion at 2 years after surgery (Anouchi, McShane et al. 1996). Ritter et al reviewed 4727 patients and found a mean ROM of 113±12° at an average of 7 years postop (Ritter, Harty et al. 2003). Rowe et al. reported on a group of TKA patients with mean ROM of 96.1±13.7° (Rowe, Myles et al. 2005). Our data reported an averaged maximal flexion of 109.2±15.2°, which is similar to those reported in literature as shown in Table 7.1.

In general, the average maximum flexion of patients following TKA has remained between 100° and 115° degrees independent of the types of the TKA components used in these studies. This range of maximal flexion angles has been accepted to be a satisfactory outcome of the TKA operations, even though a wide range of knee flexion is required to perform several activities of daily living (Laubenthal, Smidt et al. 1972; Rowe, Myles et al. 2000; Myles, Rowe et al. 2002). Rowe et al reported a mean ROM of 138° in a group of healthy subjects with similar age to a typical TKA population (Rowe, Myles et al. 2000). They also measured the amount of knee flexion needed to perform several activities in the same group of subjects. They found that it takes 80° to 100° of flexion to navigate stairs, 90° to 100° of flexion to sit and rise out of a chair, and 120° to 140° to get in and out of the bath tub.

This study evaluated a randomly recruited patient cohort, including patients using both PS and CR TKA designs and found an average maximum flexion of 110 ± 15°. Both and mean and standard deviation of our data are very consistent with what has been reported in the literature (Table 7.1). The mean maximum flexion reached what has been deemed satisfactory, but almost a third of the patients could not flex their knee passed 100°, and a little over 10% could not flex passed 90°. Only about 25% of the patients could flex passed 120°. Some have questioned the use of ROM as an indicator of patient function (Miner, Lingard et al. 2003; Mizner, Petterson et al. 2005). In the current study, the functional score was not found to be correlated with maximum flexion, which also calls into question the importance of ROM. However, when comparing the distribution of maximum flexion with the values reported by Rowe et al, 10% to 20% of TKA patients would have difficulty managing stairs or getting up from a chair, and 75% of patients would not be able to take a bath. This observation is supported by reports of limited function in TKA patients compared to age-matched healthy subjects (Finch, Walsh et al. 1998; March, Cross et al. 1999; Mizner, Petterson et al. 2005; Noble, Gordon et al. 2005; Rossi, Hasson et al. 2006). On the other hand, our analysis showed that a quarter of the patients could flex beyond 120° using current TKA components. This implies that contemporary TKA design concepts might not be an obstacle for achieving high flexion in TKA patients. Instead, further investigation is necessary to examine the specific features of the patients who could not flex beyond the averaged maximal flexion. These data highlight the need to focus on giving satisfactory maximum flexion to those with limited flexion as opposed to giving even higher flexion to those with already high or satisfactory flexion.

A statistical analysis of the data indicates that maximum flexion values are normally distributed. This suggests two possibilities. The first possibility is that the factors that affect maximum flexion after TKA are being handled consistently, but the precision necessary to allow all patients to reach high flexion is beyond the means of the current techniques. This notion is similar to statements by Maloney and Schurman, who concluded that it is difficult to correlate postoperative ROM to any factor because so many factors may affect ROM (Maloney and Schurman 1992). The second possibility is that there is an unrecognized or simply uncontrolled factor that significantly affects maximum flexion, and the normal distribution of this factor leads to a normal distribution in maximum flexion. The fact that various modifications to contemporary TKA implants and techniques have not substantially increased maximum flexion makes this second possibility seem more likely.

The answer to alleviating limited flexion probably lies in the soft tissue structures remaining after TKA. This hypothesis is not new, but is motivated by several results from the literature, the most apparent being the very fact that all the component geometries and surgical techniques yield very similar results. The notion that preoperative flexion predicts postoperative flexion implies that the structures that limit flexion preoperatively are what limit flexion postoperatively. Several groups have reported a correlation between quadriceps length or strength and ROM (Matsumoto, Tsumura et al. 2005; Mizner, Petterson et al. 2005). Studies have also warned that overstuffing the knee can limit ROM (Laskin and Beksac 2004; Argenson, Scuderi et al. 2005; Mihalko, Fishkin et al. 2006).

In the current study, patients with lift-off had greater flexion than those without lift-off. One explanation involves the extensor mechanism. A tight extensor mechanism may prevent lift-off and may also limit flexion. Accordingly, the presence of lift-off would indicate a more lax extensor mechanism, which would allow more flexion. This is very convenient and reasonable interpretation for the active flexion data, but it does not work as well when considering the passive ROM. Presuming the extensor mechanism is more lax in the passive state than when it is active, we would expect to see passive ROM that is greater than active ROM. However, there was no difference between passive and active ROM in these patients. Besides the extensor mechanism, other soft tissues, such as the posterior cruciate ligament (PCL) or the medial collateral ligament (MCL) may also affect lift-off and flexion. A tight PCL or MCL could result in a stiff knee and limit the possibility of lift-off. Tibial slope could also have an impact on lift-off, greater posterior slope increasing the likelihood of lift-off. It is important to note that the observation of lift-off in patients with greater flexion does not necessarily indicate a casual relationship. The occurrence of lift-off could be a consequence of high flexion rather than an indicator or requirement for high flexion.

All of these factors point to soft tissues determining flexion after TKA, but there has been very little investigation into how the soft tissue around the knee affects maximum flexion, especially in the native knee. In an in-vitro study, Li et al found that the knee was very constrained at high flexion, but the contribution of the various structures around the knee was not discussed (Li, Zayontz et al. 2004). There is also a lack of information regarding the change in the structure of the knee from pre- to post-surgery and how this change affects maximum flexion. Kawamura et al found a 3mm elevation of the joint line and no change in the length of the patellar tendon before and after TKA based on standing radiographs (Kawamura and Bourne 2001). They did not discuss, however, any relationship between the joint line elevation and the function of the knee. At least part of the reason for this lack of information on these topics is a lack of tools that would enable researchers to explore them.

In conclusion, this study found that even when the averaged data seems satisfactory, a significant number of patients may still be limited in their function. This suggests that it may be more appropriate to report the data in separate groups, perhaps those with flexion above the mean and those with flexion below the mean. Further investigation is necessary to analyze the biomechanical factors that may be different between the patients having flexion capability below or above the mean flexion angle. The key to alleviating limited flexion may rest in the structures around the knee as opposed to the implant itself. Such an investigation may lead to future improvements in TKA that help patients with the most limited flexion achieve greater flexion.

Chapter 8. Initial Investigation of In-vivo Stress Distribution within the Polyethylene Tibial Insert

8.1 Introduction

Wear of the polyethylene tibial insert has been reported as one of the leading causes for revision of total knee arthroplasty (Hood, Wright et al. 1983; Bohl, Bohl et al. 1999; NIH 2000; Harman, Banks et al. 2001; Banks, Harman et al. 2002; Berzins, Jacobs et al. 2002; Sharkey, Hozack et al. 2002; NIH 2003; Vince 2003; Clarke, Math et al. 2004; Huddleston, Wiley et al. 2005; Morgan, Battista et al. 2005; Wright 2005). Currently, in-vivo wear data can only be obtained from retrieved components (Engh, Dwyer et al. 1992; Lewis, Rorabeck et al. 1994; Wasielewski, Galante et al. 1994; Blunn, Joshi et al. 1997; Wimmer, Andriacchi et al. 1998; Harman, Banks et al. 2001; Currier, Bill et al. 2005; Harman, Banks et al. 2007). Wear test machines have been used to analyze tibiofemoral wear patterns, but these methods have relied on estimates of in-vivo conditions (Blunn, Walker et al. 1991; Burgess, Kolar et al. 1997; Walker, Blunn et al. 1997; Ash, Burgess et al. 2000; DesJardins, Walker et al. 2000; Benson, DesJardins et al. 2002; Andriacchi, Dyrby et al. 2003; Laz, Pal et al. 2006; Rawlinson, Furman et al. 2006).

Several models of wear have been developed that use in-vivo data acquired by various means as input (Fregly, Sawyer et al. 2005; Laz, Pal et al. 2006; Rawlinson, Furman et al. 2006). The analyses that have used in-vivo data have typically obtained used that data to constrain some of the DOF in the model, while other DOF were left free or constrained by data from a different source. Retrieval studies have noted a large amount of variability in the observed wear patterns, suggesting that a patient specific approach may be more suitable for assessing in-vivo wear (Blunn, Joshi et al. 1997; Currier, Bill et al. 2005). Previous authors have suggested using a bi-plane, model matching technique to estimate in-vivo wear by measuring the penetration of the femoral component into the polyethylene surface (Kellett, Short et al. 2004; Gill, Waite et al. 2006Short, 2005 #266). The methodology presented in those studies, however, only allowed for the analysis of the knee in a standing position rather than during functional activities.

The ability to measure contact mechanics in-vivo would be very useful in improving TKA designs with regards to diminishing polyethylene wear. This work investigates the feasibility of using in-vivo kinematics obtained using Dual Fluoroscopy to drive finite element analysis of polyethylene insert with the goal of using this methodology to calculate the stress in the insert. First, a validation of the contact area calculation is performed followed by some preliminary estimates of the polyethylene stresses in 10 cruciate-retaining TKA patients.

8.2 Methods

8.2.1 Validation of Contact Area Measurement

One fresh frozen cadaver knee specimen was used in the validation. The specimen consisted of all the bone and soft tissue 25 cm above and below the joint line. The specimen was allowed to thaw overnight at room temperature. The bone ends were stripped of soft tissue and potted in bone cement while the tissue around the joint was left intact. A CR TKA (NexGen, Zimmer, Warsaw, IN) was implanted into the knee by an orthopaedic surgeon. The specimen was installed in a robotic system by rigidly fixing one bone to a pedestal and attaching the other bone to the end effector of a 6 degree-of-freedom (DOF) robot (UZ150, Kawasaki Heavy Industry, Japan) through a 6 DOF load cell (JR3 Inc., Woodland CA, Fig. 8.1). The robot was used to apply a 400N compressive load through the knee and determine the equilibrium of the knee under the compressive load (Most 2000; Suggs, Li et al. 2006).

After the knee position under the compressive load was recorded, the soft tissue was dissected in a manner that allowed the tissue to be wrapped around the knee. The bones were then separated to allow easy access to the articulating surfaces. A fast setting silicone rubber ("Quick-Set" RTV Silicone mold-making rubber Base, Alumilite Corp., Kalamazoo, MI; Dow Corning 4 Catalyst, Dow Corning Corp., Midland, MI) was applied to the articular surfaces, and the bones were returned to their position under the 400N compressive load (Fig 8.2). Dual fluoroscopic images were acquired simultaneously using two fluoroscopes placed orthogonally to each other (Li, Suggs et al. 2006). After the silicone rubber set, the bones were again displaced to allow access to the articular surfaces. The area where the silicone had been displaced by contact between the polyethylene and the femoral component was outlined using a three-dimensional digitizing stylus (MicroScribe-3DX, Immersion Corporation, CA) (Fig. 8.3). CAD models were matched to the fluoroscopic images, and the resulting contact areas were compared to the digitized area.

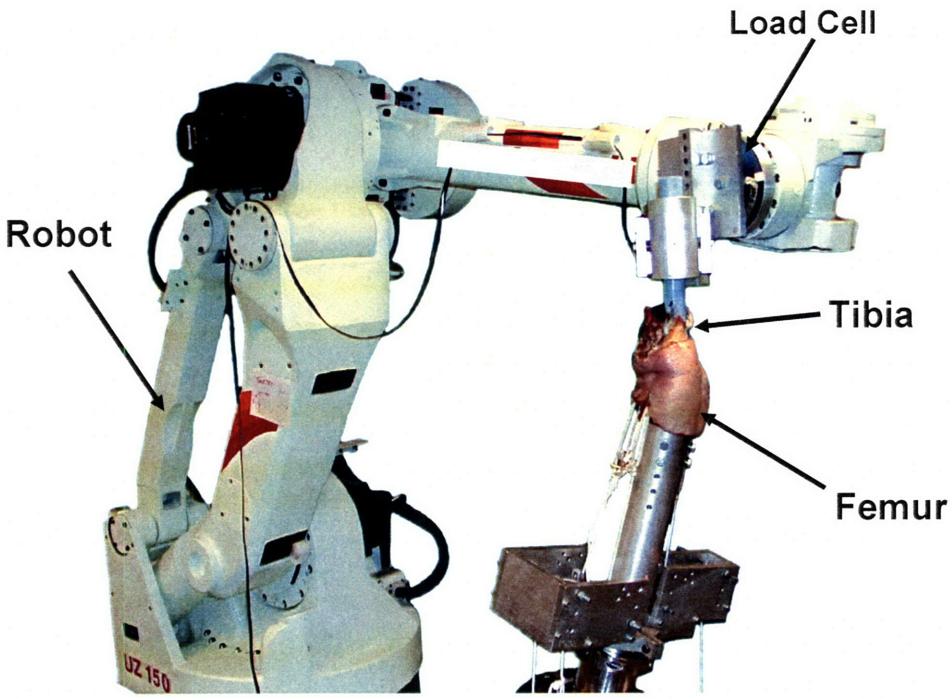

Fig. 8.1 A cadaver knee specimen installed on the Robotic testing system

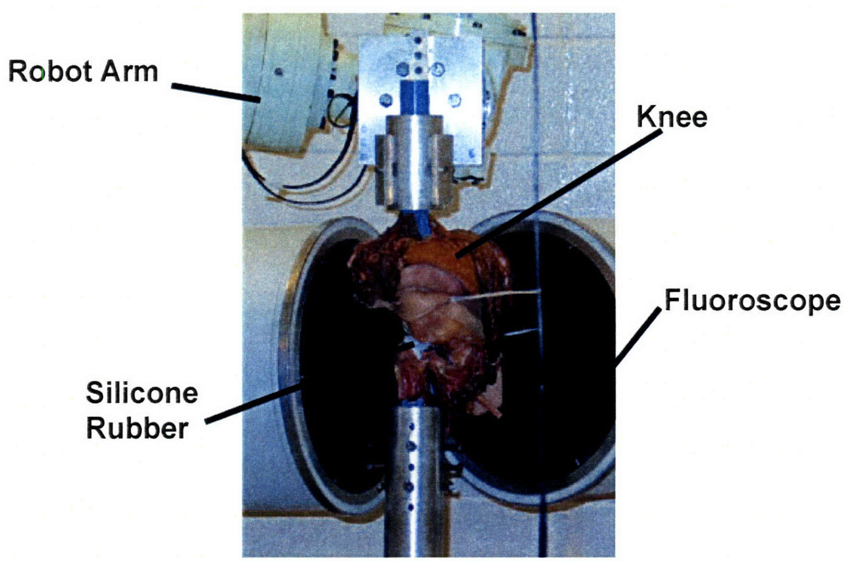

Fig. 8.2 Knee specimen under load. After the Silicone set, the soft-tissue was repositioned around the knee and fluoroscopic images were taken.

Fig. 8.3 The MicroScribe three-dimensional digitizer

The Dual Fluoroscopic imaging system was recreated in a three-dimensional modeling program (Rhinoceros®, Robert McNeel & Associates, Seattle, WA) (Li, Suggs et al. 2006). The image from each fluoroscope was then placed at the calculated intensifier location. Three dimensional computer aided design (CAD) models of the TKA components were then imported into the modeling program and matched to the fluoroscopic images in the manner discussed in Chapter 3 (Fig. 8.4). The contact area was then estimated by measuring the area of the intersection between the models of the femoral and polyethylene components. This matching process and contact area estimation was performed ten times. These estimates of the contact area were then compared to the digitized contact area denoted by the silicone rubber.

8.2.2 Estimation of In-vivo Polyethylene Stress

One patient performed a weight-bearing flexion activity with the knee of interest within the view of two fluoroscopes placed in an orthogonal manner [2]. The fluoroscopes captured images of the knee simultaneously as the patient flexed their knee to 0°, 30°, 90°, 120°, and maximum flexion. The fluoroscopic images were then imported into a solid modeling software (Rhinoceros, Robert McNeel & Associates, Seattle, WA) and oriented to mimic the relative positions of the fluoroscopes during image acquisition. The x-ray source of each fluoroscope was represented by a camera within the modeling software. 3D CAD models of the metal implants were then imported and, while viewing each fluoroscopic image from its respective camera, the models were positioned so their profiles matched their contours on the images. The matching process was performed at each flexion angle to reproduce the in-vivo knee position (Fig 8.4).

The matched models were then imported into a finite element software (ABAQUS, ABAQUS, Inc., Providence, RI). The femur was modeled as rigid. The polyethylene was modeled as elastoplastic based on data used by Huang et al with a modulus of 880 MPa and Poisson's ratio of 0.46 (Huang, Liau et al. 2007). The coefficient of friction between the femur and polyethylene was 0.04. For the analysis of each pose, the femur was initially moved normal to the base of the polyethylene such that the femur was just out of contact with the polyethylene. The femur was then returned to its matched in-vivo position. The contact area, contact force, and peak stress were calculated for the medial and lateral tibial plateaus at each pose.

8.3 Results

8.3.1 Validation of Contact Area Measurement

In the cadaver knee, the contact area obtained from digitizing the silicone rubber was 34.8 mm^2 (Fig 8.5A). The average area obtained using the dual fluoroscopic technique was 29.6±3.1 mm^2 (Fig 8.5B). Validation results are listed in Table 8.1.

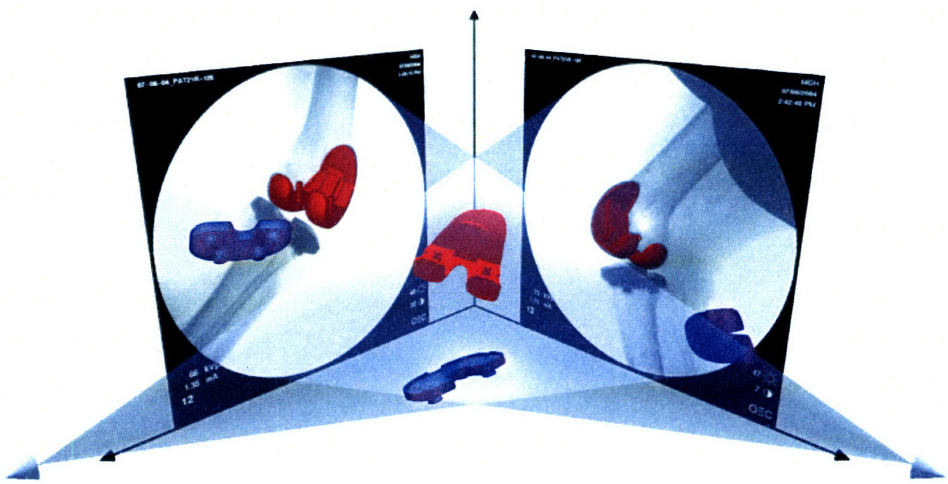

Fig. 8.4 Virtual replication of the Dual Fluoroscopic System

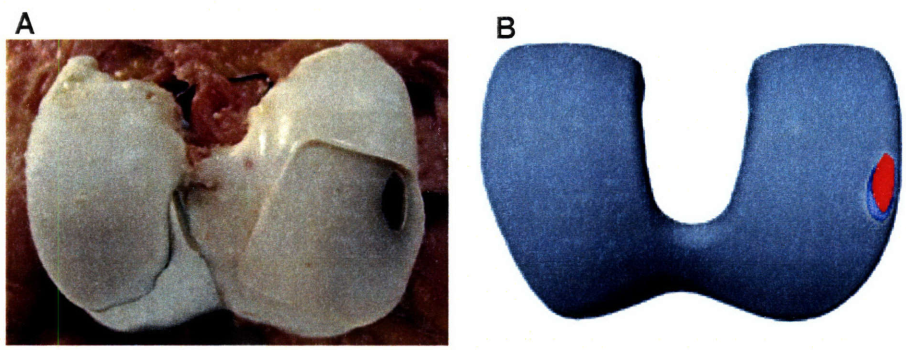

Fig. 8.5 A) View of silicone rubber and **B)** comparison of contact area from digitization (blue) and fluoroscopic analysis (red).

Table 8.1: Area Measurements using the Image Matching Technique

	Area(mm^2)	Error(mm^2)
Digitized	34.8	-
Match		
1	26.4	-8.5
2	28.3	-6.5
3	27.5	-7.4
4	25.3	-9.5
5	30.1	-4.7
6	31.0	-3.8
7	31.5	-3.4
8	32.3	-2.5
9	28.3	-6.5
10	35.7	0.9
Avg	29.6	-5.2
STD	3.1	

8.3.2 Estimation of In-vivo Polyethylene Stress

In the TKA patient, The contact area on the medial side decreased with flexion, going from 250 mm^2 at full extension to about 20 mm^2 at 90° through maximum flexion (131°) (Fig 8.6). The contact area on the lateral side varied between 25 and 80mm^2 throughout the flexion range. The maximum penetration of the medial condyle into the polyethylene decreased from 0.45 mm at 0° to 0.18 mm at 30° and varied between 0.03 and 0.18 mm through the rest of flexion (Fig. 8.7). The penetration on the lateral side ranged from 0.08 to 0.23 mm. The medial contact force decreased from 12.5 BW at full extension to about 0.4 BW at 90° and 120° (Fig 8.8). At maximum flexion, the medial contact force was 0.8 BW. On the lateral side, contact force varied between 0.5 and 2.9 BW from full extension to 90° of flexion. The lateral contact force was 1.0 BW at maximum flexion. The peak medial stress was 27 MPa at full extension, decreased to 5 MPa at 90°, and increased to 25 MPa at maximum flexion (Fig 8.9). The lateral peak stress was between 8 and 16 MPa from full extension to 90°. The lateral peak stress was 20 MPa and 30 MPa at 120° and maximum flexion.

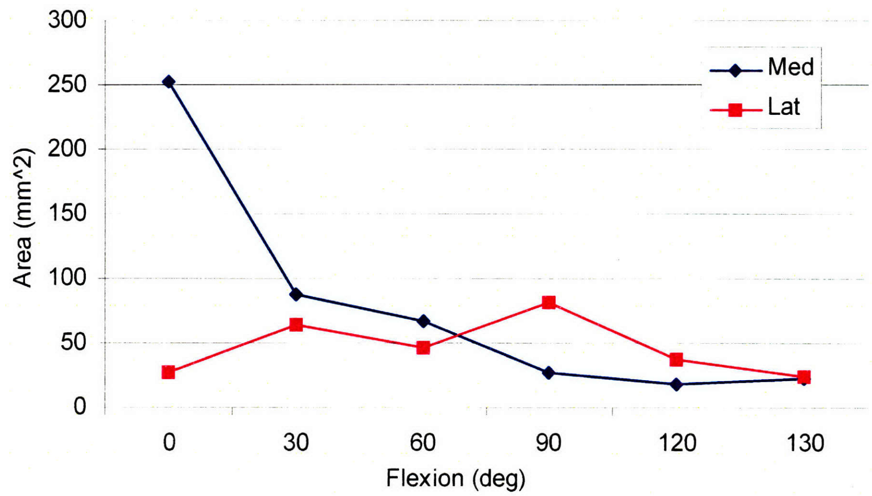

Fig. 8.6 Contact area in the medial and lateral compartments

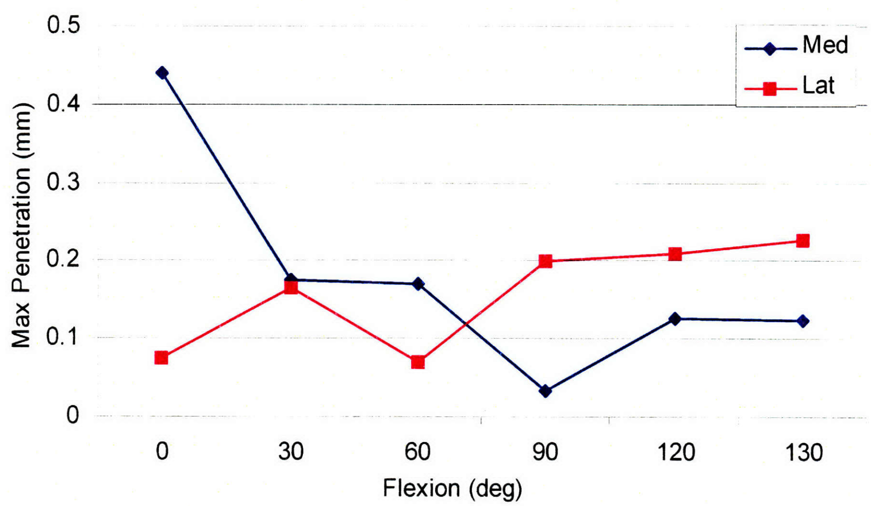

Fig. 8.7 Maximum surface penetration in the medial and lateral compartments

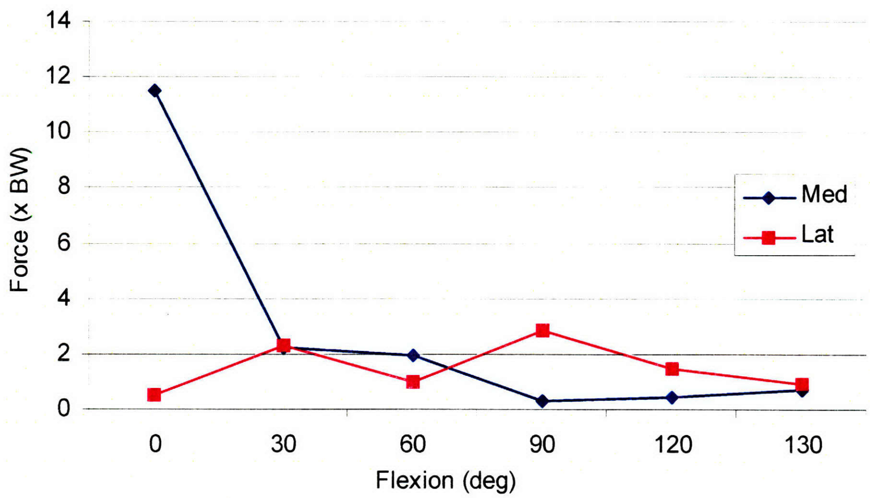

Fig. 8.8 Contact force in the medial and lateral compartments

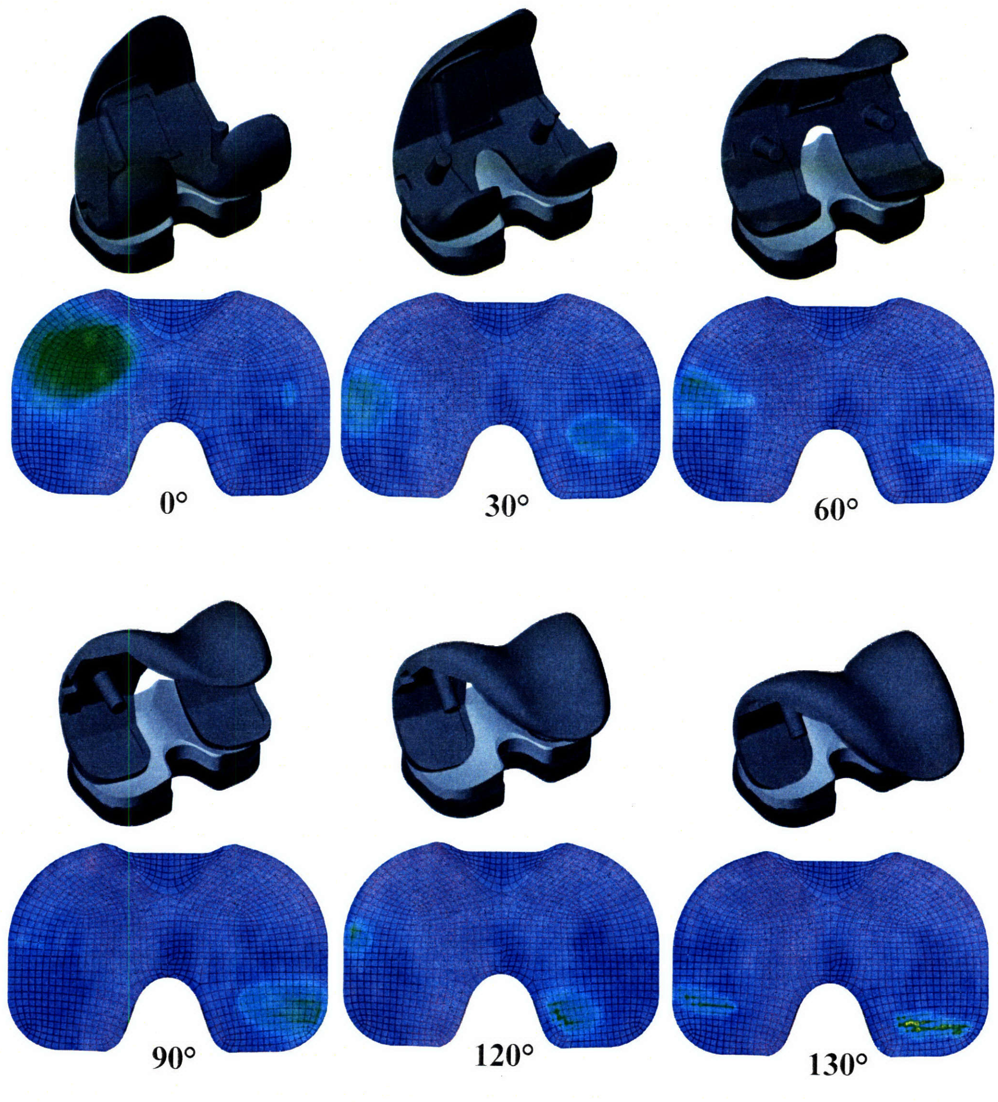

Fig. 8.9 Component positions and von Mises stress

8.4 Discussion

While one study did not find polyethylene wear to be a problem in total knee arthroplasty, most studies report polyethylene wear to be a major cause of revision after TKA (Hood, Wright et al. 1983; Feng, Stulberg et al. 1994; Bohl, Bohl et al. 1999; NIH 2000; Harman, Banks et al. 2001; Banks, Harman et al. 2002; Berzins, Jacobs et al. 2002; NIH 2003; Vince 2003; Clarke, Math et al. 2004; Huddleston, Wiley et al. 2005; Morgan, Battista et al. 2005; Wright 2005). Feng et al reported that over 10% of knees failed due to polyethylene wear (Feng, Stulberg et al. 1994). Retrieval studies have provided most of our information on the modes of polyethylene wear (Engh, Dwyer et al. 1992; Lewis, Rorabeck et al. 1994; Wasielewski, Galante et al. 1994; Blunn, Joshi et al. 1997; Wimmer, Andriacchi et al. 1998; Harman, Banks et al. 2001; Currier, Bill et al. 2005; Harman, Banks et al. 2007). Blunn et al examined 280 unicondylar and total knee arthroplasties and found that delamination was the dominant mode of wear (Blunn, Joshi et al. 1997). Currier et al. reported that the medial compartment experienced more wear then the lateral side (Currier, Bill et al. 2005). While retrieval studies offer valuable information on wear, they do not provide causative factors of wear (Rawlinson, Furman et al. 2006). It has been reported that sliding produces more wear than rolling (Blunn, Walker et al. 1991). Researchers have noted varying patterns of wear in retrievals (Blunn, Joshi et al. 1997; Currier, Bill et al. 2005) and have concluded that knee kinematics affect wear (Blunn, Walker et al. 1991; D'Lima, Hermida et al. 2001). These facts point to the need to examine wear on a patient specific basis.

The dual fluoroscopic imaging system was shown to be accurate in determining contact area and position. Further, the use of TKA kinematics obtained from dual fluoroscopy as displacement boundary conditions generally produced reasonable results. The observation that the contact area decreased with flexion is consistent with the fact that the tibiofemoral articular surfaces are the most conforming at full extension. It is interesting to note that at maximum flexion, the stresses were high even though forces were relatively low. This is due to the small contact area resulting from the posterior tips of the femoral component articulating with the polyethylene. This analysis did not account for any wear to the patient's polyethylene insert, which may have resulted in an overestimation of the stresses.

The dual fluoroscopic imaging system shows promise for analyzing the polyethylene stresses on a patient specific basis. As further validation, patients with instrumented implants have been imaged using a dynamic version of the dual fluoroscopic imaging system. Patients were imaged while performing step up/down, chair rise/sit, gait, and leg extension activities in addition to the single-leg lunge motion. The next steps in this methodology will include hyperelastic behavior, creep, and cyclic loading in the constitutive model and will utilize probabilistic methods to analyze the effect of kinematic errors on the finite element results. In future work, the calculated polyethylene stresses will be used to predict in-vivo wear with the goal of improving TKA design to better resist polyethylene wear.

Chapter 9. Conclusions

9.1 Summary

This writing completes work that has been conducted over the past 3 years and has been focused on measuring in-vivo knee kinematics after total knee arthroplasty. In Chapter 3, the methodology behind the Dual Fluoroscopic Imaging System is presented. The system was shown to be repeatable and accurate in determining the pose of the TKA components in all degrees of freedom. Having acceptable accuracy in all degrees of freedom is the advantage of this system over single-plane fluoroscopy. The importance of this advantage was demonstrated in a study of patients with anterior cruciate ligament (ACL) deficiency (Defrate, Papannagari et al. 2006; Li, Moses et al. 2006). When comparing the ACL deficient patients to healthy subjects, the ACL deficient knees demonstrated an expected increase in anterior tibial translation and internal tibial rotation. In addition, they also exhibited a small but consistent medial tibial translation (approximately 1mm), which induced an abnormal impingement between the media tibial spine and the lateral wall of the medial femoral condyle. The location of this abnormal contact is where ACL injured patients often develop osteoarthritis. Had this investigation been performed with single-plane fluoroscopy, the small medial tibial translation would have been missed due to the lack of accuracy in the out-of-plane direction.

In Chapter 4, the tibiofemoral kinematics of conventional cruciate-retaining TKA patients were measured. In Chapter 5, the kinematics of knees with a high flexion cruciate-retaining TKA were compared to the kinematics of knees with conventional cruciate-retaining TKA. No differences were detected between the high flexion and conventional designs in kinematics or maximum flexion. In the patients that reached 130°, there seemed to be a more conforming articulation in the high flexion design.

In Chapter 6, the Dual Fluoroscopic Imaging System was used to investigate the in-vivo function of posterior-stabilized total knee arthroplasty. Results from an Asian population were compared to a Western cohort. The passive range of motion of the Asian patients was significantly greater than that of the Western patients. However, no differences were detected between the Asian and Western patients during a weight-bearing single-leg lunge, including active range of motion and knee kinematics. This suggests that a large passive range of motion does not guarantee the availability of that range of motion for functional activities. The reduced active range of motion in the Asian patients compared to their passive range of motion indicates a significant role of the extensor mechanism in limiting flexion. More analysis is necessary to determine the differences between Asian and Western patients and between passive and active function.

That study also investigated cam-post engagement in posterior-stabilized TKA. Engagement did induce posterior femoral translation, but it also reduced internal tibial rotation. The timing of cam-post engagement was mildly correlated with maximum flexion. Knees with cam-post engagement later in flexion tended to achieve greater maximum flexion. If the factors that affect the timing of cam-post engagement can be established, manipulation of these factors may provide greater maximum flexion.

Chapter 7 assesses the distribution of the maximum flexion of the all the patients imaged in the previous chapters. The mean maximum flexion of these patients was very consistent with what has been published in the literature. No factors, such as age, weight, height, retention or substitution of the PCL, or use of high flexion designs, had an affect on maximum flexion. Based on the distribution of maximum flexion and reported levels of flexion necessary for various activities of daily living, a substantial portion of TKA patients will have difficulty performing these activities. This is consistent with studies that have found that while TKA significantly improves quality of life for patients, it does not return quality of life to normal levels. Improvements in TKA should be focused on helping patients with limited flexion.

In Chapter 8, the feasibility of using the kinematics from Dual Fluoroscopy as boundary conditions for finite element analysis of the polyethylene articular surface. This methodology produced reasonable results. At maximum flexion, the forces through the knee were low, but the stresses were high because the contact area was also low. A very simple constitutive model was used in this analysis and there was no accounting for any wear to the patient's polyethylene insert. These issues will be addressed in future work.

9.2 Future Steps

No factors were indicated as limiting flexion in the current data set. However, aspects of the data both in this study and in the literature suggest soft tissue structures, especially the extensor mechanism, may be responsible for determining maximum flexion. To further understand the interaction between TKA and the soft tissue around the knee, we have started analyzing patients before and after surgery. Patients first undergo magnetic resonance (MR) imaging and then perform functional activities while being dynamically imaged with the dual fluoroscopic system. The data from the MR scan will be used to build a three dimensional model of the patients femur and tibia, which will then be matched to the fluoroscopic images (DeFrate, Sun et al. 2004). Six months after surgery, patients will be imaged fluoroscopically while performing the same activities. The MR bone models and CAD models of the TKA components will then be matched to the fluoroscopic images. This technique can be used to investigate the change in the structure of the knee from the preoperative to postoperative state. This information will provide insight into the interdependence between TKA geometry and surgical technique and the remaining soft tissues around the knee joint.

One of the goals of the Bioengineer Lab is to develop a computational model that can be used to predict in-vivo wear of the polyethylene insert. While the results discussed in Chapter 8 are very promising, more validation is necessary. In that vain, 3 patients with an instrumented tibia have been imaged using an improved Dual Fluoroscopic Imaging System (D'Lima, Patil et al. 2005).

The improved system is capable of imaging patients at 30 frames/second. The patients were imaged dynamically performing the single-leg lunge along with step up/down, chair rise/sit, gait, and leg extension activities. The kinematics of the knee will be determined and used to calculate the forces through the knee through finite element analysis. The forces calculated from fluoroscopy will be compared to the forces recorded by the load cell in the instrumented tibia. The finite element analysis will utilize a hyperelastic constitutive model. While it would be very difficult to account for polyethylene wear already present at the time of imaging, the constitutive model should be able to represent plastic deformation. This method will provide valuable information about the in-vivo progression of wear in the polyethylene insert.

Appendix A. Distortion Correction

All radiographic images can suffer from distortion due to electromagnetic fields. Fluoroscopes are very useful in that they produce quality images at an order of magnitude smaller radiation dosage than standard x-ray devices. However, this benefit comes at the cost of added distortion in the image. While the distortion produced in contemporary fluoroscopes is often negligible in a clinical setting, it can be quite deleterious in a research setting. In order to correct the image distortion, an image of an object with markers in known relative locations can be acquired (Fig A.1A). Then, after identifying the markers on the image, a mathematical algorithm can be used to distort the image, moving the markers into to correct relative geometry and, thus, correcting the distortion that occurred during imaging process (Fig A.1B).

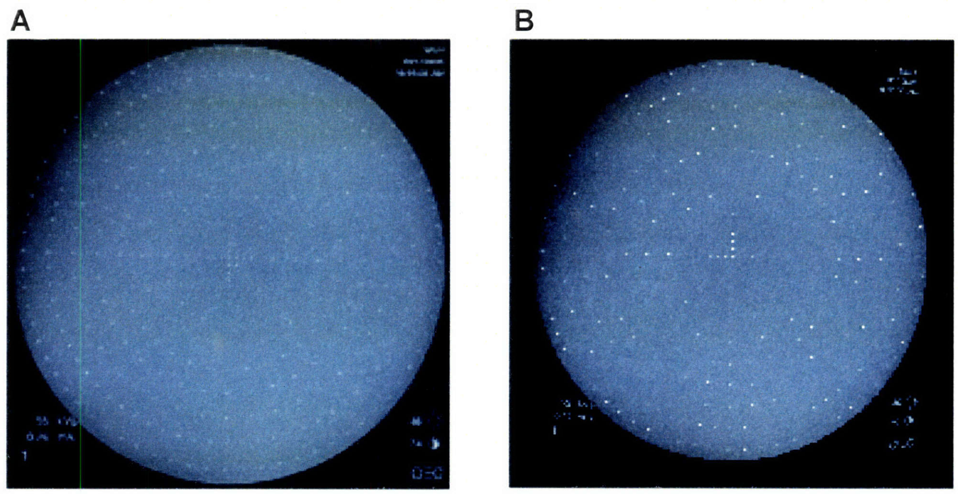

Fig. A.1 A) Original and **B)**corrected images of the calibration plate

There are many mathematical techniques available in the literature, but the global correction technique proposed by Gronenschild is robust and easy to implement (Gronenschild, 1997;Gronenschild, 1999). In this technique, two binomials are used to map the distorted points to the correct location. The following Mathematica code implements Gronenschild's global technique to correct distortion for one fluoroscope referred to as "XZ". This initial code actually performs the correction on points segmented in the image as opposed to the image itself. Executable code is in bold.

A.1 Read distorted XZ calibration data and sort

Check that calibration file exists.

```
Clear[fileexist];
fileexist = FileNames[calfileXZ<>centersuff<>calfileextXZ,caldir];
If[Length[fileexist] □ 1,
 Input[caldir<>"\\"<>calfileXZ<>centersuff<>calfileextXZ<>" does not exist.
Enter any character."];
 Interrupt[],,
 Input[caldir<>"\\"<>calfileXZ<>centersuff<>calfileextXZ<>" does not exist.
Enter any character."];
 Interrupt[]
 ]
```

Read distorted center hole and distorted zerotheta hole

```
opencenterXZ = OpenRead[caldir<>calfileXZ<>centersuff<>calfileextXZ];
distcenterXZ = Read[opencenterXZ,{Number,Number,Number}];
Close[opencenterXZ];
```

```
openzeroXZ = OpenRead[caldir<>calfileXZ<>zerosuff<>calfileextXZ];
distzeroXZ = Read[openzeroXZ,{Number,Number,Number}];
Close[openzeroXZ];
distangleXZ=ArcTan[distzeroXZ[[qXZ]]-
distcenterXZ[[qXZ]],distzeroXZ[[rXZ]]-distcenterXZ[[rXZ]]]
```

Read distorted points, calculated coordinates when zero theta is rotated to horizontal, then sort distorted points. I'll start by making an array to hold the distorted points data. There will be 10 columns as follows:

column 1 to 3 are the raw distorted coordinates,

column 4 is the radius of the point (distance from center point),

column 5 is the level,

column 6 is the angle relative to zero theta in radians,

column 7 is the modified angle based on angle tolerances in radians,

column 8 is the modified angle in degrees

column 9 is the x-coordinate in the plate coordinate system having the center hole as the origin and the zerotheta hole denoting the positive x-axis. The x-y plane of this coordinate system is in the plane of the image.

column 10 is the y-coordinate in the plate coordinate system.

```
Clear[usdistcalptsXZ,usdistcalptselemXZ];
opendistXZ = OpenRead[caldir<>calfileXZ<>allsuff<>calfileextXZ];
For[p=1,p<ncalptsXZ+1,p++,
  For[t=1,t<4,t++,usdistcalptselemXZ[p,t]=Read[opendistXZ,Number]];
  usdistcalptselemXZ[p,4]=Sqrt[Sum[(usdistcalptselemXZ[p,t]-
distcenterXZ[[t]])^2,{t,3}]];
  usdistcalptselemXZ[p,6]=
If[{usdistcalptselemXZ[p,1],usdistcalptselemXZ[p,2],usdistcalptselemXZ[p,
3]}≠distcenterXZ,ArcTan[usdistcalptselemXZ[p,qXZ]-
```

```
distcenterXZ[[qXZ]],usdistcalptselemXZ[p,rXZ]-distcenterXZ[[rXZ]]]-
distangleXZ,0.
    ];
  usdistcalptselemXZ[p,7]=
   If[Abs[usdistcalptselemXZ[p,6]]<angletolXZ,0.,

If[usdistcalptselemXZ[p,6]<0.,usdistcalptselemXZ[p,6]+2.*Pi,usdistcalptsele
mXZ[p,6]]
    ];
  usdistcalptselemXZ[p,8]=usdistcalptselemXZ[p,7]*180/Pi;
usdistcalptselemXZ[p,9]=usdistcalptselemXZ[p,qXZ]*Cos[distangleXZ]+usd
istcalptselemXZ[p,rXZ]*Sin[distangleXZ];
  usdistcalptselemXZ[p,10]=-
usdistcalptselemXZ[p,qXZ]*Sin[distangleXZ]+usdistcalptselemXZ[p,rXZ]*C
os[distangleXZ];
  ]
usdistcalptsXZ=Array[usdistcalptselemXZ,{ncalptsXZ,10}];
```

Make an extra attempt to read from the file, close the file, and check if the file was read properly. Error message is produced if the IF statement is False or Null.

```
checkdistreadXZ = Read[opendistXZ,Number];
Close[opendistXZ];
If[usdistcalptselemXZ[ncalptsXZ,3]□Reals &&
checkdistreadXZ□EndOfFile,,
   Input["Error reading XZ calibration file\n\nLast number
read\n"<>ToString[usdistcalptselemXZ[ncalptsXZ,3]]<>"\n\nExtra attempt
to read\n"<>ToString[checkdistreadXZ]<>"\n\nEnter any character, then
click Abort"];
   Interrupt[],
```

```
  Input["Error reading XZ calibration file\n\nLast number
read\n"<>ToString[usdistcalptselemXZ[ncalptsXZ,3]]<>"\n\nExtra attempt
to read\n"<>ToString[checkdistreadXZ]<>"\n\nEnter any character, then
click Abort"];
  Interrupt[] ];
```

If the pattern is rectangular, sort by y-coordinate (column 10) and add level labels to column 5. Then sort by level and x-coordinate (column 9).

If the pattern is radial, sort by radius (column 4) and add level labels to column 5. Then sort by level then modified angle (column 7) where appropriate.

```
If[patterntype==1,sortcol1=10; sortcol2=9;]
If[patterntype==2,sortcol1=4; sortcol2=7;]
srdistcalptsXZ=Sort[usdistcalptsXZ,OrderedQ[{Take[#1,{sortcol1}],Take[#2,
{sortcol1}]}]&];
lev=1;
For[p=1,p<ncalptsXZ+1,p++,
 While[p>Sum[ptspresXZ[[t]],{t,lev}],lev++];
 srdistcalptsXZ[[p,5]]=lev;
 ]
distcalptsXZ=Sort[srdistcalptsXZ,OrderedQ[{Take[#1,{5,sortcol2,sortcol2-
5}],Take[#2,{5,sortcol2,sortcol2-5}]}]&];
```

A.2 Create true points and adjust them

```
Clear[angleint,angleintelem,truecalptsXZ,truecalptselemXZ];
```

Create an array for the raw true points and place them in their initial position. Rectangular patterns are assumed to have equal spacing in the x and y directions.

```
If[patterntype==1 && plate ≠ 1 && plate ≠ 2 && plate ≠ 5,
 opentruecalptsXZ = OpenRead[caldir<>calfileXZ<>"truepoints.txt"];
 For[p=1,p<ncalptsXZ+1,p++,
    truecalptselemXZ[p,1]=Read[opentruecalptsXZ,Number];
    truecalptselemXZ[p,2]=Read[opentruecalptsXZ,Number];
    truecalptselemXZ[p,3]=Read[opentruecalptsXZ,Number];
    ]
  Close[opentruecalptsXZ];
 ]
If[patterntype==2 || plate == 1 || plate ==2 || plate ==5,
 For[t=1,t<nlevels+1,t++,
  angleintelem[t]=If[ptspresXZ[[t]]□0,2. Pi/ptspresXZ[[t]],0]
  ];
 If[plate == 1 && ptspresXZ[[12]]==71,angleintelem[12] = 2. Pi/72];
 angleint=Array[angleintelem,nlevels];
 For[p=1,p<ncalptsXZ+1,p++,
  lev=distcalptsXZ[[p,5]];
  truecalptselemXZ[p,qXZ]=Cos[angleint[[lev]]*(p-
Sum[ptspresXZ[[t]],{t,lev}]+ptspresXZ[[lev]]-1)]*levelvalue[[lev]];
  truecalptselemXZ[p,rXZ]=Sin[angleint[[lev]]*(p-
Sum[ptspresXZ[[t]],{t,lev}]+ptspresXZ[[lev]]-1)]*levelvalue[[lev]];
  truecalptselemXZ[p,sXZ]=distcalptsXZ[[p,sXZ]];
  ]
 ]
truecalptsXZ=Array[truecalptselemXZ,{ncalptsXZ,3}];
```

Adjust true points so true center coincides with distorted center and true zero-theta lines up with distorted zero-theta.

```
For[p=1,p<ncalptsXZ+1,p++,
 adjcalptselemXZ[p,qXZ]=Cos[distangleXZ]*truecalptsXZ[[p,qXZ]]-
Sin[distangleXZ]*truecalptsXZ[[p,rXZ]]+distcenterXZ[[qXZ]];

adjcalptselemXZ[p,rXZ]=Sin[distangleXZ]*truecalptsXZ[[p,qXZ]]+Cos[distan
gleXZ]*truecalptsXZ[[p,rXZ]]+distcenterXZ[[rXZ]];
 adjcalptselemXZ[p,sXZ]=truecalptsXZ[[p,sXZ]];
 ]
adjcalptsXZ=Array[adjcalptselemXZ,{ncalptsXZ,3}];
```

A.3 Set up equations, Find Polynomials and corrected points for XZ

Make lists to be used in solving for the coefficients of the correction polynomials for X and Y.

```
Clear[g,h,u,v]
For[p=1,p<ncalptsXZ+1,p++,
 Qfitpts[p,1]=distcalptsXZ[[p,qXZ]];
 Qfitpts[p,2]=distcalptsXZ[[p,rXZ]];
 Qfitpts[p,3]=adjcalptsXZ[[p,qXZ]];
 Rfitpts[p,1]=distcalptsXZ[[p,qXZ]];
 Rfitpts[p,2]=distcalptsXZ[[p,rXZ]];
 Rfitpts[p,3]=adjcalptsXZ[[p,rXZ]];
 ]
Qfitarray=Array[Qfitpts,{ncalptsXZ,3}];
Rfitarray=Array[Rfitpts,{ncalptsXZ,3}];
```

Set up the terms in the polynomials

```
Qt=1;
For[g=0,g<QporderXZ+1,g++,
 For[h=0,h<g+1,h++,
  Qterm[Qt]=u^(g-h)*v^h;
  Qt=Qt+1;
  ]
 ]
Qtermarray = Array[Qterm,Sum[k,{k,QporderXZ+1}]];
Rt=1;
For[g=0,g<RporderXZ+1,g++,
 For[h=0,h<g+1,h++,
  Rterm[Rt]=u^(g-h)*v^h;
  Rt=Rt+1;
  ]
 ]
Rtermarray = Array[Rterm,Sum[k,{k,RporderXZ+1}]];
Qtermarray
```

$\{1, u, v, u^2, u v, v^2, u^3, u^2 v, u v^2, v^3\}$

Find Polynomials for correction without and with manual rotation.

```
QpolyXZ[u_,v_]=Fit[Qfitarray,Qtermarray,{u,v}];
RpolyXZ[u_,v_]=Fit[Rfitarray,Rtermarray,{u,v}];
corrcenthole[qXZ] = QpolyXZ[distcenterXZ[[qXZ]],distcenterXZ[[rXZ]]];
corrcenthole[rXZ] = RpolyXZ[distcenterXZ[[qXZ]],distcenterXZ[[rXZ]]];
QpolyrotXZ[u_,v_]=(QpolyXZ[u,v]-
corrcenthole[qXZ])*Cos[manalpharadXZ]+(RpolyXZ[u,v]-
corrcenthole[rXZ])*(-Sin[manalpharadXZ])+corrcenthole[qXZ];
RpolyrotXZ[u_,v_]=(QpolyXZ[u,v]-
corrcenthole[qXZ])*Sin[manalpharadXZ]+(RpolyXZ[u,v]-
corrcenthole[rXZ])*Cos[manalpharadXZ]+corrcenthole[rXZ];
```

The first set of corrected points are the obtained using only the correction polynomials. The second set have a rigid body rotation adjustment.

```
For[p=1,p<ncalptsXZ+1,p++,
  corrcalptsXZ[p,qXZ]=QpolyXZ[distcalptsXZ[[p,qXZ]],distcalptsXZ[[p,rXZ]]];
  corrcalptsXZ[p,rXZ]=RpolyXZ[distcalptsXZ[[p,qXZ]],distcalptsXZ[[p,rXZ]]];
  corrcalptsXZ[p,sXZ]=distcalptsXZ[[p,sXZ]];

corrrotcalptsXZ[p,qXZ]=QpolyrotXZ[distcalptsXZ[[p,qXZ]],distcalptsXZ[[p,r
XZ]]];

corrrotcalptsXZ[p,rXZ]=RpolyrotXZ[distcalptsXZ[[p,qXZ]],distcalptsXZ[[p,rX
Z]]];
  corrrotcalptsXZ[p,sXZ]=distcalptsXZ[[p,sXZ]];
  ]
```

A.4 Calculate error for XZ

Calculate the RMS and average error of distorted positions of calibration points.

```
distrmserror = Sqrt[Sum[(distcalptsXZ[[p, qXZ]] - adjcalptsXZ[[p, qXZ]])^2 +
        (distcalptsXZ[[p, rXZ]] - adjcalptsXZ[[p, rXZ]])^2,
      {p, ncalptsXZ}] / ncalptsXZ]
distavgerror = Sum[Sqrt[(distcalptsXZ[[p, qXZ]] - adjcalptsXZ[[p, qXZ]])^2 +
        (distcalptsXZ[[p, rXZ]] - adjcalptsXZ[[p, rXZ]])^2],
    {p, ncalptsXZ}] / ncalptsXZ
```

Calculate the RMS and average error of corrected positions of calibration points.

```
corrrmserror = Sqrt[Sum[(corrrotcalptsXZ[p, qXZ] - adjcalptsXZ[[p, qXZ]])^2 +
        (corrrotcalptsXZ[p, rXZ] - adjcalptsXZ[[p, rXZ]])^2,
      {p, ncalptsXZ}] / ncalptsXZ]
corravgerror = Sum[Sqrt[(corrrotcalptsXZ[p, qXZ] - adjcalptsXZ[[p, qXZ]])^2 +
        (corrrotcalptsXZ[p, rXZ] - adjcalptsXZ[[p, rXZ]])^2],
    {p, ncalptsXZ}] / ncalptsXZ
```

Check if correction was performed properly.

```
If[corrrmserror>corrtolXZ||corravgerror>corrtolXZ,
  cont=Input["Correction error is greater than desired!!\n\nCorrection
tolerance = "<>ToString[corrtolXZ]<>"\n\nDistorted RMS and average error
= "<>ToString[distrmserror]<>",  "<>ToString[distavgerror]<>"\nCorrected
RMS and average error = "<>ToString[corrrmserror]<>",
"<>ToString[corravgerror]<>"\n\nEnter q to quit or p to plot points"];
  If[cont==q,Interrupt[]];
  If[cont==p,

distcalptsXZplot=Graphics[{RGBColor[0,0,1],PointSize[.011],Point/@Table[{
distcalptsXZ[[p,qXZ]],distcalptsXZ[[p,rXZ]]},{p,1,ncalptsXZ,1}]}];

corrcalptsXZplot=Graphics[{RGBColor[0,1,0],PointSize[.010],Point/@Table[
{corrcalptsXZ[p,qXZ],corrcalptsXZ[p,rXZ]},{p,1,ncalptsXZ,1}]}];

adjcalptsXZplot=Graphics[{RGBColor[1,0,0],PointSize[.012],Point/@Table[{
adjcalptsXZ[[p,qXZ]],adjcalptsXZ[[p,rXZ]]},{p,1,ncalptsXZ,1}]}];

corrrotcalptsXZplot=Graphics[Point/@Table[{corrrotcalptsXZ[p,qXZ],corrro
tcalptsXZ[p,rXZ]},{p,1,ncalptsXZ,1}]];


NotebookPut[Notebook[{Cell[BoxData[RowBox[{"Show","[",RowBox[{Row
Box[{"{",RowBox[{"adjcalptsXZplot",",","distcalptsXZplot"}],"}"}],",",RowB
```

```
ox[{"ImageSize","→","500"}],",",RowBox[{"AspectRatio","→","1"}]}],"]"}]],"I
nput"],Cell[BoxData[RowBox[{"Show","[",RowBox[{RowBox[{"{",RowBox[{
"adjcalptsXZplot",",","corrrotcalptsXZplot"}],"}"}],",",RowBox[{"ImageSize"
,"→","500"}],",",RowBox[{"AspectRatio","→","1"}]}],"]"}]],"Input"],Cell[Box
Data[{RowBox[{RowBox[{"cont","=",RowBox[{"Input","[","\"Examine the
plots.  You may enter c to continue evalution or any other character to
quit\"","]"}]}],";"}],RowBox[{RowBox[{"If","[",RowBox[{RowBox[{"cont","==
","c"}],",","

",RowBox[{RowBox[{"SetSelectedNotebook","[","canb","]"}],";","

",RowBox[{"SelectionMove","[",RowBox[{"canb",",","Next",",","CellGroup"
}],"]"}],";","
                    ",RowBox[{"SelectionEvaluate","[","canb","]"}]}],",","
                  ",RowBox[{"Interrupt","[","]"}]}],"
                ","]"}],";"}]}],"Input"]},FrontEndVersion→"4.1 for Microsoft
Windows",ScreenRectangle→{{0.,1024.},{0.,695.}},WindowSize→{600.,600.},
WindowMargins→{{183.,Automatic},{23.,Automatic}}]];
   adjcorrwin = SelectedNotebook[];
   SelectionMove[adjcorrwin,All,Notebook];
   SelectionEvaluate[adjcorrwin];
   SelectionMove[adjcorrwin,Before,Notebook];
   ],,
  Input["There was an error in performing the correction!!\n\nCorrection
tolerance = "<>ToString[corrtolXZ]<>"\n\nDistorted RMS and average error
= "<>ToString[distrmserror]<>",  "<>ToString[distavgerror]<>"\nCorrected
RMS and average error = "<>ToString[corrrmserror]<>",
"<>ToString[corravgerror]<>"\n\nThe program will stop.  Enter any
character"];
  Interrupt[]
  ];
```

Appendix B. Kinematics Calculations

After CAD models had been matched to a series of fluoroscopic images, those matched poses needed to be translated into meaningful kinematic parameters. This was done by calculating the relative position and orientation of coordinates systems fixed to the femoral and tibial components based on a reference position of the components (Fig B.1).

The components were in their reference position when the femoral surfaces parallel to the distal femoral cut were parallel to the tibial plate and the most distal point on the femoral condyles were at the most distal (lowest) points on the polyethylene insert. In this position, the femoral and tibial coordinate systems had the same orientation. This was chosen as the reference position because of its ease of construction and physical relevance (we would expect the femur to sit as low as possible on the tibia).

To be consistent with the past in-vitro work performed in the lab, the tibiofemoral rotations were calculated using a flexion-extension - varus-valgus - internal-external Euler rotation sequence (Most, 2000; Suggs, 2006). The calculations were initially performed using code written in Mathematica (Version 4.1, Wolfram Research, Inc., Champaign, IL), which read the coordinates of the points defining each coordinate system and calculated the translations and rotations from the reference position. Part of that code is presented here.

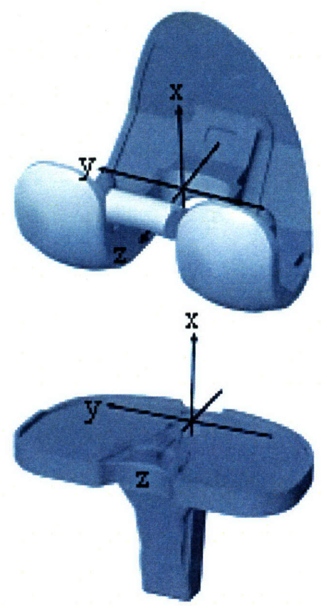

Fig. B.1 The femoral and tibial coordinate systems

B.1 Set parameters

This program was initial written to test repeatibility and accuracy, so multiple observers were used to match the same image set over multiple trials. I think I will leave these parameters in the code and set them to 1, just in case I need them later.

```
SetDirectory["C:\jfs\invivo\patients\\"<>"06-03-04_pat10R\matched"];
infile = "06-03-04_pat10";
infileext = ".CSV";
side = "R";
nfiles =11;
imgseq = {1,2,3,4,5,6,7,8,9,10,11,12,13,14,15,16,17};
outfile = "femtrantibrotV6";
outfileext = ".txt";
femtype = "CR";
femsize = "F";
femcond = "";
tibsize = "6";
polythick = "12";
outinterpdef = "intdef";
outinterpfirst="intfirst";
outinterpfirstkin = "intfirstkin";
ncol = 18;
icol = 4;
desflex={-20,-15,-10,-5,0,15,30,45,60,75,90,105,120,135,150};
zeroindex=5;
minflextol =.33;
maxflextol=.33;
label[1]="fo";
label[2]="fx";
```

```
label[3]="fy";
label[4]="fz";
label[5]="to";
label[6]="tx";
label[7]="ty";
label[8]="tz";
label[9]="go";
dummyraw={dum1,dum2,dum3};
nobservers = 1;
ntrials = 1;
intorder=1;
```

B.2 Read data

The raw data points will be read into dummy variables and then stored in vectors foraw, fxraw, fyraw...

```
For[f=1,f<nfiles+1,f++,
matchedin=OpenRead[infile<>side<>"_"<>ToString[imgseq[[f]]]<>infileext];
 For[labindex=1,labindex<9,labindex++,
  SetStreamPosition[matchedin,0];

Find[matchedin,"\""<>label[labindex]<>"\"",RecordSeparators→{"\t","\n",","
}];
  Skip[matchedin,Character, 10];
  dummyraw[[1]]=Read[matchedin,Number];
  Skip[matchedin,Character];
  dummyraw[[2]]=Read[matchedin,Number];
  Skip[matchedin,Character];
  dummyraw[[3]]=Read[matchedin,Number];
```

```
  ToExpression[label[labindex]<>"raw[f]=dummyraw",InputForm];
  ];
 Close[matchedin];
 ]
```

Read in the reference position of the femoral peg system relative to the tibial system in the tibial coordinate system. Also, read in vector from FP system to GC system, vfpgc. This vector is strictly in the FP system. However, the FP system was aligned with the tibial system when the coordinates were output from Rhino, so this vector is also in the reference position tibial system.

```
tibsizegroup = "";
If[femtype =="CR" || femtype == "LPS",
 If[tibsize=="1"||tibsize=="2",tibsizegroup="12"];
 If[tibsize=="3"||tibsize=="4",tibsizegroup="34"];
 If[tibsize=="5"||tibsize=="6",tibsizegroup="56"];

If[tibsize=="7"||tibsize=="8"||tibsize=="9"||tibsize=="10",tibsizegroup="710"
];
 refposin=OpenRead["refpos_"<>femtype<>"-"<>femsize<>"-
"<>tibsizegroup<>"-"<>polythick<>"mm.CSV"];
 ]
If[femtype == "UKA",
 tibsizegroup = tibsize;
 refposin=OpenRead["refpos_"<>femtype<>"-"<>femsize<>"-
"<>femcond<>"-"<>tibsizegroup<>"-"<>polythick<>"mm.CSV"];
 ]
Find[refposin,"\"fo\"",RecordSeparators→{"\t","\n",","}];
Skip[refposin,Character, 10];
dummyraw[[1]]=Read[refposin,Number];
Skip[refposin,Character];
```

```
dummyraw[[2]]=Read[refposin,Number];
Skip[refposin,Character];
dummyraw[[3]]=Read[refposin,Number];
refpos=dummyraw;
SetStreamPosition[refposin,0];
Find[refposin,"\"go\"",RecordSeparators→{"\t","\n",","}];
Skip[refposin,Character, 10];
dummyraw[[1]]=Read[refposin,Number];
Skip[refposin,Character];
dummyraw[[2]]=Read[refposin,Number];
Skip[refposin,Character];
dummyraw[[3]]=Read[refposin,Number];
vfpgc=dummyraw-refpos;
Close[refposin];
mllength=Sqrt[(fyraw[1]-foraw[1]).(fyraw[1]-foraw[1])];
```

B.3 Calculate kinematics and Write

At each flexion angle, calculate unit vectors corresponding to the axes of the tibial system (utibxraw, utibyraw, utibzraw) and the FP system (ufpxraw,ufpyraw,ufpzraw), calculate the vector from the tibial system to the femoral system (vtibfpraw, this vector being in the global system), and transform the vector, as well as the FP system unit vectors, from global coordinates to the tibial coordinates (vtibfptib, ufpxtib, ufpytib, ufpztib). The transformation will be carried out using a rotation matrix based on the tibial system unit vectors. If we have three orthogonal, right-handed unit vectors, ux1, uy1, and uz1, the rotation from the xyz-ref system to the xyz-1 system is given by {ux1,uy1,uz1} in *Mathematica* format. So, the rotation matrix is given by {utibxraw, utibyraw, utibzraw} in *Mathematica* format.

```
For[f=1,f<nfiles+1,f++,
 utibxraw[f]=(txraw[f]-toraw[f])/Sqrt[(txraw[f]-toraw[f]).(txraw[f]-toraw[f])];
 utibyraw[f]=(tyraw[f]-toraw[f])/Sqrt[(tyraw[f]-toraw[f]).(tyraw[f]-toraw[f])];
 utibzraw[f]=(tzraw[f]-toraw[f])/Sqrt[(tzraw[f]-toraw[f]).(tzraw[f]-toraw[f])];
 ufpxraw[f]=(fxraw[f]-foraw[f])/Sqrt[(fxraw[f]-foraw[f]).(fxraw[f]-foraw[f])];
 ufpyraw[f]=(fyraw[f]-foraw[f])/Sqrt[(fyraw[f]-foraw[f]).(fyraw[f]-foraw[f])];
 ufpzraw[f]=(fzraw[f]-foraw[f])/Sqrt[(fzraw[f]-foraw[f]).(fzraw[f]-foraw[f])];
 vtibfpraw[f]=foraw[f]-toraw[f];
 vtibfptib[f]={utibxraw[f],utibyraw[f],utibzraw[f]}.vtibfpraw[f];
 ufpxtib[f]={utibxraw[f],utibyraw[f],utibzraw[f]}.ufpxraw[f];
 ufpytib[f]={utibxraw[f],utibyraw[f],utibzraw[f]}.ufpyraw[f];
 ufpztib[f]={utibxraw[f],utibyraw[f],utibzraw[f]}.ufpzraw[f];
 ]
```

Write kinematics to file. Start by calculating a non-Eulerian rotation matrix to be used in calculating rotation kinematics. This rotation matrix will be calculated using the FP system unit vectors in tibial coordinates. The matrix that rotates the tibial system unit vectors to the FP system unit vectors is given by Transpose[{ufpxtib,ufpytib,ufpztib}] in *Mathematica* format.

Translations are calculated by combining vtibfptib, refpos, and vfpgc as appropriate. Now, vtibfptib and refpos are in tibial coordinates, but vfpgc is in FP coordinates. Remember, the FP system has the same orientation as the tibial system in the reference position but not at any given flexion angle. When combining vfpgc with vtibfptib to get the translated position of the GC origin, vfpgc will have to be transformed from the FP to the tibial system. The necessary rotation matrix is given by Transpose[{ufpxtib,ufpytib,ufpztib}]. (You can also think of vfpgc being given in tibial coordinates in the reference position and having to be rotated from the reference orientation the FP system orientation at the given flexion angle.)

The translation of the left femoral peg, leftfptrans = vtibfptib + ufpytib*mllength - (refpose + {0,mllength,0}) = fptrans + ufpytib*mllength - {0,mllength,0}. Similarly, rightfptrans = fptrans - ufpytib*mllength + {0,mllength,0}.

So the femoral kinematics are given by (See derivation of Euler matrix below) the following. **Note: some negative signs are put in artificially to make sure Proximal, medial, posterior femoral translation, and flexion, Varus, and internal tibial rotation are positive

```
For[f=1,f<nfiles+1,f++,
 components=Transpose[{ufpxtib[f],ufpytib[f],ufpztib[f]}];
 flexrad[f]=Chop[ArcTan[components[[1,1]],components[[1,3]]],10^-7];
 flex[f]=-flexrad[f]*180/Pi;
 VVrad[f]=Chop[ArcSin[-components[[1,2]]],10^-7];
 IErad[f]=Chop[ArcTan[components[[2,2]],components[[3,2]]],10^-7];
 flexproj[f]=Chop[ArcTan[ufpxtib[f][[1]],ufpxtib[f][[3]]],10^-7]*180/Pi;
 fptrans = vtibfptib[f]-refpos;
 gctrans=(vtibfptib[f]+components.vfpgc)-(refpos+vfpgc);
 proximalfp[f]=fptrans[[1]];
 proximalgc[f]=gctrans[[1]];
 posteriorfp[f]=fptrans[[3]];
 posteriorgc[f]=gctrans[[3]];
 leftfptrans= fptrans + ufpytib[f]*mllength - {0,mllength,0};
 rightfptrans=fptrans- ufpytib[f]*mllength + {0,mllength,0};
 If[side=="L",
  medialfp[f] = -fptrans[[2]];
  medialgc[f] = -gctrans[[2]];
  varus[f]=-VVrad[f]*180/Pi;
  internal[f]=IErad[f]*180/Pi;
  varusproj[f]=-Chop[ArcTan[ufpxtib[f][[1]],ufpxtib[f][[2]]],10^-7]*180/Pi;
  internalproj[f]=Chop[ArcTan[ufpytib[f][[2]],ufpxtib[f][[3]]],10^-7]*180/Pi;
  medialmfp[f]=-rightfptrans[[2]];
```

```
  proximalmfp[f]=rightfptrans[[1]];
  posteriormfp[f]=rightfptrans[[3]];
  mediallfp[f]=-leftfptrans[[2]];
  proximallfp[f]=leftfptrans[[1]];
  posteriorlfp[f]=leftfptrans[[3]];
  ];
 If[side=="R",
  medialfp[f] = fptrans[[2]];
  medialgc[f] = gctrans[[2]];
  varus[f]=VVrad[f]*180/Pi;
  internal[f]=-IErad[f]*180/Pi;
  varusproj[f]=-Chop[ArcTan[ufpytib[f][[2]],ufpytib[f][[1]]],10^-7]*180/Pi;
  internalproj[f]=-Chop[ArcTan[ufpytib[f][[2]],ufpytib[f][[3]]],10^-7]*180/Pi;
  medialmfp[f]=leftfptrans[[2]];
  proximalmfp[f]=leftfptrans[[1]];
  posteriormfp[f]=leftfptrans[[3]];
  mediallfp[f]=rightfptrans[[2]];
  proximallfp[f]=rightfptrans[[1]];
  posteriorlfp[f]=rightfptrans[[3]];
  ];
 ]
```

Put the data into an array to be used for interpolation.

```
Clear[rawdummy];
For[f=1,f<nfiles+1,f++,
 rawdummy[f,1]=proximalfp[f];
 rawdummy[f,2]=medialfp[f];
 rawdummy[f,3]=posteriorfp[f];
 rawdummy[f,4]=flex[f];
 rawdummy[f,5]=varus[f];
 rawdummy[f,6]=internal[f];
```

```
 rawdummy[f,7]=proximalgc[f];
 rawdummy[f,8]=medialgc[f];
 rawdummy[f,9]=posteriorgc[f];
 rawdummy[f,10]=proximalmfp[f];
 rawdummy[f,11]=medialmfp[f];
 rawdummy[f,12]=posteriormfp[f];
 rawdummy[f,13]=proximallfp[f];
 rawdummy[f,14]=mediallfp[f];
 rawdummy[f,15]=posteriorlfp[f];
 rawdummy[f,16]=flexproj[f];
 rawdummy[f,17]=varusproj[f];
 rawdummy[f,18]=internalproj[f];
 ]
rawarray=Array[rawdummy,{nfiles,ncol}];
```

Write the data to file.

```
kinout=
OpenWrite[infile<>side<>outfile<>outfileext,FormatType→FortranForm];
WriteString[kinout,"FP-Proximal\tFP-Medial\tFP-
Posterior\tFlexion\tVarus\tInternal\tGC-Proximal\tGC-Medial\tGC-
Posterior\tMFP-Proximal\tMFP-Medial\tMFP-Posterior\tLFP-Proximal\tLFP-
Medial\tLFP-Posterior\tProjFlexion\tProjVarus\tProjInternal\n"];
For[f=1,f<nfiles+1,f++,
 For[c=1,c<ncol,c++,
  WriteString[kinout,FortranForm[rawarray[[f,c]]],"\t"]
  ];
 WriteString[kinout,FortranForm[rawarray[[f,ncol]]],"\n"]
 ]
Close[kinout];
```

Find the minimum flexion angle to use as a reference. I also find the min and max flexion angles in the "Interpolate" section.

```
firstarray = rawarray;
ndat=nfiles;
defminflex=45;
For[p=1,p<ndat+1,p++,
  defminflex=If[rawarray[[p,icol]]<defminflex,rawarray[[p,icol]],defminflex];
  ];
For[p=1,p<ndat+1,p++,
 firstarray[[p,icol]]=rawarray[[p,icol]]-defminflex
 ]
```

B.4 Interpolate data

Find the max flexion angle and pick the greatest desired flexion angle that is still less than or within the given tolerance of the max flexion angle. Do the analogous for the minimum flexion angle. Remember that the minimum flexion angle when referencing the first pose in the series will always be zero degrees.

```
Clear[defminindex,defmaxindex,firstmaxindex];
defminflex=45;
defmaxflex=0;
For[p=1,p<ndat+1,p++,
  defminflex=If[rawarray[[p,icol]]<defminflex,rawarray[[p,icol]],defminflex];

defmaxflex=If[rawarray[[p,icol]]>defmaxflex,rawarray[[p,icol]],defmaxflex]
  ];
firstmaxflex=defmaxflex-defminflex;
defminindex=1;
```

```
defmaxindex=1;
While[desflex[[defminindex]]<defminflex-
minflextol(Abs[desflex[[defminindex]]-
desflex[[defminindex+1]]]),defminindex=defminindex+1];While[desflex[[def
maxindex+1]]<defmaxflex+maxflextol(Abs[desflex[[defmaxindex]]-
desflex[[defmaxindex+1]]]),defmaxindex=defmaxindex+1;
If[defmaxindex>14,Break[]]];
firstmaxindex=zeroindex;
While[desflex[[firstmaxindex+1]]<firstmaxflex+maxflextol(Abs[desflex[[first
maxindex]]-desflex[[firstmaxindex+1]]]),firstmaxindex=firstmaxindex+1;
If[firstmaxindex>14,Break[]]];
```

Interpolate the data referenced to the default position.

```
Off[InterpolatingFunction::"dmval"];
Clear[intdummy,coltable,intfunct]
For[c=1,c<ncol+1,c++,
 coltable[c]=Table[{rawarray[[p,icol]],rawarray[[p,c]]},{p,ndat}];
 intfunct[c]=Interpolation[coltable[c],InterpolationOrder□intorder];
 For[f=defminindex,f<defmaxindex+1,f++,
  intdummy[f-defminindex+1,c]=intfunct[c][desflex[[f]]]
  ]
 ]
intdefarray=Array[intdummy,{defmaxindex-defminindex+1,ncol}];
```

Interpolate the data referenced to the first pose in the series.

```
Clear[intdummy,coltable,intfunct]
For[c=1,c<ncol+1,c++,
 coltable[c]=Table[{firstarray[[p,icol]],firstarray[[p,c]]},{p,ndat}];
 intfunct[c]=Interpolation[coltable[c],InterpolationOrder□intorder];
 For[f=zeroindex,f<firstmaxindex+1,f++,
```

```
   intdummy[f-zeroindex+1,c]=intfunct[c][desflex[[f]]]
   ]
  ]
intfirstarray=Array[intdummy,{firstmaxindex-zeroindex+1,ncol}];
```

REFERENCES

Aglietti, P., A. Baldini, et al. (2005). "Comparison of mobile-bearing and fixed-bearing total knee arthroplasty: a prospective randomized study." J Arthroplasty 20(2): 145-53.

Aglietti, P., R. Buzzi, et al. (1988). "Patellofemoral functional results and complications with the posterior stabilized total condylar knee prosthesis." J Arthoplasty 3: 17-25.

Akagi, M., T. Nakamura, et al. (2000). "The Bisurface total knee replacement: a unique design for flexion. Four-to-nine-year follow-up study." J Bone Joint Surg Am 82-A(11): 1626-33.

Andriacchi, T. P., C. O. Dyrby, et al. (2003). "The use of functional analysis in evaluating knee kinematics." Clin Orthop 410: 44-53.

Andriacchi, T. P. and J. O. Galante (1988). "Retention of the posterior cruciate in total knee arthroplasty." J Arthroplasty 3 Suppl: S13-9.

Andriacchi, T. P., J. O. Galante, et al. (1982). "The influence of total knee-replacement design on walking and stair-climbing." J Bone Joint Surg Am 64(9): 1328-35.

Anouchi, Y. S., M. McShane, et al. (1996). "Range of motion in total knee replacement." Clin Orthop Relat Res 331: 87-92.

Anouchi, Y. S., L. A. Whiteside, et al. (1993). "The effects of axial rotational alignment of the femoral component on knee stability and patellar tracking in total knee arthroplasty demonstrated on autopsy specimens." Clin Orthop Relat Res 287: 170-7.

Argenson, J. N., R. D. Komistek, et al. (2002). "In vivo determination of knee kinematics for subjects implanted with a unicompartmental arthroplasty." J Arthroplasty 17(8): 1049-54.

Argenson, J. N., R. D. Komistek, et al. (2004). "A High Flexion Total Knee Arthroplasty Design Replicates Healthy Knee Motion." Clin Orthop 1(428): 174-179.

Argenson, J. N., G. R. Scuderi, et al. (2005). "In vivo kinematic evaluation and design considerations related to high flexion in total knee arthroplasty." J Biomech 38(2): 277-84.

Arima, J., L. A. Whiteside, et al. (1998). "Effect of partial release of the posterior cruciate ligament in total knee arthroplasty." Clin Orthop Relat Res 353: 194-202.

Asano, T., M. Akagi, et al. (2001). "In vivo three-dimensional knee kinematics using a biplanar image-matching technique." Clin Orthop 388: 157-66.

Ash, H. E., I. C. Burgess, et al. (2000). "Long-term results for Kinemax and Kinematic knee bearings on a six-station knee wear simulator." Proc Inst Mech Eng [H] 214(5): 437-47.

Bachmeier, C. J., L. M. March, et al. (2001). "A comparison of outcomes in osteoarthritis patients undergoing total hip and knee replacement surgery." Osteoarthritis Cartilage 9(2): 137-46.

Banks, S., J. Bellemans, et al. (2003). "Knee motions during maximum flexion in fixed and mobile-bearing arthroplasties." Clin Orthop Relat Res(410): 131-8.

Banks, S. A., B. J. Fregly, et al. (2005). "Comparing in vivo kinematics of unicondylar and bi-unicondylar knee replacements." Knee Surg Sports Traumatol Arthrosc 13(7): 551-6.

Banks, S. A., M. K. Harman, et al. (2002). "Mechanism of anterior impingement damage in total knee arthroplasty." J Bone Joint Surg Am 84-A Suppl 2: 37-42.

Banks, S. A., M. K. Harman, et al. (2003). "Making sense of knee arthroplasty kinematics: news you can use." J Bone Joint Surg Am 85-A Suppl 4: 64-72.

Banks, S. A. and W. A. Hodge (1996). "Accurate measurement of three-dimensional knee replacement kinematics using single-plane fluoroscopy." IEEE Trans Biomed Eng 43(6): 638-49.

Banks, S. A., G. D. Markovich, et al. (1997). "In vivo kinematics of cruciate-retaining and -substituting knee arthroplasties." J Arthroplasty 12(3): 297-304.

Bartel, D. L., V. L. Bicknell, et al. (1986). "The effect of conformity, thickness, and material on stresses in ultra-high molecular weight components for total joint replacement." J Bone Joint Surg Am 68(7): 1041-51.

Becker, M. W., J. N. Insall, et al. (1991). "Bilateral total knee arthroplasty. One cruciate retaining and one cruciate substituting." Clin Orthop Relat Res(271): 122-4.

Bellemans, J., S. Banks, et al. (2002). "Fluoroscopic analysis of the kinematics of deep flexion in total knee arthroplasty. Influence of posterior condylar offset." J Bone Joint Surg Br 84(1): 50-3.

Benson, L. C., J. D. DesJardins, et al. (2002). "Effect of stair descent loading on ultra-high molecular weight polyethylene wear in a force-controlled knee simulator." Proc Inst Mech Eng [H] 216(6): 409-18.

Berend, M. E., M. A. Ritter, et al. (2004). "Tibial component failure mechanisms in total knee arthroplasty." Clin Orthop Relat Res 428: 26-34.

Berger, R. A., L. S. Crossett, et al. (1998). "Malrotation causing patellofemoral complications after total knee arthroplasty." Clin Orthop 356: 144-153.

Berger, R. A., S. Sanders, et al. (2005). "Outpatient total knee arthroplasty with a minimally invasive technique." J Arthroplasty 20(7 Suppl 3): 33-8.

Bertin, K. C. (2005). "Cruciate-retaining total knee arthroplasty at 5 to 7 years followup." Clin Orthop Relat Res 436: 177-83.

Bertin, K. C., R. D. Komistek, et al. (2002). "In vivo determination of posterior femoral rollback for subjects having a NexGen posterior cruciate-retaining total knee arthroplasty." J Arthroplasty 17(8): 1040-8.

Berzins, A., J. J. Jacobs, et al. (2002). "Surface damage in machined ram-extruded and net-shape molded retrieved polyethylene tibial inserts of total knee replacements." J Bone Joint Surg Am 84-A(9): 1534-40.

Bin, S. I. and T. S. Nam (2007). "Early results of high-flex total knee arthroplasty: comparison study at 1 year after surgery." Knee Surg Sports Traumatol Arthrosc 15(4): 350-5.

Blunn, G. W., A. B. Joshi, et al. (1997). "Wear in retrieved condylar knee arthroplasties. A comparison of wear in different designs of 280 retrieved condylar knee prostheses." J Arthroplasty 12(3): 281-90.

Blunn, G. W., P. S. Walker, et al. (1991). "The dominance of cyclic sliding in producing wear in total knee replacements." Clin Orthop 273: 253-60.

Bohl, J. R., W. R. Bohl, et al. (1999). "The Coventry Award. The effects of shelf life on clinical outcome for gamma sterilized polyethylene tibial components." Clin Orthop Relat Res(367): 28-38.

Bolanos, A. A., W. A. Colizza, et al. (1998). "A comparison of isokinetic strength testing and gait analysis in patients with posterior cruciate-retaining and substituting knee arthroplasties." J Arthroplasty 13(8): 906-15.

Boone, D. C. and S. P. Azen (1979). "Normal range of motion of joints in male subjects." J Bone Joint Surg Am 61(5): 756-9.

Browne, C., J. C. Hermida, et al. (2005). "Patellofemoral forces after total knee arthroplasty: effect of extensor moment arm." Knee 12(2): 81-8.

Burgess, I. C., M. Kolar, et al. (1997). "Development of a six station knee wear simulator and preliminary wear results." Proc Inst Mech Eng [H] 211(1): 37-47.

Callaghan, J. J., M. R. O'Rourke, et al. (2002). "Tibial post impingement in posterior-stabilized total knee arthroplasty." Clin Orthop Relat Res 404: 83-8.

Capeci, C. M., E. C. Brown, 3rd, et al. (2006). "Component asymmetry in simultaneous bilateral total knee arthroplasty." J Arthroplasty 21(5): 749-53.

Catani, F., S. Fantozzi, et al. (2006). "Influence of tibial component posterior slope on in vivo knee kinematics in fixed-bearing total knee arthroplasty." J Orthop Res 24(4): 581-7.

Chen, B., J. R. Zimmerman, et al. (2000). "Continuous passive motion after total knee arthroplasty: a prospective study." Am J Phys Med Rehabil 79(5): 421-6.

Clarke, H. D., K. R. Math, et al. (2004). "Polyethylene post failure in posterior stabilized total knee arthroplasty." J Arthroplasty 19(5): 652-7.

Coughlin, K. M., S. J. Incavo, et al. (2007). "Kneeling kinematics after total knee arthroplasty: anterior-posterior contact position of a standard and a high-flex tibial insert design." J Arthroplasty 22(2): 160-5.

Currier, J. H., M. A. Bill, et al. (2005). "Analysis of wear asymmetry in a series of 94 retrieved polyethylene tibial bearings." J Biomech 38(2): 367-75.

DeFrate, L. E., R. Papannagari, et al. (2006). "The 6 degrees of freedom kinematics of the knee after anterior cruciate ligament deficiency: an in vivo imaging analysis." Am J Sports Med 34(8): 1240-6.

DeFrate, L. E., H. Sun, et al. (2004). "In vivo tibiofemoral contact analysis using 3D MRI-based knee models." J Biomech 37(10): 1499-504.

Delp, S. L., J. H. Kocmond, et al. (1995). "Tradeoffs between motion and stability in posterior substituting knee arthroplasty design." J Biomech 28(10): 1155-66.

Dennis, B. D., R. Komistek, et al. (2001). "In vivo three-dimensional determination of kinematics for subjects with a normal knee or a unicompartmental or total knee replacement." J Bone Joint Surg Am 83-A Suppl 2 Pt 2: 104-15.

Dennis, D. A., M. L. Clayton, et al. (1992). "Posterior cruciate condylar total knee arthroplasty. Average 11-year follow-up evaluation." Clin Orthop Relat Res 281: 168-76.

Dennis, D. A., R. D. Komistek, et al. (1998). "In vivo anteroposterior femorotibial translation of total knee arthroplasty: a multicenter analysis." Clin Orthop 356: 47-57.

Dennis, D. A., R. D. Komistek, et al. (1998). "Range of motion after total knee arthroplasty: the effect of implant design and weight-bearing conditions." J Arthroplasty 13(7): 748-52.

Dennis, D. A., R. D. Komistek, et al. (1996). "In vivo knee kinematics derived using an inverse perspective technique." Clin Orthop 331: 107-17.

Dennis, D. A., R. D. Komistek, et al. (2003). "In vivo fluoroscopic analysis of fixed-bearing total knee replacements." Clin Orthop Relat Res 410: 114-30.

Dennis, D. A., R. D. Komistek, et al. (2004). "A Multicenter Analysis of Axial Femorotibial Rotation after Total Knee Arthroplasty." Clin Orthop 1(428): 180-189.

Dennis, D. A., R. D. Komistek, et al. (1998). "Range of motion after total knee arthroplasty: the effect of implant design and weight-bearing conditions." J Arthroplasty 13(7): 748-52.

DesJardins, J. D., P. S. Walker, et al. (2000). "The use of a force-controlled dynamic knee simulator to quantify the mechanical performance of total knee replacement designs during functional activity." J Biomech 33(10): 1231-42.

Diduch, D., J. Insall, et al. (1997). "Total knee replacement in young, active patients. Long-term follow-up and functional outcome." J Bone Joint Surg Am 79(4): 575-582.

D'Lima, D. D., P. C. Chen, et al. (2001). "Polyethylene contact stresses, articular congruity, and knee alignment." Clin Orthop Relat Res 392: 232-8.

D'Lima, D. D., P. C. Chen, et al. (2003). "Impact of patellofemoral design on patellofemoral forces and polyethylene stresses." J Bone Joint Surg Am 85-A Suppl 4: 85-93.

D'Lima, D. D., J. C. Hermida, et al. (2001). "Polyethylene wear and variations in knee kinematics." Clin Orthop Relat Res 392: 124-30.

D'Lima, D. D., S. Patil, et al. (2005). "The Chitranjan Ranawat Award: in vivo knee forces after total knee arthroplasty." Clin Orthop Relat Res 440: 45-9.

D'Lima, D. D., S. Patil, et al. (2006). "Tibial forces measured in vivo after total knee arthroplasty." J Arthroplasty 21(2): 255-62.

D'Lima, D. D., C. Poole, et al. (2001). "Quadriceps moment arm and quadriceps forces after total knee arthroplasty." Clin Orthop Relat Res 392: 213-20.

D'Lima, D. D., C. P. Townsend, et al. (2005). "An implantable telemetry device to measure intra-articular tibial forces." J Biomech 38(2): 299-304.

Emerson, R. J., C. Ayers, et al. (1996). "Surgical Closing in Primary Total Knee Arthroplasties: Flexion Versus Extension." Clin Orthop 331: 74-80.

Emerson, R. J., C. Ayers, et al. (1999). "Surgical Closing in Total Knee Arthroplasty: A Series Followup." Clin Orthop 368: 176-181.

Emmerson, K. P., C. G. Moran, et al. (1996). "Survivorship analysis of the Kinematic Stabilizer total knee replacement: a 10- to 14-year follow-up." J Bone Joint Surg Br 78(3): 441-5.

Engh, G. A., K. A. Dwyer, et al. (1992). "Polyethylene wear of metal-backed tibial components in total and unicompartmental knee prostheses." J Bone Joint Surg Br 74(1): 9-17.

Evans, M. C., E. M. Parsons, et al. (2006). "Comparative flexion after rotating-platform vs fixed-bearing total knee arthroplasty." J Arthroplasty 21(7): 985-91.

Fantozzi, S., F. Catani, et al. (2006). "Femoral rollback of cruciate-retaining and posterior-stabilized total knee replacements: In vivo fluoroscopic analysis during activities of daily living." J Orthop Res 24(12): 2222-2229.

Finch, E., M. Walsh, et al. (1998). "Functional ability perceived by individuals following total knee arthroplasty compared to age-matched individuals without knee disability." J Orthop Sports Phys Ther 27(4): 255-63.

Foster, D. L., F. Werner, et al. (1980). "Telemetry instrumentation for kinesiologic studies of knee motion." Med Res Eng 13(2): 17-21.

Fox, J. L. and R. Poss (1981). "The role of manipulation following total knee replacement." J Bone Joint Surg Am 63(3): 357-62.

Frankowski, J. J. and S. Watkins-Castillo (2002). Primary Total Knee and Hip Arthroplasty Projections for the U.S. Population to the Year 2030. Am Acad Orthop Surgeons.

Fregly, B. J., Y. Bei, et al. (2003). "Experimental evaluation of an elastic foundation model to predict contact pressures in knee replacements." J Biomech 36(11): 1659-68.

Fregly, B. J., H. A. Rahman, et al. (2005). "Theoretical accuracy of model-based shape matching for measuring natural knee kinematics with single-plane fluoroscopy." J Biomech Eng 127(4): 692-9.

Fregly, B. J., W. G. Sawyer, et al. (2005). "Computational wear prediction of a total knee replacement from in vivo kinematics." J Biomech 38(2): 305-14.

Gill, H. S., J. C. Waite, et al. (2006). "In vivo measurement of volumetric wear of a total knee replacement." Knee 13(4): 312-7.

Godest, A. C., C. S. de Cloke, et al. (2000). "A computational model for the prediction of total knee replacement kinematics in the sagittal plane." J Biomech 33(4): 435-42.

Goldberg, V. M., M. P. Figgie, et al. (1988). "Use of a total condylar knee prosthesis for treatment of osteoarthritis and rheumatoid arthritis. Long-term results." J Bone Joint Surg Am 70(6): 802-811.

Gronenschild, E. (1997). "The accuracy and reproducibility of a global method to correct for geometric image distortion in the x-ray imaging chain." Med Phys 24(12): 1875-88.

Gronenschild, E. (1999). "Correction for geometric image distortion in the x-ray imaging chain: local technique versus global technique." Med Phys 26(12): 2602-16.

Guess, T. M. and L. P. Maletsky (2005). "Computational modeling of a dynamic knee simulator for reproduction of knee loading." J Biomech Eng 127(7): 1216-21.

Guess, T. M. and L. P. Maletsky (2005). "Computational modelling of a total knee prosthetic loaded in a dynamic knee simulator." Med Eng Phys 27(5): 357-67.

Gupta, S. K., A. S. Ranawat, et al. (2006). "The P.F.C. sigma RP-F TKA designed for improved performance: a matched-pair study." Orthopedics 29(9 Suppl): S49-52.

Halloran, J. P., A. J. Petrella, et al. (2005). "Explicit finite element modeling of total knee replacement mechanics." J Biomech 38(2): 323-31.

Hanson, G. R., J. F. Suggs, et al. (2006). "Investigation of in vivo 6DOF total knee arthoplasty kinematics using a dual orthogonal fluoroscopic system." J Orthop Res 24(5): 974-81.

Hanson, G. R., J. F. Suggs, et al. (2007). "In vivo anterior tibial post contact after posterior stabilizing total knee arthroplasty." J Orthop Res.

Harman, M. K., S. A. Banks, et al. (2001). "Polyethylene damage and knee kinematics after total knee arthroplasty." Clin Orthop Relat Res 392: 383-93.

Harman, M. K., S. A. Banks, et al. (2007). "Backside damage corresponding to articular damage in retrieved tibial polyethylene inserts." Clin Orthop Relat Res 458: 137-44.

Harman, M. K., G. D. Markovich, et al. (1998). "Wear patterns on tibial plateaus from varus and valgus osteoarthritic knees." Clin Orthop 352: 149-58.

Harvey, I. A., K. Barry, et al. (1993). "Factors affecting the range of movement of total knee arthroplasty." J Bone Joint Surg Br 75(6): 950-5.

Hefzy, M. S., B. P. Kelly, et al. (1997). "Knee kinematics in-vivo of kneeling in deep flexion examined by bi-planar radiographs." Biomed Sci Instrum 33: 453-8.

Hemmerich, A., H. Brown, et al. (2006). "Hip, knee, and ankle kinematics of high range of motion activities of daily living." J Orthop Res 24(4): 770-781.

Hoff, W. A., R. D. Komistek, et al. (1998). "Three-dimensional determination of femoral-tibial contact positions under in vivo conditions using fluoroscopy." Clin Biomech (Bristol, Avon) 13(7): 455-472.

Hood, R. W., T. M. Wright, et al. (1983). "Retrieval analysis of total knee prostheses: a method and its application to 48 total condylar prostheses." J Biomed Mater Res 17(5): 829-42.

Huang, C. H., J. J. Liau, et al. (2007). "Stress analysis of the anterior tibial post in posterior stabilized knee prostheses." J Orthop Res.

Huang, H. T., J. Y. Su, et al. (2005). "The early results of high-flex total knee arthroplasty: a minimum of 2 years of follow-up." J Arthroplasty 20(5): 674-9.

Huddleston, J. I., J. W. Wiley, et al. (2005). "Zone 4 femoral radiolucent lines in hybrid versus cemented total knee arthroplasties: are they clinically significant?" Clin Orthop Relat Res 441: 334-9.

Incavo, S. J., E. R. Mullins, et al. (2004). "Tibiofemoral kinematic analysis of kneeling after total knee arthroplasty." J Arthroplasty 19(7): 906-10.

Insall, J. N., R. Binazzi, et al. (1985). "Total knee arthroplasty." Clin Orthop Relat Res 192: 13-22.

Insall, J. N., R. W. Hood, et al. (1983). "The total condylar knee prosthesis in gonarthrosis. A five to nine-year follow-up of the first one hundred consecutive replacements." J Bone Joint Surg Am 65(5): 619-28.

Jacobs, W. C., D. J. Clement, et al. (2005). "Retention versus removal of the posterior cruciate ligament in total knee replacement: a systematic literature review within the Cochrane framework." Acta Orthop 76(6): 757-68.

Jain, N. B., L. D. Higgins, et al. (2005). "Trends in epidemiology of knee arthroplasty in the United States, 1990-2000." Arthritis Rheum 52(12): 3928-33.

Jevsevar, D. S., P. O. Riley, et al. (1993). "Knee kinematics and kinetics during locomotor activities of daily living in subjects with knee arthroplasty and in healthy control subjects." Phys Ther 73(4): 229-39; discussion 240-2.

Jones, R. E. (2006). "High-flexion rotating-platform knees: rationale, design, and patient selection." Orthopedics 29(9 Suppl): S76-9.

Kaptein, B. L., E. R. Valstar, et al. (2003). "A new model-based RSA method validated using CAD models and models from reversed engineering." J Biomech 36(6): 873-82.

Karrholm, J., H. Jonsson, et al. (1994). "Kinematics of successful knee prostheses during weight-bearing: three-dimensional movements and positions of screw axes in the Tricon-M and Miller-Galante designs." Knee Surg Sports Traumatol Arthrosc 2(1): 50-9.

Kaufman, K. R., N. Kovacevic, et al. (1996). "Instrumented implant for measuring tibiofemoral forces." J Biomech 29(5): 667-71.

Kawamura, H. and R. B. Bourne (2001). "Factors affecting range of flexion after total knee arthroplasty." J Orthop Sci 6(3): 248-52.

Keating, E. M., P. M. Faris, et al. (1999). "Comparison of the midvastus muscle-splitting approach with the median parapatellar approach in total knee arthroplasty." J Arthroplasty 14(1): 29-32.

Kellett, C. F., A. Short, et al. (2004). "In vivo measurement of total knee replacement wear." Knee 11(3): 183-7.

Kim, H., R. R. Pelker, et al. (1997). "Rollback in posterior cruciate ligament-retaining total knee arthroplasty. A radiographic analysis." J Arthroplasty 12(5): 553-61.

Kim, Y. H., K. S. Sohn, et al. (2005). "Range of motion of standard and high-flexion posterior stabilized total knee prostheses. A prospective, randomized study." J Bone Joint Surg Am 87(7): 1470-5.

Kirking, B., J. Krevolin, et al. (2006). "A multiaxial force-sensing implantable tibial prosthesis." J Biomech 39(9): 1744-51.

Knight, L. A., S. Pal, et al. (2007). "Comparison of long-term numerical and experimental total knee replacement wear during simulated gait loading." J Biomech 40(7): 1550-1558.

Kocmond, J. H., S. L. Delp, et al. (1995). "Stability and range of motion of Insall-Burstein condylar prostheses. A computer simulation study." J Arthroplasty 10(3): 383-8.

Komistek, R. D., J. Allain, et al. (2002). "In vivo kinematics for subjects with and without an anterior cruciate ligament." Clin Orthop Relat Res 404: 315-25.

Komistek, R. D., D. A. Dennis, et al. (2003). "In vivo fluoroscopic analysis of the normal human knee." Clin Orthop 410: 69-81.

Komistek, R. D., D. A. Dennis, et al. (2004). "In Vivo Polyethylene Bearing Mobility Is Maintained in Posterior Stabilized Total Knee Arthroplasty." Clin Orthop 428: 207-213.

Komistek, R. D., T. R. Kane, et al. (2005). "Knee mechanics: a review of past and present techniques to determine in vivo loads." J Biomech 38(2): 215-28.

Kotani, A., A. Yonekura, et al. (2005). "Factors influencing range of motion after contemporary total knee arthroplasty." J Arthroplasty 20(7): 850-6.

Kramers-de Quervain, I. A., E. Stussi, et al. (1997). "Quantitative gait analysis after bilateral total knee arthroplasty with two different systems within each subject." J Arthroplasty 12(2): 168-79.

Kumar, P., E. McPherson, et al. (1996). "Rehabilitation after total knee arthroplasty." Clin Ortho 331: 93-101.

Kurosaka, M., S. Yoshiya, et al. (2002). "Maximizing flexion after total knee arthroplasty: the need and the pitfalls." J Arthroplasty 17(4 Suppl 1): 59-62.

Kurtz, S., F. Mowat, et al. (2005). "Prevalence of primary and revision total hip and knee arthroplasty in the United States from 1990 through 2002." J Bone Joint Surg Am 87(7): 1487-97.

Kuwano, T., K. Urabe, et al. (2005). "Importance of the lateral anatomic tibial slope as a guide to the tibial cut in total knee arthroplasty in Japanese patients." J Orthop Sci 10(1): 42-7.

Laskin, R. S. (2005). "Minimally invasive total knee arthroplasty: the results justify its use." Clin Orthop Relat Res 440: 54-9.

Laskin, R. S. and B. Beksac (2004). "Stiffness after total knee arthroplasty." J Arthroplasty 19(4 Suppl 1): 41-6.

Laubenthal, K., G. Smidt, et al. (1972). "A quantitative analysis of knee motion during activities of daily living." Phys Ther 52: 34.

Lavallee, S. and R. Szeliski (1995). "Recovering the Position and Orientation of Free-Form Objects from Image Contours Using 3D Distance Maps." IEEE TPAMI 17(4): 378-390.

Laz, P. J., S. Pal, et al. (2006). "Effects of knee simulator loading and alignment variability on predicted implant mechanics: a probabilistic study." J Orthop Res 24(12): 2212-21.

Laz, P. J., S. Pal, et al. (2006). "Probabilistic finite element prediction of knee wear simulator mechanics." J Biomech 39(12): 2303-10.

Leach, W., J. Reid, et al. (2006). "Continuous passive motion following total knee replacement: a prospective randomized trial with follow-up to 1 year." Knee Surg Sports Traumatol Arthrosc 14(10): 922-6.

Lee, J. G., E. M. Keating, et al. (1990). "Review of the all-polyethylene tibial component in total knee arthroplasty. A minimum seven-year follow-up period." Clin Orthop Relat Res 260: 87-92.

Lee, S. Y., N. Matsui, et al. (2005). "A posterior-stabilized total knee arthroplasty shows condylar lift-off during deep knee bends." Clin Orthop Relat Res 435: 181-4.

Lewis, P., C. H. Rorabeck, et al. (1994). "Posteromedial tibial polyethylene failure in total knee replacements." Clin Orthop Relat Res 299: 11-7.

Li, G., L. E. DeFrate, et al. (2005). "In vivo articular cartilage contact kinematics of the knee: an investigation using dual-orthogonal fluoroscopy and magnetic resonance image-based computer models." Am J Sports Med 33(1): 102-7.

Li, G., T. J. Gill, et al. (2002). "Biomechanical consequences of PCL deficiency - an in-vitro experimental study." J Orthop Res 20: 887-892.

Li, G., J. M. Moses, et al. (2006). "Anterior cruciate ligament deficiency alters the in vivo motion of the tibiofemoral cartilage contact points in both the anteroposterior and mediolateral directions." J Bone Joint Surg Am 88(8): 1826-34.

Li, G., E. Most, et al. (2002). "Biomechanics of posterior-substituting total knee arthroplasty: an in vitro study." Clin Orthop 404: 214-25.

Li, G., E. Most, et al. (2004). "Knee kinematics with a high-flexion posterior stabilized total knee prosthesis: an in vitro robotic experimental investigation." J Bone Joint Surg Am 86-A(8): 1721-9.

Li, G., R. Papannagari, et al. (2005). Stretching of Extensor Mechanism after Total Knee Arthroplasty. Orthopaedic Research Society, Washington D.C.

Li, G., R. Papannagari, et al. (Accepted). "The six degrees-of-freedom in-vivo kinematics of the knee: The coupling of the femoral and patellar kinematics." J Biomech Eng.

Li, G., S. L. Schule, et al. (2003). Improving Flexion in Total Knee Arthroplasty. The Adult Knee. J. J. Callaghan, A. G. Rosenberg, H. E. Rubash, P. T. Simonian and T. L. Wickiewicz. Philadelphia, Lippincott Williams and Wilkins. 2: 1233-44.

Li, G., J. Suggs, et al. (2006). "Three-dimensional tibiofemoral articular contact kinematics of a cruciate-retaining total knee arthroplasty." J Bone Joint Surg Am 88(2): 395-402.

Li, G., T. H. Wuerz, et al. (2004). "Feasibility of using orthogonal fluoroscopic images to measure in vivo joint kinematics." J Biomech Eng 126(2): 314-8.

Li, G., S. Zayontz, et al. (2004). "Kinematics of the knee at high flexion angles: an in vitro investigation." J Orthop Res 22(1): 90-5.

Li, G., S. Zayontz, et al. (2001). "Cruciate-retaining and cruciate-substituting total knee arthroplasty: an in vitro comparison of the kinematics under muscle loads." J Arthroplasty 16(8 Suppl 1): 150-6.

Lizaur, A., L. Marco, et al. (1997). "Preoperative factors influencing the range of movement after total knee arthroplasty for severe osteoarthritis." J Bone Joint Surg Br 79(4): 626-9.

Luger, E., S. Sathasivam, et al. (1997). "Inherent differences in the laxity and stability between the intact knee and total knee replacements." Knee 4(1): 7-14.

MacDonald, S. J., R. B. Bourne, et al. (2000). "Prospective randomized clinical trial of continuous passive motion after total knee arthroplasty." Clin Orthop Relat Res(380): 30-5.

Mahfouz, M. R., W. A. Hoff, et al. (2003). "A robust method for registration of three-dimensional knee implant models to two-dimensional fluoroscopy images." IEEE Trans Med Imaging 22(12): 1561-74.

Mahfouz, M. R., W. A. Hoff, et al. (2005). "Effect of segmentation errors on 3D-to-2D registration of implant models in X-ray images." J Biomech 38(2): 229-39.

Mahomed, N. N., M. H. Liang, et al. (2002). "The importance of patient expectations in predicting functional outcomes after total joint arthroplasty." J Rheumatol 29(6): 1273-9.

Malkani, A. L., J. A. Rand, et al. (1995). "Total knee arthroplasty with the kinematic condylar prosthesis. A ten-year follow-up study." J Bone Joint Surg Am 77(3): 423-31.

Maloney, W. and D. Schurman (1992). "The effects of implant design on range of motion after total knee arthroplasty laxity after ACL reconstructive surgery." Clin Orthop 278: 147-152.

Maloney, W. J. and D. J. Schurman (1992). "The effects of implant design on range of motion after total knee arthroplasty. Total condylar versus posterior stabilized total condylar designs." Clin Orthop Relat Res 278: 147-52.

March, L. M., M. J. Cross, et al. (1999). "Outcomes after hip or knee replacement surgery for osteoarthritis. A prospective cohort study comparing patients' quality of life before and after surgery with age-related population norms." Med J Aust 171(5): 235-8.

Masri, B. A., R. S. Laskin, et al. (1996). "Knee closure in total knee replacement: a randomized prospective trial." Clin Orthop Relat Res(331): 81-6.

Matsuda, S., H. Miura, et al. (1999). "Knee stability in posterior cruciate ligament retaining total knee arthroplasty." Clin Orthop Relat Res 366: 169-73.

Matsueda, M. and R. B. Gustilo (2000). "Subvastus and medial parapatellar approaches in total knee arthroplasty." Clin Orthop Relat Res(371): 161-8.

Matsumoto, T., N. Tsumura, et al. (2005). "Influence of hip position on knee flexion angle in patients undergoing total knee arthroplasty." J Arthroplasty 20(5): 669-73.

Mihalko, W., Z. Fishkin, et al. (2006). "Patellofemoral overstuff and its relationship to flexion after total knee arthroplasty." Clin Orthop Relat Res 449: 283-7.

Mihalko, W. M., L. A. Whiteside, et al. (2003). "Comparison of ligament-balancing techniques during total knee arthroplasty." J Bone Joint Surg Am 85-A Suppl 4: 132-5.

Miller, R. K., J. W. Goodfellow, et al. (1998). "In vitro measurement of patellofemoral force after three types of knee replacement." J Bone Joint Surg Br 80(5): 900-6.

Miller, R. K., D. W. Murray, et al. (1997). "In vitro patellofemoral joint force determined by a non-invasive technique." Clin Biomech (Bristol, Avon) 12(1): 1-7.

Miner, A. L., E. A. Lingard, et al. (2003). "Knee range of motion after total knee arthroplasty: how important is this as an outcome measure?" J Arthroplasty 18(3): 286-94.

Mizner, R. L., S. C. Petterson, et al. (2005). "Quadriceps strength and the time course of functional recovery after total knee arthroplasty." J Orthop Sports Phys Ther 35(7): 424-36.

Mizu-Uchi, H., S. Matsuda, et al. (2006). "Anteroposterior stability in posterior cruciate ligament-retaining total knee arthroplasty." J Arthroplasty 21(4): 592-8.

Moffet, H., J. P. Collet, et al. (2004). "Effectiveness of intensive rehabilitation on functional ability and quality of life after first total knee arthroplasty: A single-blind randomized controlled trial." Arch Phys Med Rehabil 85(4): 546-56.

Morgan, H., V. Battista, et al. (2005). "Constraint in primary total knee arthroplasty." J Am Acad Orthop Surg 13(8): 515-24.

Moro-Oka, T. A., M. Muenchinger, et al. (2006). "Comparing in vivo kinematics of anterior cruciate-retaining and posterior cruciate-retaining total knee arthroplasty." Knee Surg Sports Traumatol Arthrosc 15(1): 93-9.

Morris, B. A., D. D. D'Lima, et al. (2001). "e-Knee: evolution of the electronic knee prosthesis. Telemetry technology development." J Bone Joint Surg Am 83-A Suppl 2(Pt 1): 62-6.

Most, E. (2000). Development of a 6-DOF Robotic Test System for Studying the Biomechanics of Total Knee Replacement. Dept of Mech Eng. Cambridge, MA, Massachusetts Institute of Technology.

Most, E., G. Li, et al. (2003). "The kinematics of fixed- and mobile-bearing total knee arthroplasty." Clin Orthop 416: 197-207.

Most, E., P. G. Sultan, et al. (2006). "Tibiofemoral contact behavior is improved in high-flexion cruciate retaining TKA." Clin Orthop Relat Res 452: 59-64.

Most, E., S. Zayontz, et al. (2003). "Femoral rollback after cruciate-retaining and stabilizing total knee arthroplasty." Clin Orthop 410: 101-13.

Mulholland, S. J. and U. P. Wyss (2001). "Activities of daily living in non-Western cultures: range of motion requirements for hip and knee joint implants." Int J Rehab Res 24(3): 191-8.

Myles, C. M., P. J. Rowe, et al. (2002). "Knee joint functional range of movement prior to and following total knee arthroplasty measured using flexible electrogoniometry." Gait Posture 16(1): 46-54.

Nagura, T., C. Dyrby, et al. (2002). "Mechanical loads at the knee joint during deep flexion." J Ortho Res 20(4): 881-6.

Nagura, T., T. Otani, et al. (2005). "Is high flexion following total knee arthroplasty safe?: evaluation of knee joint loads in the patients during maximal flexion." J Arthroplasty 20(5): 647-51.

Nakagawa, S., Y. Kadoya, et al. (2000). "Tibiofemoral movement 3: full flexion in the living knee studied by MRI." J Bone Joint Surg Br 82(8): 1199-200.

NIH (2000). Improving Medical Implant Performance Tthrough Retrieval Information: Challenges and Opportunities. NIH Technology Assessment Conference.

NIH (2003). NIH Consensus Development Conference on Total Knee Replacement. National Institutes of Health Consensus Development Conference.

Nilsson, K. G., J. Karrholm, et al. (1990). "Knee motion in total knee arthroplasty. A roentgen stereophotogrammetric analysis of the kinematics of the Tricon-M knee prosthesis." Clin Orthop Relat Res 256: 147-61.

Nilsson, K. G., J. Karrholm, et al. (1991). "Abnormal kinematics of the artificial knee. Roentgen stereophotogrammetric analysis of 10 Miller-Galante and five New Jersey LCS knees." Acta Orthop Scand 62(5): 440-6.

Noble, P. C., M. J. Gordon, et al. (2005). "Does total knee replacement restore normal knee function?" Clin Orthop Relat Res 431: 157-65.

Nozaki, H., S. A. Banks, et al. (2002). "Observations of femoral rollback in cruciate-retaining knee arthroplasty." Clin Orthop Relat Res 404: 308-14.

Parentis, M. A., M. N. Rumi, et al. (1999). "A comparison of the vastus splitting and median parapatellar approaches in total knee arthroplasty." Clin Orthop Relat Res(367): 107-16.

Parsley, B. S., G. A. Engh, et al. (1992). "Preoperative flexion. Does it influence postoperative flexion after posterior-cruciate-retaining total knee arthroplasty?" Clin Orthop Relat Res 275: 204-10.

Parsley, B. S., G. A. Engh, et al. (1992). "Preoperative flexion. Does it influence postoperative flexion after posterior-cruciate-retaining total knee arthroplasty?" Clin Orthop Relat Res(275): 204-10.

Patil, S., C. W. Colwell, Jr., et al. (2005). "Can normal knee kinematics be restored with unicompartmental knee replacement?" J Bone Joint Surg Am 87(2): 332-8.

Penney, G. P., J. Weese, et al. (1998). "A comparison of similarity measures for use in 2-D-3-D medical image registration." IEEE Trans Med Imaging 17(4): 586-95.

Piazza, S. J. and S. L. Delp (2001). "Three-dimensional dynamic simulation of total knee replacement motion during a step-up task." J Biomech Eng 123(6): 599-606.

Piazza, S. J., S. L. Delp, et al. (1998). "Posterior tilting of the tibial component decreases femoral rollback in posterior-substituting knee replacement: a computer simulation study." J Orthop Res 16(2): 264-70.

Pope, R. O., S. Corcoran, et al. (1997). "Continuous passive motion after primary total knee arthroplasty. Does it offer any benefits?" J Bone Joint Surg Br 79(6): 914-7.

Praemer, A., S. Furner, et al. (1999). Musculoskeletal Conditions in the United States. Rosemont, IL, American Academy of Orthopaedic Surgeons.

Ranawat, A. S., S. K. Gupta, et al. (2006). "The P.F.C. sigma RP-F total knee arthroplasty: designed for improved performance." Orthopedics 29(9 Suppl): S28-9.

Ranawat, C. S. (2003). "Design may be counterproductive for optimizing flexion after TKR." Clin Orthop Relat Res 416: 174-6.

Ranawat, C., W. J. Flynn, et al. (1993). "Long-term results of the total condylar knee arthroplasty: a 15-year survivorship study." Clin Orthop 286(94-102).

Ranawat, C. S., C. P. Luessenhop, et al. (1997). "The press-fit condylar modular total knee system. Four-to-six-year results with a posterior-cruciate-substituting design." J Bone Joint Surg Am 79(3): 342-348.

Ranawat, C. S., D. E. Padgett, et al. (1989). "Total knee arthroplasty for patients younger than 55 years." Clin Orthop Relat Res(248): 27-33.

Rand, J. (1993). "Comparison of metal-backed and all-polyethelene tibial components in cruciate condylar total knee arthroplasty." J Arthoplasty 8: 307-313.

Rawlinson, J. J., B. D. Furman, et al. (2006). "Retrieval, experimental, and computational assessment of the performance of total knee replacements." J Orthop Res 24(7): 1384-94.

Ritter, M. A. (2006). "High-flexion knee designs: more hype than hope? In the affirmative." J Arthroplasty 21(4 Suppl 1): 40-1.

Ritter, M. A., L. D. Harty, et al. (2003). "Predicting range of motion after total knee arthroplasty. Clustering, log-linear regression, and regression tree analysis." J Bone Joint Surg Am 85-A(7): 1278-85.

Ritter, M. A. and E. A. Stringer (1979). "Predictive range of motion after total knee replacement." Clin Orthop Relat Res 143: 115-9.

Rittman, N., D. B. Kettelkamp, et al. (1981). "Analysis of patterns of knee motion walking for four types of total knee implants." Clin Orthop Relat Res 155: 111-7.

Robertsson, O., M. Dunbar, et al. (2000). "Patient satisfaction after knee arthroplasty: a report on 27,372 knees operated on between 1981 and 1995 in Sweden." Acta Orthop Scand 71(3): 262-7.

Romness, D. W. and J. A. Rand (1988). "The role of continuous passive motion following total knee arthroplasty." Clin Orthop Relat Res(226): 34-7.

Rosenberg, A. G., R. M. Barden, et al. (1990). "Cemented and ingrowth fixation of the Miller-Galante prosthesis. Clinical and roentgenographic comparison after three- to six-year follow-up studies." Clin Orthop Relat Res 260: 71-9.

Rossi, M. D., S. Hasson, et al. (2006). "Mobility and perceived function after total knee arthroplasty." J Arthroplasty 21(1): 6-12.

Rowe, P. J., C. M. Myles, et al. (2000). "Knee joint kinematics in gait and other functional activities measured using flexible electrogoniometry: how much knee motion is sufficient for normal daily life?" Gait Posture 12(2): 143-55.

Rowe, P. J., C. M. Myles, et al. (2005). "The effect of total knee arthroplasty on joint movement during functional activities and joint range of motion with particular regard to higher flexion users." J Orthop Surg (Hong Kong) 13(2): 131-8.

Sathappan, S. S., B. Wasserman, et al. (2006). "Midterm results of primary total knee arthroplasty using a dished polyethylene insert with a recessed or resected posterior cruciate ligament." J Arthroplasty 21(7): 1012-6.

Sathasivam, S. and P. S. Walker (1997). "A computer model with surface friction for the prediction of total knee kinematics." J Biomech 30(2): 177-84.

Schurman, D. J., A. Matityahu, et al. (1998). "Prediction of postoperative knee flexion in Insall-Burstein II total knee arthroplasty." Clin Orthop Relat Res 353: 175-84.

Schurman, D. J., J. N. Parker, et al. (1985). "Total condylar knee replacement. A study of factors influencing range of motion as late as two years after arthroplasty." J Bone Joint Surg Am 67(7): 1006-14.

Seon, J. K., E. K. Song, et al. (2005). "Comparison of range of motion of high-flexion prosthesis and mobile-bearing prosthesis in total knee arthroplasty." Orthopedics 28(10 Suppl): s1247-50.

Sharkey, P. F., W. J. Hozack, et al. (2002). "Insall Award paper. Why are total knee arthroplasties failing today?" Clin Orthop Relat Res 404: 7-13.

Silva, M., E. F. Shepherd, et al. (2003). "Knee strength after total knee arthroplasty." J Arthroplasty 18(5): 605-11.

Singerman, R., J. Dean, et al. (1996). "Decreased posterior tibial slope increases strain in the posterior cruciate ligament following total knee arthroplasty." J Arthroplasty 11(1): 99-103.

Singerman, R., H. D. Pagan, et al. (1997). "Effect of femoral component rotation and patellar design on patellar forces." Clin Orthop Relat Res 334: 345-53.

Steinberg, N., I. Hershkovitz, et al. (2005). "Range of Joint Movement in Female Dancers and Nondancers Aged 8 to 16 Years: Anatomical and Clinical Implications." Am J Sports Med In press.

Stiehl, J. B., D. A. Dennis, et al. (2000). "In vivo kinematic comparison of posterior cruciate ligament retention or sacrifice with a mobile bearing total knee arthroplasty." Am J Knee Surg 13(1): 13-8.

Stiehl, J. B., R. D. Komistek, et al. (2000). "The cruciate ligaments in total knee arthroplasty: a kinematic analysis of 2 total knee arthroplasties." J Arthroplasty 15(5): 545-50.

Stiehl, J. B., R. D. Komistek, et al. (1995). "Fluoroscopic analysis of kinematics after posterior-cruciate-retaining knee arthroplasty." J Bone Joint Surg Br 77(6): 884-9.

Sugama, R., Y. Kadoya, et al. (2005). "Preparation of the flexion gap affects the extension gap in total knee arthroplasty." J Arthroplasty 20(5): 602-7.

Suggs, J. F., G. Li, et al. (2004). "Function of the anterior cruciate ligament after unicompartmental knee arthroplasty: an in vitro robotic study." J Arthroplasty 19(2): 224-9.

Suggs, J. F., G. Li, et al. (2006). "ACL--Knee biomechanics after UKA and its relation to the a robotic investigation." J Orthop Res 24(4): 588-94.

Sugita, T., K. Sato, et al. (2005). "In vivo determination of knee kinematics for Japanese subjects having either a low contact stress rotating platform or an anteroposterior glide total knee arthroplasty." J Arthroplasty 20(2): 154-61.

Sultan, P. G., E. Most, et al. (2003). "Optimizing flexion after total knee arthroplasty: advances in prosthetic design." Clin Orthop 416: 167-73.

Szabo, G., G. Lovasz, et al. (2000). "A prospective comparative analysis of mobility in osteoarthritic knees." J Bone Joint Surg Br 82(8): 1167-9.

Tanavalee, A., S. Thiengwittayaporn, et al. (2004). "Rapid ambulation and range of motion after minimally invasive total knee arthroplasty." J Med Assoc Thai 87 Suppl 2: S195-201.

Taylor, S. J. and P. S. Walker (2001). "Forces and moments telemetered from two distal femoral replacements during various activities." J Biomech 34(7): 839-48.

Taylor, M. and D. S. Barrett (2003). "Explicit finite element simulation of eccentric loading in total knee replacement." Clin Orthop Relat Res 414: 162-71.

Taylor, S. J., P. S. Walker, et al. (1998). "The forces in the distal femur and the knee during walking and other activities measured by telemetry." J Arthroplasty 13(4): 428-37.

Teeny, S. M., S. C. York, et al. (2005). "Does shortened length of hospital stay affect total knee arthroplasty rehabilitation outcomes?" J Arthroplasty 20(7 Suppl 3): 39-45.

Tew, M., I. W. Forster, et al. (1989). "Effect of total knee arthroplasty on maximal flexion." Clin Orthop Relat Res 247: 168-74.

Uvehammer, J., J. Karrholm, et al. (2000). "In vivo kinematics of total knee arthroplasty. Concave versus posterior-stabilised tibial joint surface." J Bone Joint Surg Br 82(4): 499-505.

Victor, J., S. Banks, et al. (2005). "Kinematics of posterior cruciate ligament-retaining and -substituting total knee arthroplasty: A PROSPECTIVE RANDOMISED OUTCOME STUDY." J Bone Joint Surg Br 87-B(5): 646-655.

Vince, K. G. (2003). "Why knees fail." J Arthroplasty 18(3 Suppl 1): 39-44.

Walker, P. S., G. W. Blunn, et al. (1997). "A knee simulating machine for performance evaluation of total knee replacements." J Biomech 30(1): 83-9.

Walker, P. and A. Garg (1991). "Range of motion in Total Knee Arthroplasty: A computer analysis." Clin Orthop 262: 227-35.

Walker, P. S. and H. Haider (2003). "Characterizing the motion of total knee replacements in laboratory tests." Clin Orthop Relat Res 410: 54-68.

Walker, P. S. S., Sathasivam. (2000). "Design forms of total knee replacement." Proc Instn Mech Engrs 214(H): 101-119.

Wasielewski, R. C., J. O. Galante, et al. (1994). "Wear patterns on retrieved polyethylene tibial inserts and their relationship to technical considerations during total knee arthroplasty." Clin Orthop Relat Res 299: 31-43.

Watanabe, T., T. Yamazaki, et al. (2004). "In vivo kinematics of mobile-bearing knee arthroplasty in deep knee bending motion." J Orthop Res 22(5): 1044-9.

Weale, A. E., J. Feikes, et al. (2002). "In vitro evaluation of the resistance to dislocation of a meniscal-bearing total knee prosthesis between 30 degrees and 90 degrees of knee flexion." J Arthroplasty 17(4): 475-83.

Weale, A. E., O. A. Halabi, et al. (2001). "Perceptions of outcomes after unicompartmental and total knee replacements." Clin Orthop 382: 143-53.

Weiss, J. M., P. C. Noble, et al. (2002). "What functional activities are important to patients with knee replacements?" Clin Orthop Relat Res 404: 172-88.

Werner, F. W., D. C. Ayers, et al. (2005). "The effect of valgus/varus malalignment on load distribution in total knee replacements." J Biomech 38(2): 349-55.

Whiteside, L. A., M. R. Kasselt, et al. (1987). "Varus-valgus and rotational stability in rotationally unconstrained total knee arthroplasty." Clin Orthop Relat Res 219: 147-57.

Wilson, S. A., P. D. McCann, et al. (1996). "Comprehensive gait analysis in posterior-stabilized knee arthroplasty." J Arthroplasty 11(4): 359-67.

Wimmer, M. A. and T. P. Andriacchi (1997). "Tractive forces during rolling motion of the knee: implications for wear in total knee replacement." J Biomech 30(2): 131-7.

Wimmer, M. A., T. P. Andriacchi, et al. (1998). "A striated pattern of wear in ultrahigh-molecular-weight polyethylene components of Miller-Galante total knee arthroplasty." J Arthroplasty 13(1): 8-16.

Wright, T. M. (2005). "Polyethylene in knee arthroplasty: what is the future?" Clin Orthop Relat Res 440: 141-8.

Yamazaki, J., S. Ishigami, et al. (2002). "Hy-Flex II total knee system and range of motion." Arch Orthop Trauma Surg 122(3): 156-60.

Yamazaki, T., T. Watanabe, et al. (2005). "Visualization of femorotibial contact in total knee arthroplasty using X-ray fluoroscopy." Eur J Radiol 53(1): 84-9.

Yau, W. P., K. Y. Chiu, et al. (2005). "Residual posterior femoral condyle osteophyte affects the flexion range after total knee replacement." Int Orthop 29(6): 375-9.

Yoshiya, S., N. Matsui, et al. (2005). "In vivo kinematic comparison of posterior cruciate-retaining and posterior stabilized total knee arthroplasties under passive and weight-bearing conditions." J Arthroplasty 20(6): 777-83.

You, B. M., P. Siy, et al. (2001). "In vivo measurement of 3-D skeletal kinematics from sequences of biplane radiographs: application to knee kinematics." IEEE Trans Med Imaging 20(6): 514-25.

Zavatsky, A. B. (1997). "A kinematic-freedom analysis of a flexed-knee-stance testing rig." J Biomech 30(3): 277-80.

Zhao, D., S. A. Banks, et al. (2007). "In vivo medial and lateral tibial loads during dynamic and high flexion activities." J Orthop Res 25(5): 593-602.

Zimmer (2004). "NexGen Complete Knee Solution: design rationale. Warsaw, IN: Zimmer."

Zuffi, S., A. Leardini, et al. (1999). "A model-based method for the reconstruction of total knee replacement kinematics." IEEE Trans Med Imaging 18(10): 981-91.